MULTIDISCIPLINARY CENTER FOR EARTHQUAKE ENGINEERING RESEARCH
A National Center of Excellence in Advanced Technology Applications

ISSN 1520-295X

The Performance-Based Design Paradigm

by

Michael J. Astrella and Andrew S. Whittaker
University at Buffalo, State University of New York
Department of Civil, Structural and Environmental Engineering
Ketter Hall
Buffalo, New York 14260

Technical Report MCEER-05-0011

December 15, 2005

This research was conducted at the University at Buffalo, State University of New York and was supported primarily by the Earthquake Engineering Research Centers Program of the National Science Foundation under award number EEC-9701471.

NOTICE

MULTIDISCIPLINARY CENTER FOR EARTHQUAKE ENGINEERING RESEARCH
A National Center of Excellence in Advanced Technology Applications

The Performance-Based Design Paradigm

by

Michael J. Astrella[1] and Andrew S. Whittaker[2]

Publication Date: December 15, 2005
Submittal Date: June 17, 2005

Technical Report MCEER-05-0011

Task Number 8.2.4

NSF Master Contract Number EEC 9701471

1 Structural Engineer, Weidlinger Associates; Former Graduate Assistant, Department of Civil, Structural and Environmental Engineering, University at Buffalo, State University of New York
2 Professor, Department of Civil, Structural and Environmental Engineering, University at Buffalo, State University of New York

MULTIDISCIPLINARY CENTER FOR EARTHQUAKE ENGINEERING RESEARCH
University at Buffalo, State University of New York
Red Jacket Quadrangle, Buffalo, NY 14261

Preface

The Multidisciplinary Center for Earthquake Engineering Research (MCEER) is a national center of excellence in advanced technology applications that is dedicated to the reduction of earthquake losses nationwide. Headquartered at the University at Buffalo, State University of New York, the Center was originally established by the National Science Foundation in 1986, as the National Center for Earthquake Engineering Research (NCEER).

Comprising a consortium of researchers from numerous disciplines and institutions throughout the United States, the Center's mission is to reduce earthquake losses through research and the application of advanced technologies that improve engineering, pre-earthquake planning and post-earthquake recovery strategies. Toward this end, the Center coordinates a nationwide program of multidisciplinary team research, education and outreach activities.

MCEER's research is conducted under the sponsorship of two major federal agencies: the National Science Foundation (NSF) and the Federal Highway Administration (FHWA), and the State of New York. Significant support is derived from the Federal Emergency Management Agency (FEMA), other state governments, academic institutions, foreign governments and private industry.

MCEER's NSF-sponsored research objectives are twofold: to increase resilience by developing seismic evaluation and rehabilitation strategies for the post-disaster facilities and systems (hospitals, electrical and water lifelines, and bridges and highways) that society expects to be operational following an earthquake; and to further enhance resilience by developing improved emergency management capabilities to ensure an effective response and recovery following the earthquake (see the figure below).

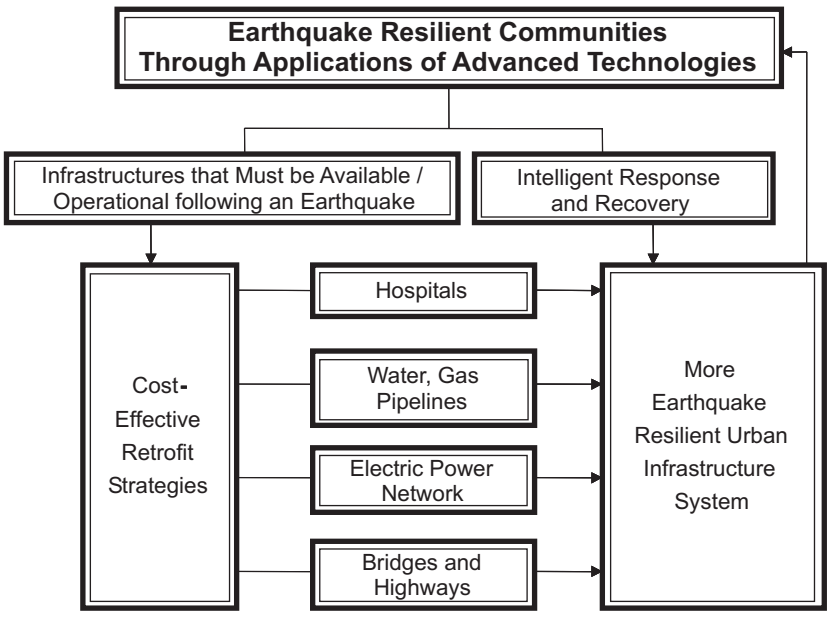

A cross-program activity focuses on the establishment of an effective experimental and analytical network to facilitate the exchange of information between researchers located in various institutions across the country. These are complemented by, and integrated with, other MCEER activities in education, outreach, technology transfer, and industry partnerships.

The study described in this report provides ground work toward the development of performance-based design tools for buildings. The focus is on nonstructural components and building contents. The study assesses the response of different seismic framing systems to a broad range of earthquake ground motions and the impact of framing system choice on the demands of nonstructural components and building contents. This is illustrated through response-history analysis of two conventional hospital buildings located in Southern California, which represent typical 1960's and 1970's-era construction, and 10 models of alternate (retrofit) construction. Three bins of earthquake histories with different probabilities of exceedence are used for the response-history analysis. Three types of protective systems are considered in the study: steel yielding devices (buckling restrained braces), fluid viscous dampers and base-isolation. Six of the models are base-isolated with three types of isolators. The performance of the base-isolated frames is superior to that of the other frames as gauged by the smallest drift and acceleration demands on the nonstructural components. Of the non-isolated models, those equipped with fluid viscous dampers offer superior performance. No single type of isolator (of the three types considered) outperforms the others across all three bins of earthquake histories. The work complements performance-based earthquake engineering tools currently under development by MCEER, the Pacific Earthquake Engineering Center (PEER) and the ATC-58 project.

ABSTRACT

The principal investments in building construction are made in non-structural components and contents (NCCs). An efficient performance-based design paradigm should focus on these key investments and a new design paradigm is needed to do so. The impact of structural framing system type on the NCCs demands is illustrated through response-history analysis of two conventional hospital buildings located in Southern California, which represent typical 1960s-era and 1970s-era construction, and 10 models of alternate (retrofit) construction. Three bins of earthquake histories with different probabilities of exceedence are used for the response-history analysis. Three types of protective systems are considered in the study: steel yielding devices (buckling restrained braces), fluid viscous dampers and base-isolation. Six of the models are base-isolated with three types of isolators. The performance of the base-isolated frames is superior to that of the other frames as gauged by the smallest drift and acceleration demands on the NCCs. Of the non-isolated models, those equipped with fluid viscous dampers offer superior performance. No single type of isolator (of the three types considered) outperforms the other two isolator types across all 3 bins of earthquake histories.

ACKNOWLEDGEMENTS

Funding for this work was provided by the Multidisciplinary Center for Earthquake Engineering Research through grants from the National Science Foundation (Award Number EEC-9701471) and the State of New York. These studies are part of the MCEER research program on the seismic resilience of acute-care facilities.

TABLE OF CONTENTS

TABLE OF CONTENTS

LIST OF FIGURES

LIST OF FIGURES

LIST OF FIGURES

LIST OF TABLES

CHAPTER 1

INTRODUCTION

1.1 Performance-Based Earthquake Engineering of Buildings

In the past, decisions regarding target building performance during earthquake shaking have been made by structural engineers with little consultation with building owners, insurers and regulators (hereafter termed stakeholders) because tools for risk computations and decision-making, cast in a format understood by and accessible to the stakeholders, did not exist.

The first-generation tools for performance-based earthquake engineering (PBEE-1) that were published in 1997 as the FEMA 273, *Guidelines for the Seismic Rehabilitation of Buildings* (FEMA, 1997) included a decision-making process for building performance that was based solely on estimating the response of structural and nonstructural components and comparing those estimates with predefined (default) limits for discrete performance levels. No formal risk-based mechanism was provided in that document to engage stakeholders in the decision-making process.

Since the publication of FEMA 273 and its derivative, FEMA 356, *Prestandard and Commentary for the Seismic Rehabilitation of Buildings* (FEMA, 2000b), much effort has been spent to engage stakeholders in decision-making related to the performance of buildings during earthquake shaking and to present performance data in an efficient and useful format for the stakeholders. On the basis of a workshop conducted as part of the ATC-58 project in 2002 (FEMA, 2005), insight was gained into the needs and interests of stakeholders related to building performance in earthquake shaking. Key insights included a) stakeholders have a strong interest in the societal and economic (direct and indirect) impacts of earthquakes beyond the traditional life-safety considerations, b) stakeholders have a wide range of needs for performance characterization, and c) expressions of risk (exposure to loss) should be available as probabilistic expressions (e.g., expected annualized loss) and for deterministic scenarios. Further, the traditional measures of

performance (e.g., component plastic hinge rotation) for structural engineers were of little-to-no value to stakeholders.

To engage stakeholders in the decision-making process, decision-support infrastructure and tools must be developed that express performance in a language understood by the stakeholders. A decision-support system developed by one of the National Science Foundation Earthquake Engineering Research Centers, the Multidisciplinary Center for Earthquake Engineering Research (MCEER) is presented in figure 1-1. The focus of the work at MCEER is hospital construction in California and the MCEER decision-support system specifically addresses the unique needs and constraints of hospital construction in California. This decision-support system is scenario-based and includes traditional steps in the building analysis and design process, including characterization of the earthquake hazard, site response analysis, structural analysis and engineering. The process is constructed around concepts of fragility and resilience (Bruneau et al., 2003).

Similar infrastructure and tools have also been developed for the ATC-58 project (see www.atcouncil.org) and by another National Science Foundation Earthquake Engineering Research Center: the Pacific Earthquake Engineering Research (PEER) Center (peer.berkeley.edu). Much is common to the infrastructure and tools produced by the ATC-58 project, PEER and MCEER.

1.2 MCEER Decision Support Framework

Fragility and resilience are two measures of building performance. Fragility can be defined as the median probability that a system (component) will exceed a level of damage given a level of demand on that system (component). At each point on a fragility curve there is a distribution about the central tendency that depends on uncertainties and randomness in system (component) properties and loading characteristics. A sample fragility curve is presented in figure 1-2a. Seismic resilience represents a) the capability of a building (through design and construction) to resist damage, and b) a measure of the recovery time required to return the building to full operation. An example resilience curve is shown in figure 1-2b.

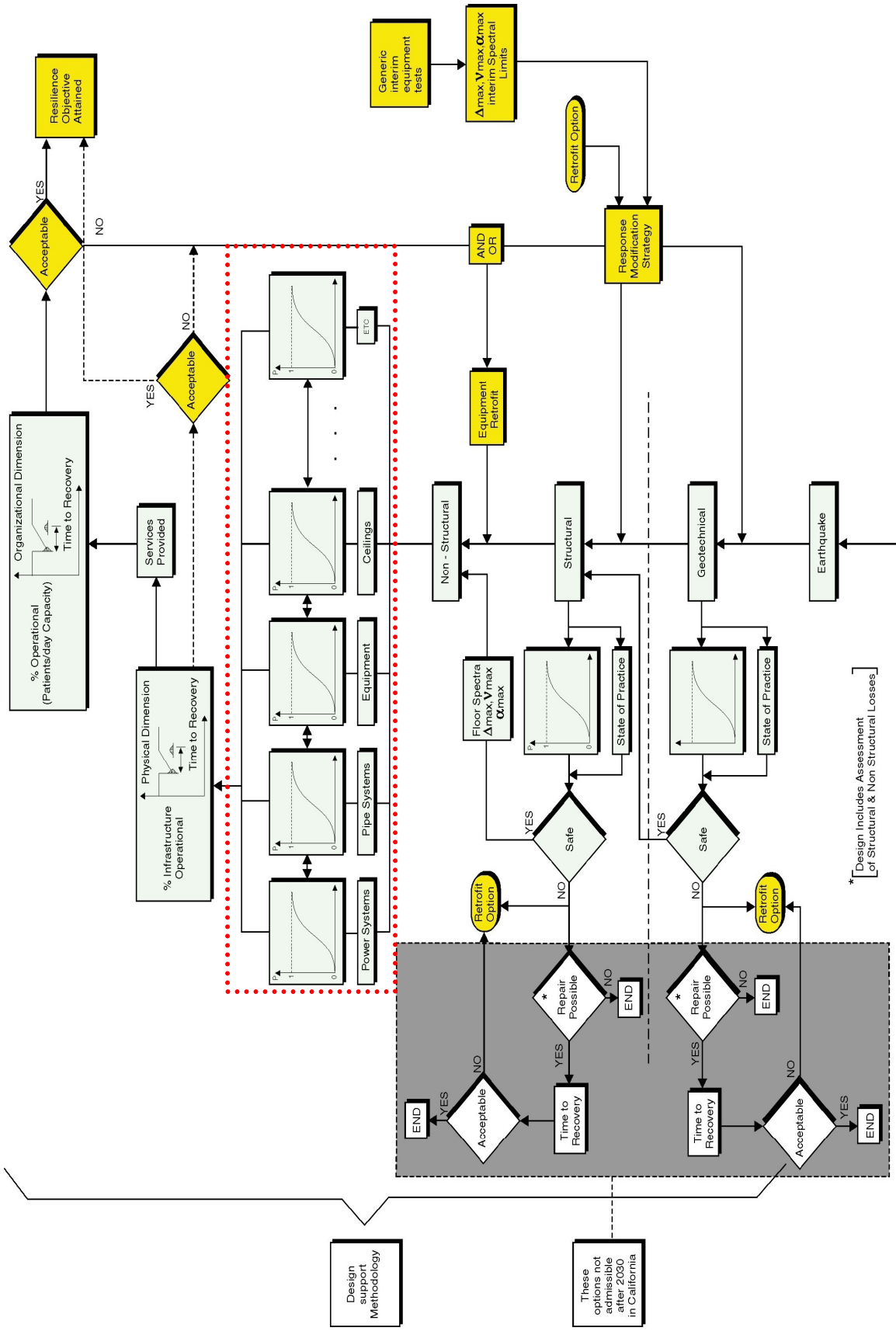

FIGURE 1-1: MCEER Fragility-Oriented Decision Support System

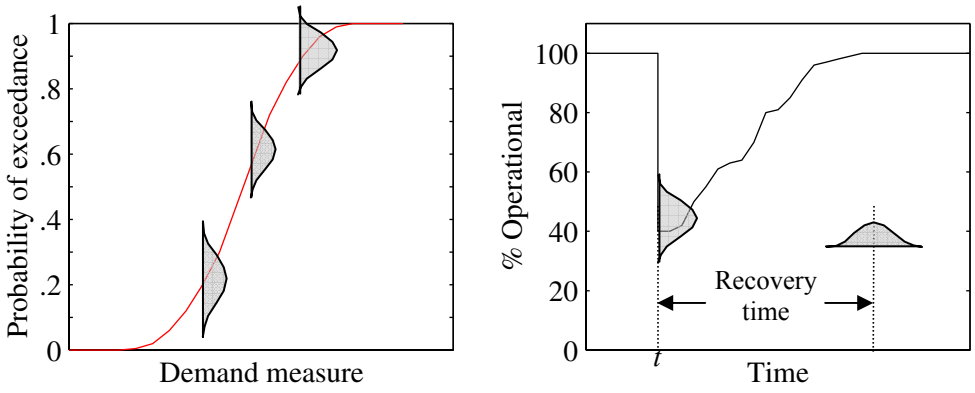

a. Fragility curve b. Resilience function

FIGURE 1-2: Sample Fragility and Resilience Functions

The figure shows the occurrence of a seismic event at time t that causes an immediate reduction in the operation of the building to 40% (median estimate) of maximum. The percent reduction for a given event is a random variable with an associated distribution. The time to full recovery (or 100% operation) that is shown in the figure is also a random variable with an associated distribution. Resilience can also be measured in terms of direct and indirect economic losses, which are performance metrics used in the ATC-58 project (www.atcouncil.org) and the PEER project (www.peer.berkeley.edu).

The decision-support framework of figure 1-1 is hospital building, building site and earthquake-scenario based. Focusing solely on the assessment components of the figure, the process begins with the selection of a hospital building (new or existing) and a characterization of the scenario earthquake hazard, represented in a format appropriate for structural analysis (e.g., a response spectrum for linear static and dynamic analysis; earthquake records for response-history analysis). The building is assumed to be fully defined in terms of its structural and nonstructural components and the fragilities of these components are assumed to be known.

The response of the structural framing to the prescribed seismic input will yield two key products. First, the structural analysis will enable the engineer to determine the probability that a structural limit state will be exceeded at the component or system level, where the limit state could be any number of response quantities such as system displacement, component deformation, floor acceleration and velocity. Second, the response of the structural framing-system will serve as the

seismic input to the non-structural components and facilitate the fragility-based assessment of these components. The nonstructural component fragility curves shown in the dotted box of figure 1-1 enable the calculation of the probability of exceeding a specified level of damage as a function of the seismic input, where the seismic input to the non-structural components corresponds to the response of the structural framing at the points of attachment of these components. Different framing-system response quantities will be critical for different non-structural components or systems (i.e., drift-sensitive or acceleration-sensitive).

Four key developments are needed to enable the use of the MCEER decision support systems for assessment of the resilience of hospital buildings, namely, 1) reliable methods of, and models for, nonlinear response-history analysis must be developed; 2) the structural and nonstructural component fragility curves must be sufficiently well populated; 3) damage-cost relationships (loss functions) must be developed for structural and nonstructural components as well as a method for the aggregation of loss over an entire building system; and 4) structural framing systems capable of limiting acceleration- and displacement-responses in nonstructural components and contents (NCCs) for a given level of earthquake shaking must be identified.

The studies described herein support the last of the four developments. Two broad classes of structural framings systems are studied, namely, 1) framing systems including traditional (conventional) moment-frame and bracing elements, and 2) framing systems equipped with protective systems. The reader is assumed to be familiar with the behavior of traditional framing systems. Introductory information on seismic protective systems is provided in Section 1.3 below.

1.3 Seismic Protective Systems

Protection of structural framing systems and nonstructural components against damage during design and maximum capable earthquake shaking motivated the development and implementation of seismic protective systems, assumed herein to include seismic isolation bearings and passive damping devices. The basic principles of operation of both isolation bearings and damping devices are well established and are summarized in books, journal articles and conference papers

(e.g., Bozorgnia and Bertero, 2004; Constantinou et al., 1998; Constantinou et al., 1999; FEMA, 2000b; Hanson and Soong, 2001; Naeim and Kelly, 1999).

In the United States, two classes of seismic isolation bearings are used in building construction: elastomeric and sliding. Three types of elastomeric (rubber) bearings are available: low-damping rubber (LDR), high-damping rubber (HDR) and lead-rubber (LR). The Friction Pendulum (FP) bearing is the common sliding isolation bearing for building construction. Some near-fault applications of seismic isolation have involved the use of supplemental fluid viscous dampers to control displacements across the isolation interface. Seismically isolated buildings are generally designed to restrict substantial (or all) inelastic action to the isolators in design-basis and maximum-capable earthquake shaking.

Two types of supplemental damping devices dominate the building market in the United States at this time: fluid viscous dampers and buckling-restrained (unbonded) braces. Buildings incorporating supplemental dampers are generally designed to restrict substantial (or all) inelastic action to the (disposable) damping devices in design-basis and maximum-capable earthquake shaking and eliminate damage to components of the gravity-load-resisting system.

1.4 Report Organization

This report contains 6 chapters, a list of references, and 2 appendices. Chapter 2 describes the state-of-practice and recent developments in performance-based earthquake engineering. Chapter 3 presents the MCEER West Coast Demonstration Hospital (Section 3.1), the OpenSees models that were created for the analysis of the hospital building (Section 3.2), and discusses the earthquake records from the SAC Steel Project, which were used for the response-history analysis of the building (Section 3.3). Analysis results are presented in Chapter 4. The responses of the base-isolated models of the hospital building are studied in more detail in Chapter 5. A summary and conclusions are provided in Chapter 6. Appendix A presents supplemental information on the construction of the hospital building. Appendix B presents ground motion data and analysis results from supplemental analyses performed using two ground motion bins from the MCEER hospital project.

CHAPTER 2

PERFORMANCE-BASED EARTHQUAKE ENGINEERING OF HOSPITALS

2.1 Hospital Construction

The focus of the MCEER decision-support system is hospital construction. Emphasis is placed on construction in California, where the seismic hazard is high and hospital design and construction is tightly regulated.

Hospital construction represents a unique type of building construction, wherein buildings are designed (albeit indirectly in many cases) for performance that is far superior to typical commercial and office building construction. Performance-based analysis and design tools are far more likely to be used for hospital construction than commercial and office building construction because a) hospital owners are required by law to provide higher levels of performance, b) hospital owners are long-term owners of buildings with a greater financial interest in the risk posed to (hospital) buildings by earthquakes, and c) hospital construction is significantly more expensive than commercial and office building construction (costs exceeding $400 per square foot as opposed to $100 to $150 per square foot).

Figure 2-1 displays the average percent investment in structural framing, nonstructural components and building contents for three types of building structures: office, hotel and hospital. In all cases, the investment in the structural framing is less than 20% of the total investment, and the percent investment in hospital construction is a mere 8% of the total. Clearly, performance-based analysis and design of hospital construction must explicitly address nonstructural components and contents (NCCs). Section 2.4 proposes a change in the design paradigm to shift emphasis to NCCs in hospital construction.

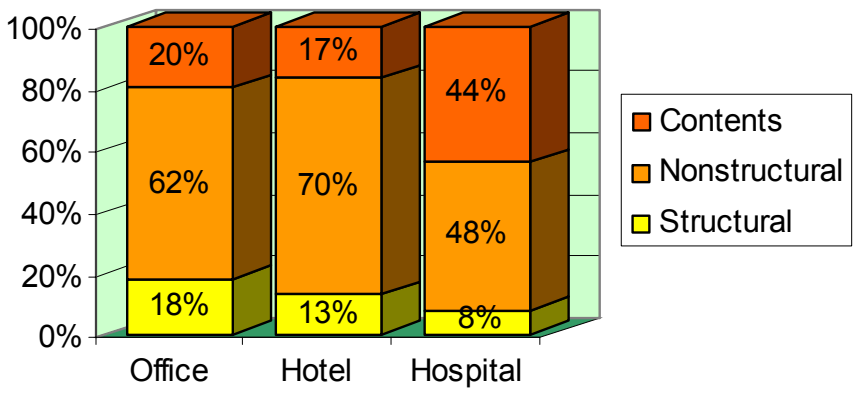

FIGURE 2-1: Investments in Building Construction (after E. Miranda)

Sections 2.2 and 2.3 below present summaries of the state of the practice in performance-based earthquake engineering (describing procedures in use at this time for the assessment and design of hospital construction) and recent developments in performance-based earthquake engineering, respectively.

2.2 State of Practice in Performance-Based Earthquake Engineering

Modern seismic codes such as the 2003 International Building Code (ICBO, 2004) and the 2003 *NEHRP Recommended Provisions for Seismic Regulations for Buildings and Other Structures* (FEMA, 2004) adopt a deterministic load and resistance factor design format, which compares demand and capacity as follows,

$$\sum_i \gamma_i D_i \le \phi_i C_i \tag{2-1}$$

where γ_i is a load factor, D_i is a demand action (dead load, earthquake effect, etc.), ϕ_i is a capacity reduction factor, and C_i is the capacity associated with the action D_i. Demands and capacities are expressed as forces. Randomness in the load effect is recognized using γ_i. Satisfaction of the force-based design equation of (2-1) together with the use of prescriptive details are assumed to deliver the intended performance, which is typically either life safety in a design earthquake or collapse prevention in a maximum earthquake. Such force-based design practice has been used in the United States for many years, and can be traced back to rudimentary procedures adopted following the 1906 San Francisco earthquake (ATC, 1995).

The poor performance of structural and non-structural components in buildings during the 1989 Loma Prieta earthquake and the 1994 Northridge earthquake prompted the earthquake engineering community into its first fundamental reassessment of force-based seismic design practice since the 1970s. Products of this assessment included SEAOC Vision 2000 (SEAOC, 1995), FEMA 273/274 (FEMA, 1997), FEMA 283 (FEMA, 1993), and FEMA 356 (FEMA, 2000b): all documents related to performance-based earthquake engineering. Vision 2000 identified issues related to the development of tools to enable structural engineers to design and deliver performance-oriented products. FEMA 283 presented an action plan for the development of performance-based earthquake engineering.

Guidelines and commentary for the seismic rehabilitation of buildings were published in FEMA 273/274, and re-published with modest amendments as FEMA 356. These Federal Emergency Management Agency (FEMA) documents presented deterministic performance-oriented procedures for seismic evaluation based on explicit displacement calculations, and extended work on displacement-based design that was initiated by Sozen and his graduate students at the University of Illinois at Urbana Champaign (UIUC) in the mid-1970s. The basic FEMA 356 design equation for ductile component actions took the form of (2-1) wherein demands and capacities are expressed, either directly or indirectly, in terms of deformations. The corresponding equation for brittle component actions takes the form of (2-1) wherein median estimates of force demand were compared with lower bound estimates of force capacity. The performance-oriented procedures of FEMA 273/274/356 represented a paradigm shift in the practice of earthquake engineering and shifted the focus of evaluation work from forces to deformations. However, these procedures remained deterministic and the reliability (level of confidence) of the resultant designs is unknown.

2.3 Developments in Performance-Based Earthquake Engineering

The past ten years has seen the widespread introduction of probability theory into the practice of structural earthquake engineering. (Note that probability theory was first introduced in the field of earthquake engineering by Cornell in a landmark paper in 1968 related to probabilistic seismic

hazard assessment.) Advances prior to the Northridge earthquake include work on redundancy published by the Applied Technology Council (ATC, 1995). Other advances are described below.

2.3.1 SAC Steel Project

Following the 1994 Northridge earthquake and the formation of the SAC Joint Venture, significant new work was undertaken on the application of probability theory to performance assessment of steel moment frame building structures responding in the nonlinear range. Funding was provided by the Federal Emergency Management Agency (FEMA).

Cornell et al. (2002) extended the displacement-based checking procedures of FEMA 273/274/356 and presented a probabilistic framework for the seismic analysis and design of steel moment-resisting frames. The framework presented by Cornell et al. (2002) is based on the expression of a performance objective as the probability of exceeding a specified performance level. The framework facilitates the development of quantitative statements of confidence regarding the likelihood of the performance objective being met. The formulation involves the characterization of three random variables: ground shaking intensity, displacement demand, and displacement capacity, where the variables are denoted by S_a, D, and C, respectively. The ground shaking intensity is characterized using the commonly adopted measure of spectral acceleration, S_a. Displacement demand (drift) and displacement capacity are calculated at the story level. Figure 2-2 from Cornell et al. shows the basic components of the formulation. The paper also provides a systematic and holistic treatment of the (epistemic) uncertainty present in the three random elements identified above. The paper introduces the epistemic uncertainty in each of the elements and deduces the subsequent implied uncertainty in the calculation of the annual probability that the performance level (in this instance drift capacity) is exceeded.

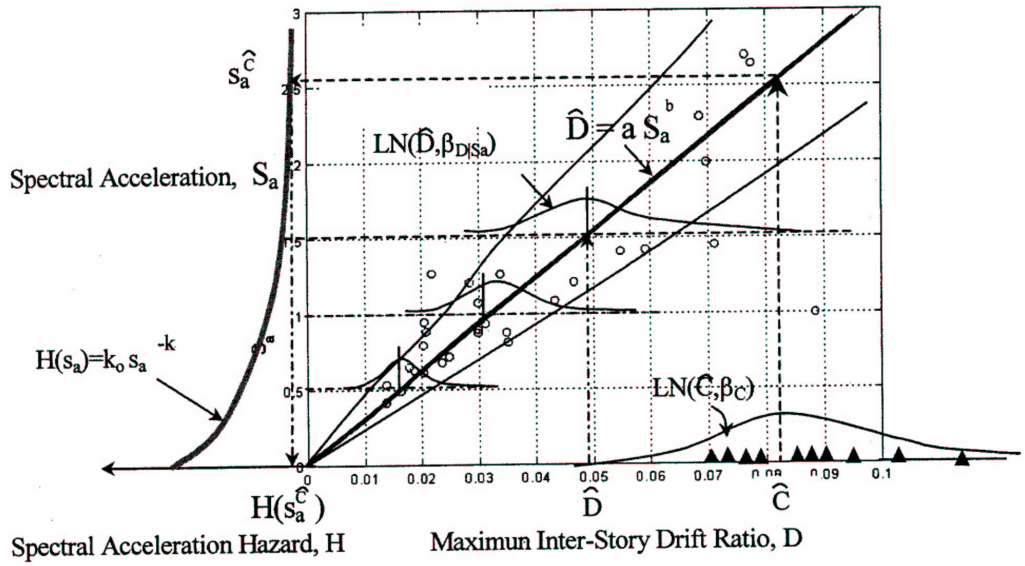

FIGURE 2-2: Basic Elements of Performance-Based Design (Cornell et al., 2002)

2.3.2 ATC-58 and PEER projects

The ATC-58 project is funded by the Federal Emergency Management Agency for the purpose of implementing the *second* generation of tools for performance-based earthquake engineering design. Most of the technical underpinnings of the ATC-58 work are provided by researchers affiliated with the Pacific Earthquake Engineering Research (PEER) Center (Moehle, 2003): a National Science Foundation-funded earthquake engineering research center, similar to MCEER. Information on the ATC-58 and PEER projects can be found at www.atcouncil.org and www.peer.berkeley.edu.

As part of the ATC-58 project, Hamburger (2003) developed a probabilistic loss modeling process using a fragility framework. A general outline of the process proposed by Hamburger (2003) is illustrated in figure 2-3 and is most similar to the PEER framework (Moehle, 2003). The MCEER resilience framework shown in figure 1-1 could be considered to be a scenario-based version of the ATC-58 framework.

The ATC-58 (and PEER) performance-based design process begins with the selection of a performance objective. In the *first* generation of performance-based documents such as FEMA 356 (FEMA, 2000b) and Vision 2000 (SEAOC, 2000), performance objectives are described as the marriage of a performance level and a hazard level, where performance levels are qualitative descriptions of damage. In contrast, Hamburger uses an allowable level of risk as a performance objective, where risk can be quantified in a number of different ways, including but not limited to, average annual cost of restoration, potential loss of life, and time to restore the facility to service.

The development of a preliminary design is not discussed in the paper by Hamburger. Current methods, such as that of 2003 NEHRP (FEMA, 2004), could be used to develop trial designs for the iterative process of figure 2-3. Verification that the trial design will satisfy the performance objective(s) to a specified level of confidence is the core of the process, and is illustrated in figure 2-3 by that part of the procedure contained within the box. Procedures for seismic hazard characterization are well established, and Hamburger does not introduce new concepts for their development. Hamburger emphasizes the importance of selecting an intensity measure (IM) that is both useful and efficient, where the intensity measure must be compatible with the selected analysis method, correlate well with structural (and nonstructural) response data, and be predictable as a function of the source, travel path, and site characteristics.

The fragility curves of figure 1-2 (structural and nonstructural) can be generated in two ways: (1) Monte Carlo simulation in which each source of uncertainty is treated as a random variable, and multiple analyses using different combinations of the assigned values are performed at each level of hazard, and (2) a single analysis at each intensity level to establish a median estimate of response, and the subsequent assumption of a statistical shape for the calculation of a probability of exceedance. Whichever method is used, the development of fragility curves requires the designation of a damage level, and thus a measure of damage. The damage to the structural system can either be recorded in conventional response quantities, such as inter-story drift, plastic

rotation, element ductility, or strength demand, or recorded as a numerical damage index (e.g., Park and Ang, 1985).

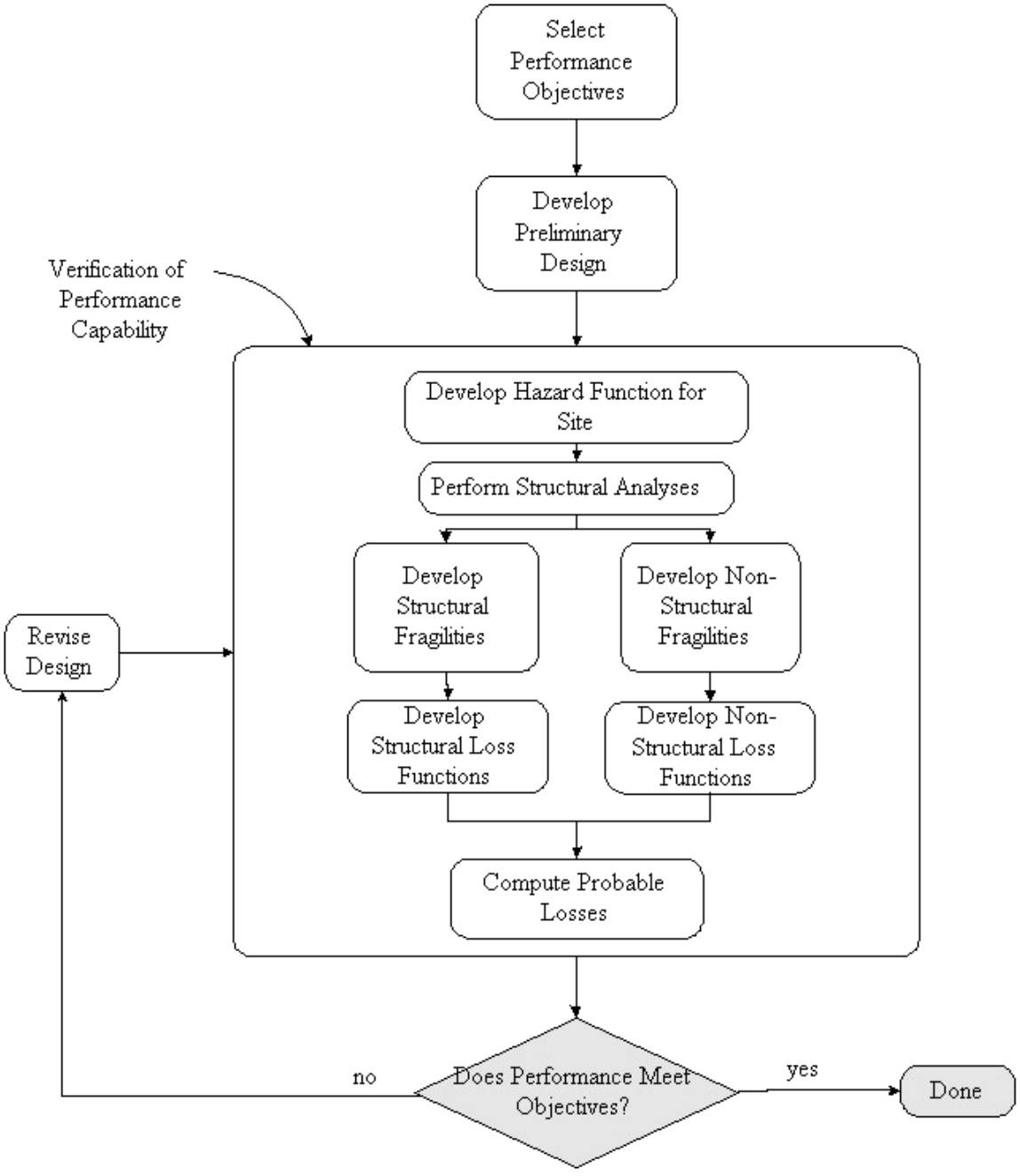

FIGURE 2-3: Fragility Framework for Loss Computation (adapted from Hamburger)

A key development of the work described by Hamburger (2003) is the development of loss estimates from available fragility and hazard data. Loss functions are the probability of various levels of loss given a level of damage. Loss can be expressed in any parameter that is applicable to the function of the building (e.g., repair cost, lives lost, hours of service lost) and can be quantified by postulating damage to the building. Hamburger demonstrated the process for two example parameters, namely, the mean loss in dollars, and the probable maximum loss (PML) in dollars, given the scenario that an earthquake with the exceedance probability of 10% in 50 years has occurred.

Hamburger (2003) provided a snapshot view of the state of performance-based design. This paper served as the basis for FEMA 445, *Program Plan for Development of Next-Generation Performance-Based Seismic Design Guidelines for New and Existing Buildings* (FEMA, 2005), which presents the proposed two-phase plan and schedule for developing and organizing tools needed for the *second* generation of performance-based design in the ATC-58 project. Phase 1 will continue to develop performance assessment procedures; Phase 2 will develop design tools. The work to be completed in Phase 2 serves as part motivation for the studies described in this report. A crucial step in the design process is the development of a preliminary design. Selection of an appropriate preliminary design is critical to effectively and efficiently implementing the performance-based design process by avoiding multiple design iterations.

Hamburger (2003) included the development of fragilities and loss functions for nonstructural components and contents (NCCs) into the ATC-58 framework, but did not describe methods to integrate and aggregate the fragilities. Porter and Kiremidjian (2000) presented one strategy for aggregating structural and nonstructural fragilities but noted that the procedures did not apply to cases where the structural framing system suffered widespread damage.

Miranda and Taghavi (2003) proposed a methodology for estimating the expected annual loss for a building as a summation of the annual expected losses in each individual component using the PEER framework described above. The probability that the loss in the component will exceed a

threshold level given that it is in a selected damage state is calculated from a cost function, where the function is a probability distribution of repair/replacement cost for a certain damage state. A cost function is required for each component. A taxonomy was proposed to define appropriate damage states.

2.4 Fragility Data

A major obstacle to the development and implementation of the MCEER, PEER and ATC-58 performance-based design frameworks is the lack of usable component fragility data, especially for non-structural components and contents (NCCs). Some component-specific fragility data are now available for NCCs such as ceiling systems (Badillo, 2003), partition walls (Restrepo, 2004), laboratory equipment (Hutchinson, 2003), and book shelves (Filiatrault, 2004) but these data must be used and interpreted with care for the reasons given by Badillo (2003).

Nonstructural components and contents in most buildings, and always in hospitals, are installed as part of integrated systems. For example, sprinkler heads are generally installed in the same plane as ceiling tiles and so it is the fragility of the integrated system that must be established in addition to the fragility of the stand-alone components. No reliable procedures exist at the time of this writing to combine the fragilities of independent systems and likely detailed system testing will be required to provide the necessary fragility data.

2.5 Changing the Design Paradigm

If a goal of performance-based earthquake engineering is to protect financial investments by minimizing total cost (including construction cost, annual maintenance cost and annualized earthquake-damage-related cost), close attention must be paid to those parts of a building in which the greatest investment is made (Astrella and Whittaker, 2003). Figure 2-1 showed that nonstructural components and contents (NCCs) represent the greatest investment in most buildings and in excess of 90% of the total investment in hospital construction.

Earthquake-damage-related cost includes the reparation and replacement of damaged components and the cost associated with loss of function of the building. NCCs are not only expensive to repair and replace, but many components are essential to the operation of a building. Traditionally, structural engineers have paid scant attention to NCCs because their design and detailing had not formed part of the structural-engineering scope of work. In those cases where structural engineers have designed and detailed NCCs, the components have been analyzed and designed (albeit indirectly) for the output of the structural framing.

Such an approach is inappropriate in a performance-oriented design framework. The performance-based design process should focus first and foremost on the most significant investments in the building, namely, the nonstructural components and contents. In a process like that shown in figure 2-3, NCCs should be considered in the development of a preliminary design. That said, "…Presently, the engineer has little guidance on how to develop an appropriate preliminary design to meet a specified performance objective. . ." (FEMA, 2005).

The research work described in this report takes first steps towards considering the demands on NCCs in the development of a preliminary design by investigating the effect of framing system type on the amplitude and distribution of demands on NCCs. The remaining chapters of this report describe dynamic analyses of 11 mathematical models that represent two acute care facilities and a number of retrofit schemes for each. Each model is analyzed for three levels of seismic hazard. Each level of hazard is characterized by a bin of 20 ground motions. Use of a suite of ground motions to characterize a single level of hazard creates a distribution of response values (e.g., maximum displacements, maximum accelerations and floor acceleration spectra) that considers the randomness in ground motion. Response data from the 11 models were harvested to understand the distributions of demand on NCCs, which is determined by the response of the points of connection of the NCCs to the structural framing. Distributions of maximum floor acceleration, floor acceleration spectra and story drift are presented together with performance points and performance spaces.

CHAPTER 3

MCEER DEMONSTRATION HOSPITAL

3.1 MCEER Demonstration Hospital

The MCEER Demonstration Hospital is located in Northridge, California. It was designed in 1974 to conform to the 1970 Uniform Building Code (ICBO, 1970). The hospital is a four-story steel frame structure with a penthouse. The plan dimensions of the building are 17.25 m x 83.8 m (56.5 ft x 275 ft). The typical story height is 3.8 m (12.5 ft), except for the ground floor, which is 4.1 m (13.5 ft) in height. These dimensions do not include the entryway, which extends North from the front of the building.

The steel frame of the hospital is composed of thirteen transverse frames in the North-South (N-S) direction, and four longitudinal frames in the East-West (E-W) direction. All structural steel is Grade A36 except for those members that are part of the moment-resisting frames, which are composed of ASTM A572 Grade 50 steel.

The MCEER Demonstration Hospital uses moment resisting frames to provide lateral load resistance. Figure 3-1 shows a half-plan view of a typical floor in the building. In the E-W direction, the two moment-resisting frames are located on column lines 2 and 5. The four moment resisting frames in the N-S direction are located on column lines B, F, J, and N, noting that lines J and N are not shown in figure 3-1. Moment resisting frames are denoted in figure 3-1 by arrowheads that indicate rigid connections. Typical rigid beam flange-column flange and rigid beam-column web connections are shown in figure 3-2, both are welded flange, bolted web connections. The majority of the rigid connections are beam-column flange connections. These connections are detailed with continuity plates to prevent flange distortions and column web crippling and 4.45 cm (1.75 in.) doubler plates to increase the strength of the panel zone.

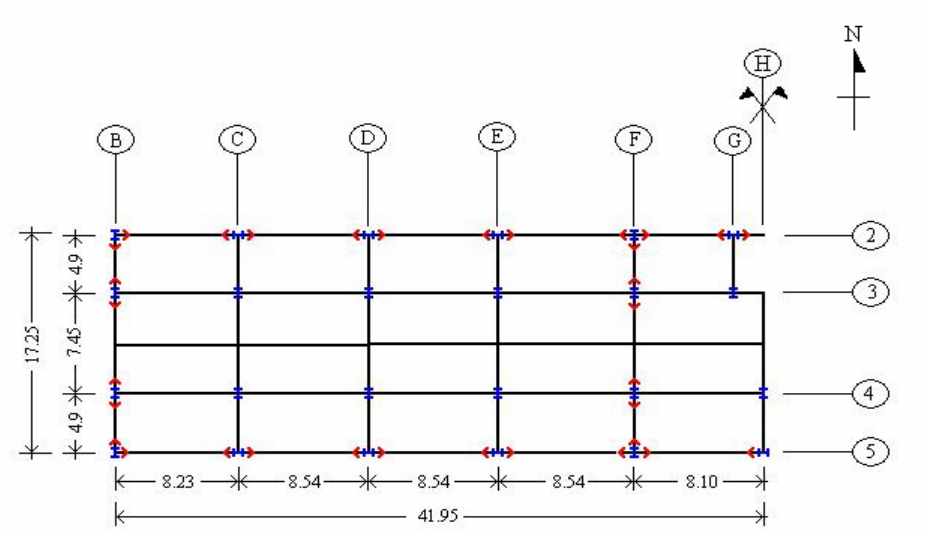

FIGURE 3-1: Half Plan View of Structural Framing System of the MCEER Demonstration Hospital (units in meters)

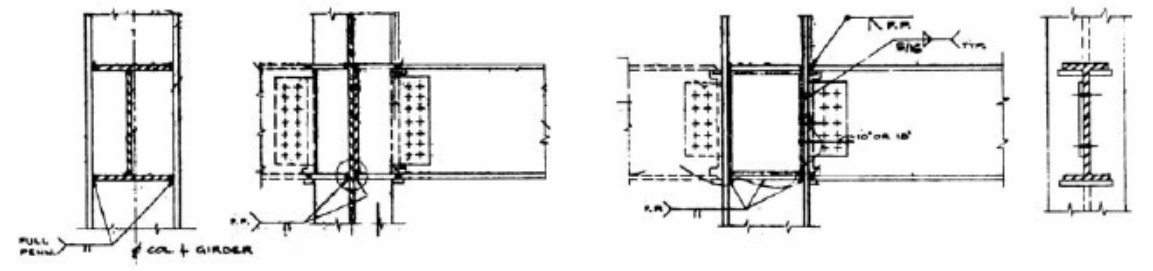

FIGURE 3-2: Typical Rigid Connection Details

Gravity loads are supported by 14 cm (5.5 in.) thick reinforced concrete slabs on metal decking, which span between the longitudinal beams. A cross-section of the gravity load carrying system is shown in figure 3-3. Beam-column and girder-column connections are bolted shear tab connections for members with a depth less than 61cm (24 in.) and bolted top and seat angle connections for beams with a depth of 61 cm or more. Beam-girder (non-moment) connections are bolted shear-tab connections. Typical connections are shown in figure 3-4 for beam depths (d_b) less than 24 inches.

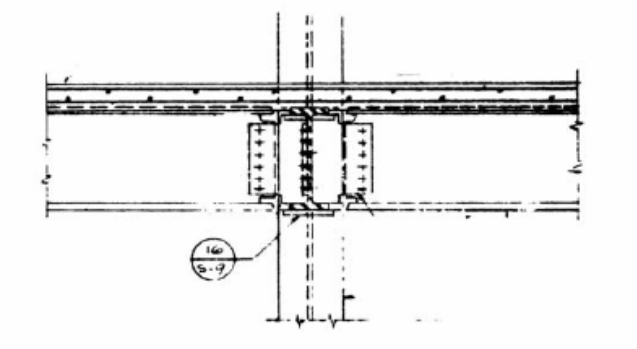

FIGURE 3-3: Typical Cross-Section Through the Flooring System

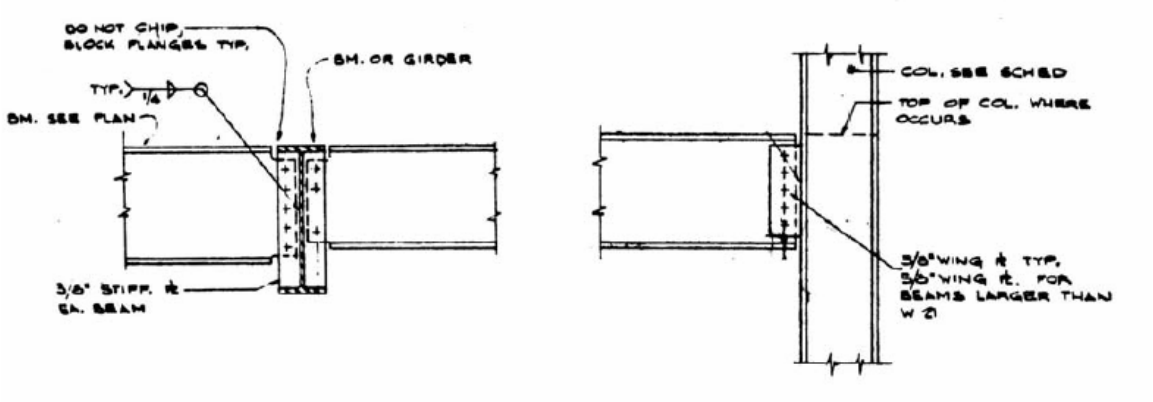

FIGURE 3-4: Non-Moment Beam-Girder and Beam-Column Connections (d_b<24")

Column bases are supported by individual piled footings, which consist of a pile cap atop four tapered piles. A typical pile cap has plan dimensions of 1.7 m x 1.7 m (5.5 ft x 5.5 ft) and a depth of 1.1 m (3.5 ft.). Piles typically reach a depth of 14.6 m (48 ft.). All columns are welded to base-plates. Every base-plate sits atop a 3.8 cm (1.5 in.) layer of dry pack grout, and is connected to the pile cap with four anchor bolts at its corners. Those columns that are part of the moment-resisting frames are embedded in 137 cm (54 in.) deep concrete grade beams that are supported on pile caps. A cross-section through one of the grade beams is shown in figure 3-5. Columns that are not part of the moment-resisting frames are engaged by a 35.5 cm (14 in.) thick slab-on-grade, which can also be seen in the cross-section of figure 3-5.

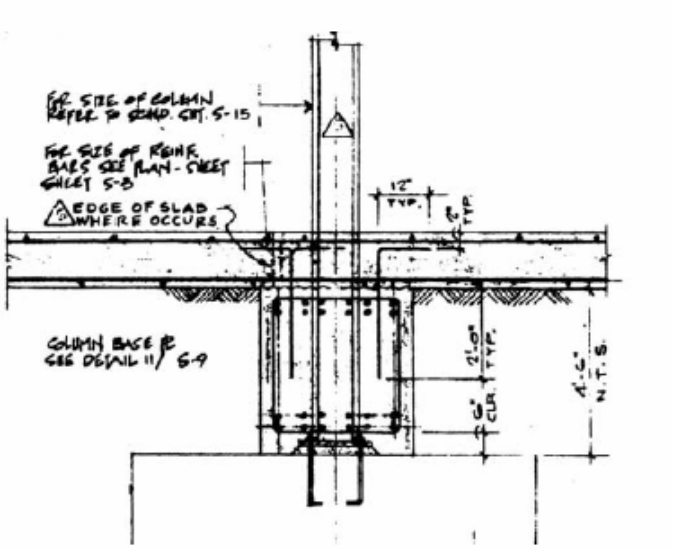

FIGURE 3-5: Typical Grade Beam Cross-Section at Base of MRF Columns

3.2 Baseline and Retrofit Hospital Models

3.2.1 Open System for Earthquake Engineering Simulation (OpenSEES)

Modeling and analysis was undertaken using the program OpenSEES (opensees.berkeley.edu). OpenSEES is a general purpose program for the 3D analysis of structures. This program contains a model builder and a computational framework. Models can be created using TCL procedures, which allows the program to be used like a language. OpenSEES is object oriented and allows for the seamless addition of elements to, or removal of elements from, existing models.

Steel column and beam elements were defined by force-deformation properties in each of the six degrees of freedom. Moment-curvature in the strong and weak directions were assigned bilinear hysteretic properties while axial, torsional and shear force-deformation relationships were assumed elastic. Force-deformation relationships were calculated using best estimate steel yield and ultimate strengths (Frank, 1996). Beams and columns were modeled with the *beamWithHinges* element that uses a lumped plasticity model. To model a pinned connection between a beam and a column in the non-moment-resisting frames, the beam hinge within the element was assigned negligible stiffness.

3.2.2 Baseline Models

Two simplified baseline mathematical models for the hospital building described in Section 3.1 were prepared for analysis. The first baseline model, West Coast 1970 (denoted WC70 herein), represents the in-service building that was designed in 1974 using the 1970 Uniform Building Code (ICBO, 1970). The second model is a 1960s-era version of WC70 and is denoted WC60 (West Coast 1960s) herein. WC60 is weaker and more flexible than WC70 because the 1970 Uniform Building Code (UBC) imposed drift limits that were not part of previous codes. Satisfaction of these limits led to significant increases in component strength and stiffness over those required for strength alone. A number of retrofit strategies were applied to these two base models to judge the influence of choice of structural framing on the demands on non-structural components and contents.

A number of minor geometric changes were made to the hospital building to impose symmetry and regularity and improve computational efficiency. The mathematical models were created with half the floor area of the actual structure (half the length in the East-West direction) and do not include the entryway or the penthouse. For symmetry, the building was modeled with moment frames at the exterior column lines. In the transverse direction (N-S), the moment-resisting frame (MRF) originally from line F (figure 3-1) was used as the typical MRF. The span of all longitudinal bays was set at 8.54 m (28 ft). Because the analyses focus on the effects of lateral loading, the longitudinal beams that span from girder to girder were omitted from the model. The gravity loads associated with those beams were added to the remaining framing. The design gravity dead (D) and live (L) loads are listed in table 3-1. The masses used for evaluation of horizontal earthquake shaking effects were calculated using the values in table 3-1 and the load case of 1.0D+0.5L.

TABLE 3-1: Gravity loads

Dead loads		Live loads	
Floors	4.77 kN/m^2 (99.6 psf)	Floors	1.92 kN/m^2 (40.0 psf)
Roof	4.59 kN/m^2 (95.9 psf)	Roof	0.58 kN/m^2 (12.0 psf)
External Walls	2.50 kN/m^2 (52.2 psf)		
Structural Frame	Self weight		

All member lengths were defined using centerline dimensions and rigid offsets were not considered. Member schedules and drawings of the two models can be found in figures A1-1 through A1-6 for WC70 (for Model M3, see below) and A1-7 through A1-9 for WC60 (Model M6, see below) in Appendix A. Figure 3-6 provides the terminology used to identify the different levels and stories in the models used throughout this report.[1]

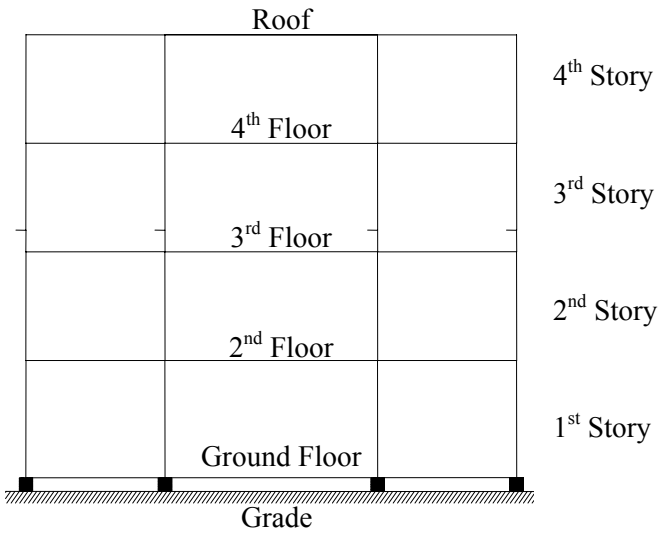

FIGURE 3-6: Floor and Story Designation for the Levels of all Models

[1] The ground floor and grade levels are identical for models M3, M6, M7, M8 and M9, but are separated by seismic isolators for models M10 through M15. See Table 3.2 for more details.

The baseline models were assigned 5% Rayleigh damping. The damping in each model is discussed further below. The dynamic properties of models M3 and M6 are presented in table 3-2 and figures 3-7 and 3-8.

3.2.3 Retrofit Models

Ten retrofitted variants of Models M3 (WC70) and M6 (WC60) were created to study the impact of framing-system choice on demands on nonstructural components and contents (NCCs). Six isolation systems were developed as retrofit schemes for WC70 (M3). Four retrofit schemes were developed for the WC60 (M6) structure using supplemental damping devices.

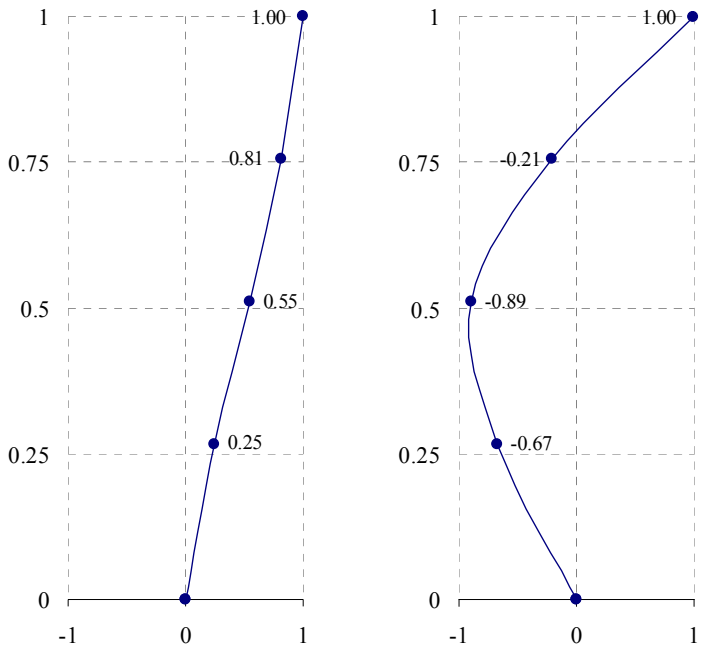

a. 1st mode b. 2nd mode

FIGURE 3-7: Mode Shapes for Model M3

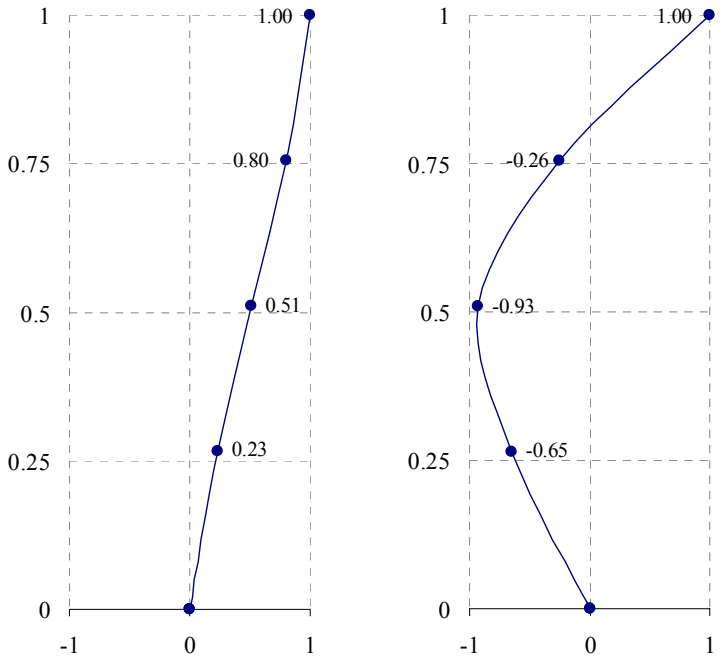

a. 1st mode b. 2nd mode

FIGURE 3-8: Mode Shapes for Models M6, M9 and M10

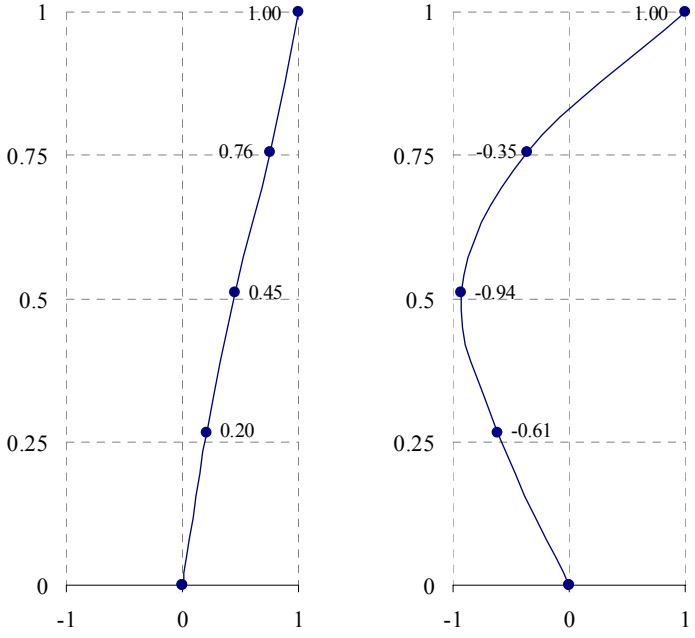

a. 1st mode b. 2nd mode

FIGURE 3-9: Mode Shapes for Model M7 and M8

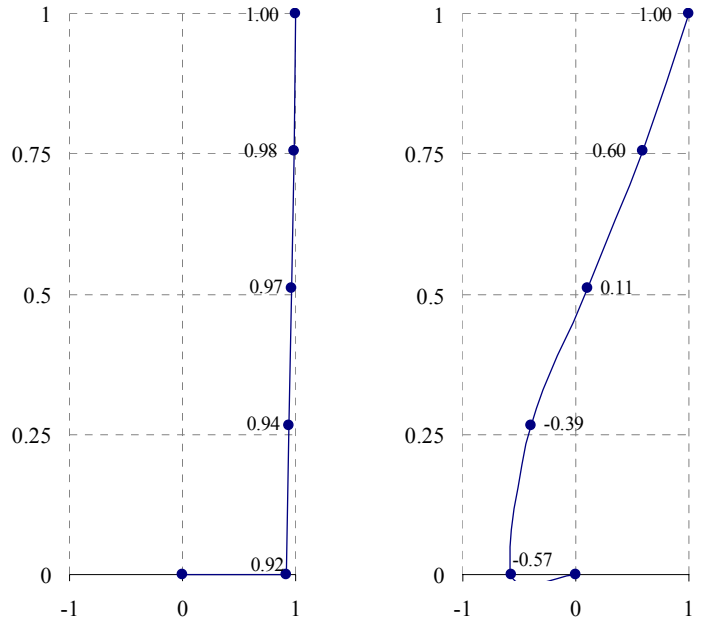

a. 1st mode b. 2nd mode

FIGURE 3-10: Mode Shapes for Models M11, M12 and M15

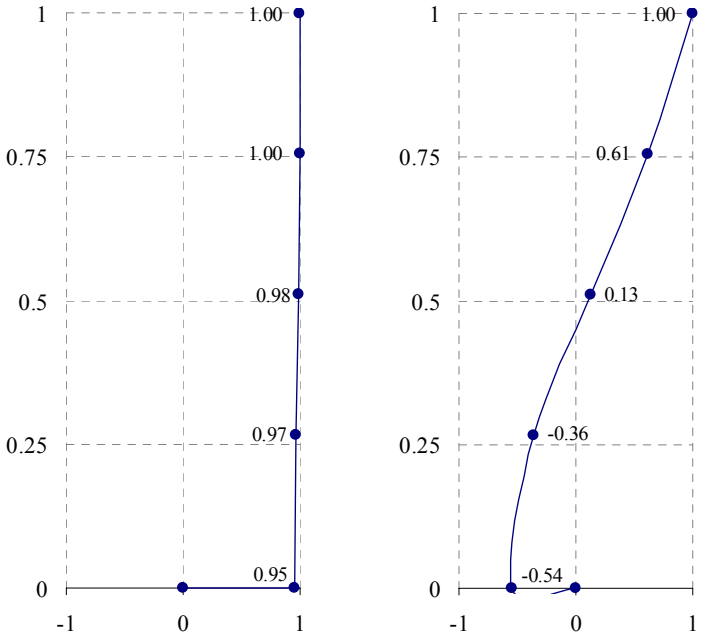

a. 1st mode b. 2nd mode

FIGURE 3-11: Mode Shapes for Models M13, M14 and M16

TABLE 3-2: Description of mathematical models

Model	Description	T_1 [1] (s)	T_2 [1] (s)
M1	Baseline model of 1970s in-situ building; best-estimate model for non-moment-resisting connections.	0.70	0.24
M2	Similar to M1 except rigid connections used for non-moment-resisting connections.	0.68	0.23
M3	Similar to M1 except pinned connections used for non-moment-resisting connections.	0.70	0.24
M4	1960s variant of M1: design drift limits of M1 not imposed.	1.74	0.60
M5	Similar to M4 except rigid connections used for non-moment-resisting connections.	1.58	0.58
M6	Similar to M4 except pinned connections used for non-moment-resisting connections.	1.81	0.61
M7	M6 augmented with buckling restrained braces (BRBs) to provide approximately a 300% increase in lateral stiffness. Braces have a yield stress of 250 MPa (36 ksi)	0.97	0.37
M8	M6 augmented with BRBs to provide approximately a 300% increase in lateral stiffness. Braces have a yield stress of 140 MPa (20 ksi)	0.97	0.37
M9	M6 equipped with fluid viscous dampers (FVDs) to provide approximately 25% of critical damping in the first mode.	1.81	0.62
M10	M6 equipped with fluid viscous dampers (FVDs) to provide approximately 40% of critical damping in the first mode.	1.81	0.62
M11	M3 equipped with viscoelastic seismic isolation bearings; isolated period is 2.5 seconds; approximately 10% of critical damping in the first mode.	2.60	0.47
M12	M3 equipped with viscoelastic seismic isolation bearings; isolated period is 2.5 seconds; approximately 20% of critical damping in the first mode.	2.60	0.47
M13	M3 equipped with viscoelastic seismic isolation bearings; isolated period is 3.5 seconds; approximately 10% of critical damping in the first mode.	3.57	0.47
M14	M3 equipped with viscoelastic seismic isolation bearings; isolated period is 3.5 seconds; approximately 20% of critical damping in the first mode.	3.57	0.47
M15	M3 equipped with coupled bilinear seismic isolation bearings: $Q_d = 0.06W$; second-slope isolation period is 2.5 seconds; isolator yield displacement is 25 mm.	2.60[2]	0.47
M16	M3 equipped with coupled bilinear seismic isolation bearings: $Q_d = 0.06W$; second-slope isolation period is 3.5 seconds; isolator yield displacement is 25 mm.	3.57[2]	0.47

1. First and second mode period in transverse (short) direction.
2. Period calculation based on second slope (post-yield) isolator stiffness.

A summary of the baseline and retrofit models is presented below. The dynamic properties of the models are listed in table 3-2 and figures 3-7 through 3-11 present the first two mode shapes of each model.

- M1, M2 and M3: All three of these models represent WC70. The three models differ from one another in the modeling of the joints of the non-moment resisting frames. Model M1 uses a semi-rigid bilinear model for these joints, Model M2 uses a perfectly rigid connection model, and Model M3 uses a simple pinned connection model. Only the analysis results from M3 are presented in this report. Model M3 was assigned 5% Rayleigh damping in the first two lateral modes of vibration in the N-S direction.
- Models M4, M5 and M6: These three models represent WC60, and differ from one another in the same manner that Models M1, M2 and M3 differ from one another. Model M6 was assigned 5% Rayleigh damping in the first two lateral modes of vibration in the N-S direction.
- Models M7 and M8: These models are Model M6 retrofitted with Buckling Restrained Braces (BRBs). The braces were placed diagonally in the outside bays of the N-S running moment frames. The BRBs were modeled in OpenSEES as non-buckling truss elements with bilinear hystereses. The braces were designed for a target drift of 1% in 10/50 shaking using the procedures set forth in FEMA 356 (FEMA, 2000b). This drift corresponds to a lateral stiffness of the braced frame of approximately 44 kN/mm. The brace areas were assumed to decrease from the bottom story to the top story by a prescribed ratio and optimized using nonlinear static analysis in an attempt to obtain brace yielding in all stories. The braces of Models M7 and M8 were assigned yield strengths of 250 MPa (36 ksi) and 140 MPa (20 ksi), respectively[2]. Models M7 and M8 were assigned 5% Rayleigh damping in the first two lateral modes of vibration in the N-S direction.
- Models M9 and M10: These models are Model M6 retrofitted with fluid viscous dampers. The dampers have the same locations as the braces in Models M7 and M8. The

[2] Low-yield steels (20 ksi) have been tested in Japan for use in hysteretic dampers (Nakashima, 1995).

dampers in both M9 and M10 were designed to limit drifts to approximately 1% for 10/50 shaking following the equations of Section 9 in FEMA 356 (FEMA, 2000b). The design of Model M9 used the damping coefficient(s) of Ramirez (2000) and resulted in a damping ratio of approximately 25% of critical. The design of Model M10 used the damping coefficient(s) of FEMA 356 and resulted in a damping coefficient of 40% of critical. The frames of Models M9 and M10, excluding the dampers, were also assigned 5% Rayleigh damping in the first two modes of vibration in the N-S direction. The viscous dampers were designed to *add* 20% and 35% viscous damping in the first mode for Models M9 and M10, respectively. The procedures set forth in Chapter 9 of FEMA 356 (FEMA, 2000b) were used to compute the damping constant, *C*, for the viscous dampers.

- Models M11, M12, M13 and M14: The first four isolated models represent M3 retrofitted with linear viscous isolation bearings, which have been used in past studies to model low-damping rubber (LDR) and high-damping rubber (HDR) bearings[3]. A simple spring/dashpot model was used to represent the isolation systems in these models. The ground and the ground floor are defined by a different set of nodes, but are located at the same vertical position (as is evident in figures 3-10 and 3-11). A rigid diaphragm was added to the ground floor to constrain the displacement of each isolator. The isolation systems of M11 and M12 were designed to have a period of 2.5 seconds and the isolation systems of M13 and M14 were designed to have a period of 3.5 seconds[4]. The superstructures of Models M11 through M14 were assigned 5% Rayleigh damping in the first and third lateral modes of vibration in the N-S direction. The damping constants for the isolator dashpots in Models M11 and M13 were selected to provide 10% viscous

[3] In the United States, seismic isolation is used for high-performance structures such as hospitals and mission-critical structures. Superstructures in isolated buildings are designed to remain essentially elastic for maximum-capable earthquake shaking. To maintain such an approach, the strength of M6 would have to be increased substantially. To avoid preparing a strengthened version of M6 for use with the isolation systems, Model M3 was used as the superstructure model.

[4] The periods of 2.5 and 3.5 seconds assume a rigid superstructure, that is, the only source of flexibility is the isolators.

damping; the damping constants for the isolator dashpots in Models M12 and M14 were selected to provide 20% viscous damping.

- Model M15 and M16: M15 and M16 were isolated using coupled bilinear isolation bearings, which have been used typically to model lead rubber and Friction Pendulum bearings. The isolation system of M15 was assigned a second slope period of 2.5 seconds and the isolation system of M16 was assigned a second slope period of 3.5 seconds[5]. The characteristic strength or zero-displacement force intercept (Q_d) of both systems was set at $0.06W$, where W is the supported weight. The superstructure of Models M15 and M16 were assigned 5% Rayleigh damping at the first and third lateral modes of vibration in the N-S direction.

3.3 Ground motion records

3.3.1 SAC Steel Project ground motions

Seismic demands on NCCs in the 12 buildings were assessed by nonlinear response-history analysis in the transverse (north-south) direction only. The earthquake histories used for the response-history analysis were those generated for a NEHRP Soil Type S_D (firm soil) site in Los Angeles as part of the SAC Steel Project (Somerville et al. 1997). Three bins of 20 histories were developed, each representing a different probability of exceedance: 50% in 50 years (hereafter denoted 50/50), 10% in 50 years (10/50), and 2% in 50 years (2/50). The ground motion histories selected by Somerville et al. for the 50/50 and 10/50 bins are actual records. These records were selected based on a deaggregation of the seismic hazard for the region. Some of the records included in the 2/50 bin are broadband strong-motion simulations. The ground motions in each of the three bins were scaled to minimize the weighted sum of the squared error between the USGS target spectrum and each ground motion (Somerville et al. 1997).

[5] The second-slope stiffness of the bilinear isolators was back-calculated from the second-slope period based on a) the supported mass, and b) a rigid superstructure.

The response spectrum for each history in the 50/50 bin is shown in figure 3-12a. The median, 16th and 84th percentile spectra are shown in figure 3-12b together with the target spectral ordinates (shown circled) at periods of 0.3, 1, 2 and 4 seconds, to provide the reader with information on the variability in the earthquake histories used in the response-history analysis. Similar figures are shown for the 10/50 bin and the 2/50 bin in figures 3-12c through 3-12f. Additional information about the variability of the shaking characteristics of the ground motions within each bin is provided in table 3-3 in the form of coefficients of variation at periods that are relevant to the results presented in this report. Figure 3-13 presents the median acceleration and displacement spectra for each bin.

TABLE 3-3: Coefficients of variation in spectral acceleration at selected periods

	Bin		
Period (sec)	50/50	10/50	2/50
0.24	0.47	0.50	0.48
0.37	0.67	0.50	0.43
0.47	0.58	0.41	0.41
0.61	0.70	0.39	0.31
0.71	0.90	0.38	0.35
0.97	0.64	0.32	0.38
1.81	0.36	0.36	0.40
2.61	0.37	0.36	0.45
3.57	0.58	0.42	0.43

3.3.2 MCEER ground motions

Analysis was also performed using two bins of ground motions from the Multidisciplinary Center for Earthquake Engineering Research (MCEER) hospital project. These ground motions were developed by Wanitkorkul and Filiatrault (2005) for a site in Northridge, California. These ground motions represent a near-fault site condition and are composed of a low-frequency

component, or pulse, and a high-frequency component that was developed using the Specific Barrier Model (Papageorgiou and Aki, 1983). Scaling was performed only on the high frequency component to minimize the sum of the square of the errors between the mean spectrum for a bin and the uniform hazard spectrum at periods of 0.1 s, 0.2 s, 0.3 s, 0.5 s, and 1 s. The low frequency components were added back in after scaling. Four ground motion bins were created representing probabilities of exceedence of 20% in 50 years (2/50), 10% in 50 years (10/50), 5% in 50 years (5/50), and 2% in 50 years (2/50).

Analysis was performed using only the 10/50 and 2/50 bins because a direct comparison can be made with the results from the corresponding SAC ground motion bins presented above. Acceleration response spectra for the individual ground motions of the two selected MCEER bins are presented in figure B1-1a and B1-1c in Appendix B. Median, 16th percentile and 84th percentile spectra for each bin are presented in figures B1-1b and B1-1d. Two differences between the MCEER spectra and the SAC spectra are evident (by comparing figure B1-1 with figure 3-12). First, the spectral acceleration demands in the MCEER ground motion bins are higher at short periods (0.01 – 0.4 Hz) but decrease rapidly with increased period (Median spectral acceleration at a period of 1.5 s for the SAC 2/50 bin is double that for the MCEER 2/50 bin). Second, the scatter in the spectral accelerations at any given period is greater in the SAC ground motion bins than in the corresponding MCEER ground motion bin. Results of the analysis using these two bins of ground motions are presented in Appendix B as supplemental information. A summary comparison of the results obtained using the SAC Steel Project and MCEER ground motions is presented in Section 4.5.

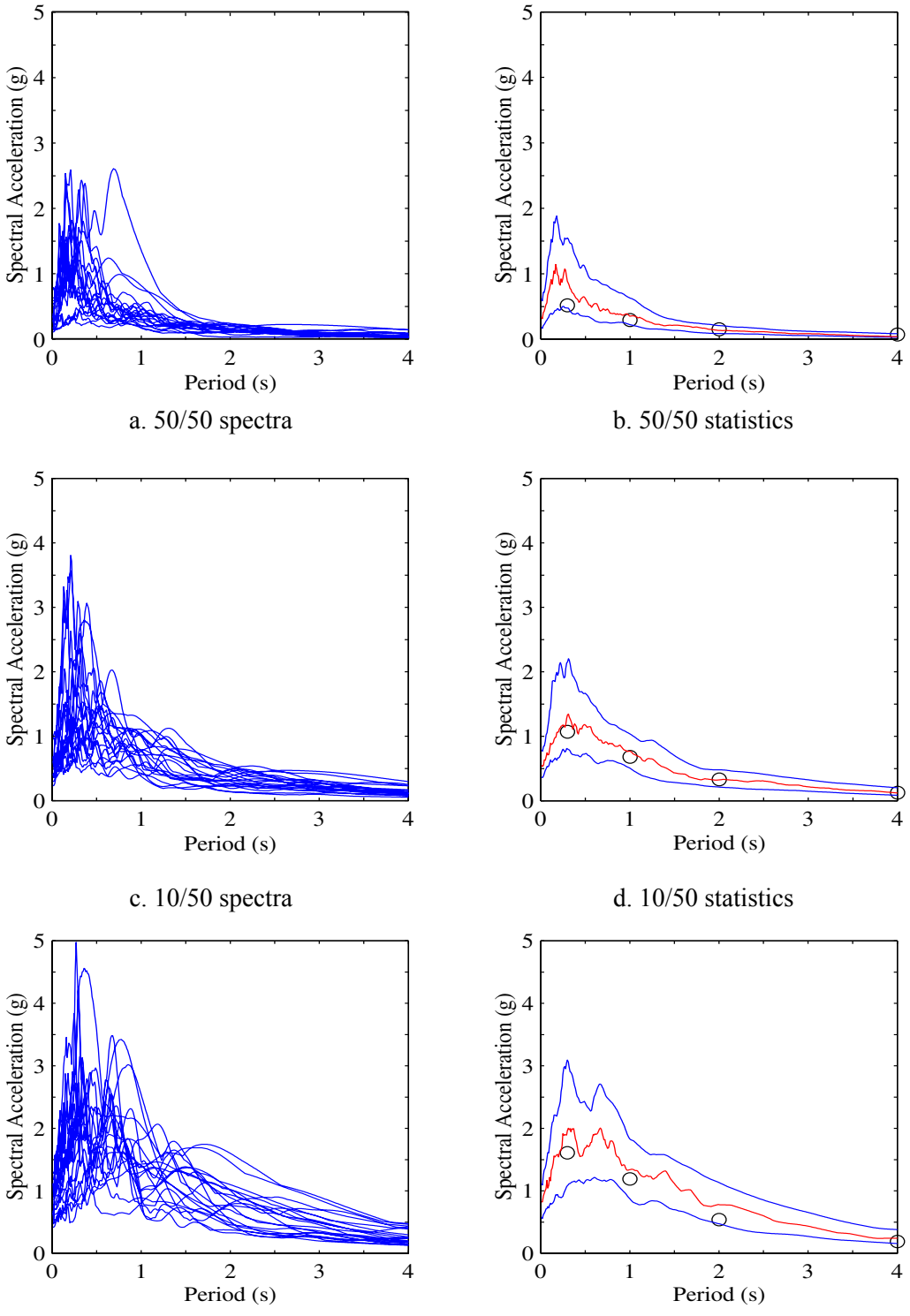

FIGURE 3-12: Acceleration Spectra and Distribution for Three Ground Motion Bins for Los Angeles from the SAC Steel Project. (Somerville et al., 1997)

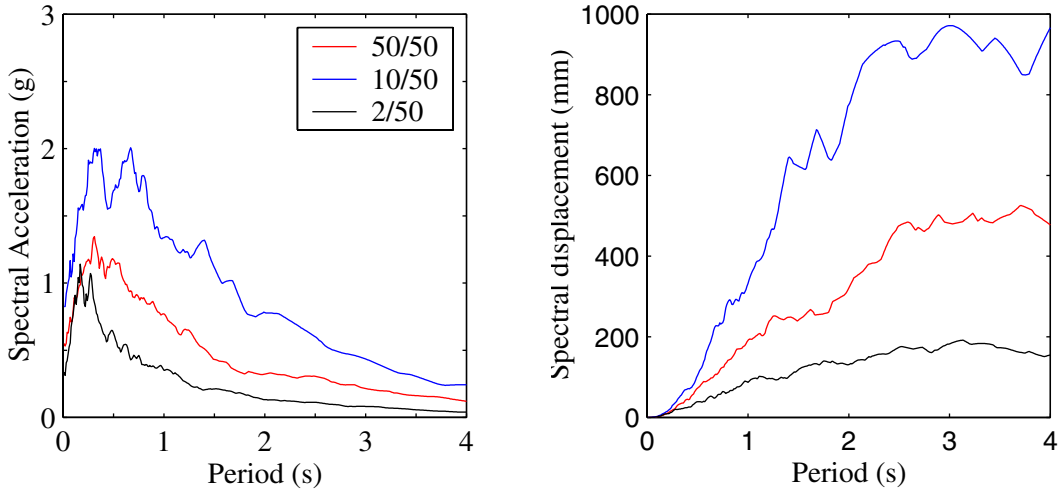

a. Acceleration b. Displacement

FIGURE 3-13: Median Spectra for the 50/50, 10/50 and 2/50 Earthquake Bins

CHAPTER 4

PERFORMANCE ASSESSMENT BY RESPONSE-HISTORY ANALYSIS

4.1 Introduction

Chapter 4 presents the results of the nonlinear response-history analysis of the 12 models introduced in Section 3.2 using the 3 bins of the SAC Steel Project earthquake histories described in Section 3.3.1. Demands on acceleration-sensitive and displacement-sensitive nonstructural components and contents (NCCs) are presented in the form of distributions of peak floor acceleration, peak story drift, and floor acceleration response spectra. Performance points and performance spaces are introduced to aid in the assessment of framing system choice on demands on NCCs.

A direct comparison of the performance of the isolated (M11 through M16) and damped (M7 though M10) models is not possible because the baseline buildings are different: M3 for the isolated buildings and M6 for the damped buildings. The effect of adding dampers to M3 instead of M6 would be to reduce interstory drifts and increase floor accelerations.

4.2 Bin 1: 50% exceedence in 50 years (50/50)

Results of response-history analysis using the 20 ground motion histories of the 50/50 bin from the SAC Steel Project are presented in this section. Figure 4-1 presents a summary of the distribution of peak drift responses. Figures 4-1a, b, c, d, and e present drifts for stories 1, 2, 3, 4 and global building drift, respectively, where the story numbers are identified in figure 3-6. Figure 4-1 presents the median, maximum, minimum, 16th percentile, and 84th percentile values of maximum response. These values assume a lognormal distribution for the maximum

responses[1]. Drift is presented as a percentage of story height (or building height in figure 4-1e). The horizontal axis labels denote the model numbers (e.g., M8), per table 3-2. The approximate yield drift for each story for M3 and M6, the two conventional MRFs, based on non-linear static analysis, are shown in each figure to identify the degree of inelastic action (damage) in each *moment* frame.[2]

The trends of figures 4-1 are well established, namely, that the addition of lateral stiffness, damping, and seismic isolation reduces drifts. As expected, drifts in the isolated frames (M11 through M16) are substantially smaller than the drifts in the non-isolated frames and the addition of displacement- and velocity-dependent dampers led to a significant reduction in the median maximum drift response of the weak and flexible frame (M6). Based on median values of maximum response and the yield drifts shown in figure 4-1, the conventional frames (M3 and M6) experience minimal damage (only in the 3rd story) for the 50/50 shaking.

For the non-isolated buildings (M3, M6, M7, M8, M9 and M10), the coefficient of variation in the peak roof drift is greatest (0.826) for M3 (mean peak roof drift = 0.52 %) and smallest (0.716) for M9 (mean peak roof drift = 0.53 %). The addition of viscous dampers (M9 and M10) to the weak and flexible building (M6) reduced the mean peak roof drift (by 54 % for M9 and 64 % for M10). Table 4-1 presents coefficients of variation of roof drifts for all three bins and all 11 models.

TABLE 4-1: Coefficients of Variation in Roof Drift

	M3	M6	M7	M8	M9	M10	M11	M12	M13	M14	M15	M16
50/50	0.826	0.768	0.725	0.775	0.716	0.729	0.606	0.616	0.619	0.606	0.495	0.484
10/50	0.672	0.697	0.703	0.694	0.608	0.577	0.579	0.531	0.540	0.483	0.474	0.434
2/50	0.702	N/A	0.816	0.844	0.682	0.676	0.727	0.668	0.643	0.633	0.640	0.506

[1] Maximum response values are assumed to follow a lognormal distribution, consistent with Cornell et al. (2002).

[2] The addition of the BRBs in models M7 and M8 will reduce the yield drift below that of M6 alone.

Figure 4-2 summarizes the distribution of the peak total floor acceleration at each level in the building. Similar to figure 4-1, median, maximum, minimum, 16th percentile, and 84th percentile values are presented assuming that the peak responses are lognormally distributed. The trends seen in figure 4-2 are also well established, namely that adding lateral stiffness increases peak floor accelerations, and adding viscous damping or seismic isolation reduces peak floor accelerations. Figure 4-2a presents total acceleration data for the ground floor, and was included to illustrate the behavior of the isolated models versus that of the non-isolated models. The isolators in Models M11 through M16 were placed below the ground floor and above the grade level (see figure 3-6). Therefore, the ground floor acceleration is equal to the ground acceleration for all non-isolated models but represents the acceleration of the ground floor diaphragm for the isolated models.

For the non-isolated models, the coefficient of variation in the peak 2nd floor acceleration is greatest (0.846) for M10 (mean peak acceleration = 0.25 g) and smallest (0.746) for M6 (mean peak acceleration = 0.34 g). Table 4-2 presents coefficients of variation in peak acceleration at the 2nd floor level for all models.

TABLE 4-2: Coefficients of Variation in Maximum Acceleration of the 2nd Floor

	M3	M6	M7	M8	M9	M10	M11	M12	M13	M14	M15	M16
50/50	0.791	0.746	0.777	0.783	0.830	0.846	0.671	0.706	0.730	0.746	0.642	0.652
10/50	0.623	0.582	0.637	0.587	0.609	0.612	0.537	0.534	0.543	0.555	0.489	0.492
2/50	0.521	N/A	0.553	0.530	0.504	0.524	0.627	0.611	0.599	0.578	0.607	0.514

As discussed in Chapter 1, FEMA 273/356 defines a performance point, first introduced by Nishkian (1937), as the intersection of the median capacity (pushover) and median demand (hazard) curves. Although a performance point is instructive, it provides no information about the impact of uncertainty and randomness on the capacity and demand calculations, and by extension, on the predicted building performance. Figure 4-3 presents performance points using median

peak drift response (ID*) and median peak floor acceleration (A*) as the performance metrics; ID* and A* are defined in figure 4-3e.

Figure 4-4 presents one possible form of the performance space, in which only the variability in ground motion has been considered. The performance spaces presented are boxes defined by the 16th and 84th percentile values of the peak drift and peak floor acceleration. In terms of demands on NCCs, performance points adjacent to the origin are preferable to points remote from the origin, and an optimal performance space should be small in size, indicating a small variability in peak displacement and acceleration response. On the basis of the chosen metrics, the buildings equipped with seismic isolators display the lowest magnitude and variability of response. The building equipped with fluid viscous dampers (FVDs) shows a reduction in magnitude and variability in response when compared to the responses of the traditional moment frames (M3 and M6) and the frames equipped with BRBs (M7 and M8).

To this point, response has been characterized by peak values of drift and floor acceleration. For many acceleration-sensitive NCCs, peak floor acceleration alone is an inefficient predictor of damage. NCCs attached to a floor may have a significant range of fundamental frequencies from 0.25 Hz (flexible) to 100 Hz (rigid). Better estimates of the vulnerability of these acceleration-sensitive components can be developed using floor acceleration spectra. Figure 4-5 presents median 5% damped floor acceleration spectra of the 12 models for the 50/50 earthquake histories developed using floor total acceleration histories. Again, the trends are well established. The stiff and strong moment frame building (M3) and the braced frames (M7 and M8) produce the highest spectral acceleration demands across a frequency range from 0.25 Hz to 100 Hz (periods from 4 sec. to 0.01 sec.). The viscous damped frames (M9 and M10) and the isolated frames (M11 through M16) produced much smaller spectral accelerations. Figure 4-6 presents normalized floor acceleration spectra for the six non-isolated buildings to show the decrease in variation of spectral accelerations with the addition of fluid viscous dampers. In these figures, peak floor accelerations were normalized to 1 g. It can be seen that for the same peak floor acceleration, the performance of the viscous damped buildings (M9 and M10) is superior to the performance of the traditional

frames when considering the predictability of the response of NCCs because the variation in spectral response with NCCs period is small. The isolated models were not included in this figure because the demands on the NCCs in the base-isolated models were substantially smaller than those in Models M3 through M10. Much additional information on the response of the isolated models is presented in Chapter 5.

4.3 Bin 2: 10% exceedence in 50 years (10/50)

Results of response-history analysis using the 20 ground motion histories of the 10/50 bin from the SAC Steel Project are presented in this section. Figures 4.7a, b, c, d, and e present a summary of the distribution of peak drift responses of stories 1, 2, 3, 4 and global building drift, respectively. These figures present the median, maximum, minimum, 16th percentile, and 84th percentile values of maximum response. Drift is presented as a percentage of story height (or building height in figure 4-7e). The horizontal axis labels denote the model numbers (e.g., M8), per table 3-2. The approximate yield drift for each story for M3 and M6 are shown in each figure.

The trends of figures 4-7 follow those of figure 4-1. The increased demand of the 10/50 event produces significantly higher levels of interstory drift. The conventional 1960s moment frame (M6) sustained significant structural damage. Again, drifts in the isolated frames (M11 through M16) are substantially smaller than the drifts in the non-isolated frames. As expected, the addition of displacement- and velocity-dependent dampers led to a significant reduction in the median maximum drift response of the weak and flexible frame (M6). Using the approximate yield drifts for the baseline models as thresholds for damage, it can be observed that the addition of protective devices to Models M3 (M7 through M10) and M6 (M11 through M16) reduced or eliminated damage. Model M7 experienced lower median drifts than M8 because of the yield strength (36 ksi) of the BRB. The viscous damped frames (M9 and M10) experienced significantly lower median drifts than either braced frame.

For the non-isolated buildings (M3, M6, M7, M8, M9 and M10), the coefficient of variation in the peak roof drift is greatest (0.703) for M7 (mean peak roof drift = 1.51 %) and smallest (0.58) for M10 (mean peak roof drift = 0.88 %). The addition of viscous dampers (M9 and M10) to the weak and flexible building (M6) reduced substantially the median maximum roof drift (by 54% for M9 and 65% for M10) and the coefficient of variation in the maximum roof drift (from 0.697 for M6 to 0.608 for M9 and 0.577 for M10). Table 4-1 presents coefficients of variation of roof drifts for all three bins and all 12 models.

Figure 4-8 summarizes the distribution of the peak total floor acceleration at each floor level. Similar to figure 4-2, median, maximum, minimum, 16th percentile, and 84th percentile values are presented assuming that the peak responses are lognormally distributed. The trends seen in figures 4-8 are also well established, namely that adding lateral stiffness increases peak floor acceleration and adding viscous damping or seismic isolation reduces peak floor acceleration.

For the non-isolated models, the coefficient of variation in the peak 2nd floor acceleration is greatest (0.637) for M7 (mean peak acceleration = 0.60 g) and smallest (0.582) for M6 (mean peak acceleration = 0.51 g). Table 4-2 presents coefficients of variation in peak acceleration at the 2nd floor level for all models.

Figures 4-9 and 4-10 are similar to figures 4-3 and 4-4. Figure 4-9 presents performance points using median peak drift response (ID*) and median peak floor acceleration (A*) as the performance metrics. ID* and A* are defined in figure 4-9e[3]. Figure 4-10 presents performance spaces for the 10/50 bin. Similar to figure 4-4, only the variability in ground motion has been considered. The performance spaces presented are boxes defined by the 16th and 84th percentile values of the peak drift and peak floor acceleration.

3 Alternate groupings of ID* and A* (e.g. A2/ID1) may be more appropriate for NCCs such as suspended ceiling systems, depending on the points of connection to the structural frame.

On the basis of the chosen metrics, the buildings equipped with seismic isolators show the lowest magnitude and variability of response. The building equipped with fluid viscous dampers (M9 and M10) show a reduction in magnitude and variability in response when compared to the responses of the conventional moment frames (M3 and M6) and the frames equipped with BRBs (M7 and M8).

Figure 4-11 presents median 5% damped floor acceleration spectra of the 12 models for the 10/50 earthquake histories. Again, the trends are well established. The stiff and strong moment-frame building (M3) and the braced frames (M7 and M8) produce the highest spectral acceleration demands across a frequency range from 0.25 Hz to 100 Hz. The viscous damped frames (M9 and M10) and the isolated frames (M11 through M16) produced much smaller spectral accelerations than the respective parent frames (M6 and M3).

Figure 4-12 presents floor acceleration spectra for the five non-isolated buildings with the peak floor accelerations normalized to 1 g. For the same peak floor acceleration, the performance of the viscous damped buildings (M9 and M10) is superior to the performance of the other frames because the variation in spectral response with NCC frequency is far smaller.

4.4 Bin 3: 2% exceedence in 50 years (2/50)

Results of response-history analysis using the 20 ground motion histories of the 2/50 bin from the SAC Steel Project are presented in this section. Figures 4-13a, b, c, d and e present a summary of the distribution of peak drift of stories 1, 2, 3, 4 and global building drift, respectively. These figures present the median, maximum, minimum, 16th percentile, and 84th percentile values of maximum response for the 2/50 bin. These values assume a lognormal distribution for the maximum responses. Drift is presented as relative displacement as a percentage of story height (or building height in figure 4-13e). The horizontal axis labels denote the model numbers (e.g., M8), per table 3-2. The yield drift for each story of M3 and M6 are shown in each figure.

Demands on the non-isolated structures and their NCCs for the 2/50 shaking are substantially greater than for the 10/50 shaking. All framing systems except those equipped with seismic isolators suffer significant damage in the 2/50 shaking[4]. On the basis of the response-history analysis, the weak and flexible moment frame (M6) is likely to collapse in four of the twenty ground motions of the 2/50 bin. The results from these four ground motions (LA 24, LA 35, LA 36, and LA 38) were not useful because the solutions did not converge and only the median response is reported for M6. The addition of the supplemental damping devices in Models M7, M8, M9 and M10 substantially reduced the level of damage to M6 but an alternate baseline system would be required to eliminate damage to the structures equipped with damping devices. The isolated framing systems suffer no structural damage. Median interstory drifts in the isolated structures ranged between 0.14 and 0.51%: likely sufficiently small to limit or prevent damage to most displacement-sensitive components such as exterior cladding, interior partitions and vertical piping.

For the non-isolated buildings (M3, M6, M7, M8, M9 and M10), the coefficient of variation in the peak roof drift is smallest (0.676) for M10 (mean peak roof drift = 1.86%) and greatest (0.844) for M8 (mean peak roof drift = 5.0%)[5]. The addition of viscous dampers (M9 and M10) to the weak and flexible building (M6) reduced substantially the median maximum roof drift (by 58 % for M9 and 70 % for M10). Table 4-1 presents coefficients of variation of roof drifts for all three bins and all 12 models.

Figure 4-14 summarizes the distribution of the peak total floor acceleration at each floor level. Similar to figure 4-13, median, maximum, minimum, 16th percentile, and 84th percentile values are presented assuming that the peak responses are lognormally distributed. Maximum floor accelerations across the 12 models do not vary as much as interstory drifts for the 2/50 shaking. The 2/50 shaking leads to yielding and damage in the non-isolated buildings but the yielding of

[4] The bilinear models used to characterize component behavior are inaccurate at large story drifts. As such, only trends and likely outcomes are reported for this level of shaking for the non-isolated structures.

[5] Model M6 is not included in Table 4.1 for the 2/50 bin because of the infinite displacements associated with the four collapses.

the non-isolated framing systems limits the accelerations that can develop in these superstructures. The addition of the fluid viscous dampers to M6, namely, M9 and M10, do not substantially reduce the peak floor accelerations, and increase the floor accelerations at the roof level. In figure 4-14, the distribution of floor accelerations for model M6 was omitted for the same reason that it was omitted from figure 4-13.

For the non-isolated models, the coefficient of variation in the peak 2nd floor acceleration is greatest (0.553) for M7 (mean peak acceleration = 0.80 g) and smallest (0.504) for M9 (mean peak accelerations = 0.58 g). The addition of viscous dampers to the weak and flexible building (M6) reduced the median peak acceleration (29 % for M8 and 21 % for M9). Table 4-2 presents coefficients of variation in peak acceleration at the 2nd floor level for all models.

Similar to figures 4-3 and 4-9, figure 4-15 presents performance points using median peak drift response (ID*) and median peak floor acceleration (A*) as the performance metrics. ID* and A* are defined in the figure 4-14d. Figure 4-16 presents performance spaces similar to those of figures 4-4 and 4-10, in which only the variability in ground motion has been considered. The performance spaces presented are boxes defined by the 16th and 84th percentile values of the peak drift and peak floor acceleration.

Figure 4-17 presents median 5% damped floor acceleration spectra of the 12 models for the 2/50 earthquake histories. Again, the trends are well established. The stiff and strong moment frame building (M3) and the braced frames (M7 and M8) produce the highest spectral acceleration demands across a frequency range from 0.25 Hz to 100 Hz. The viscous damped frames (M9 and M10) and the isolated frames (M11 through M16) produced much smaller spectral accelerations than the respective parent frames (M6 and M3).

Figure 4-18 presents floor acceleration spectra for the five non-isolated buildings. In these figures, peak floor accelerations are normalized to 1 *g*. For the same peak floor acceleration, the performance of the viscous damped buildings (M9 and M10) is superior to the performance of the other frames.

4.5 MCEER ground motion analysis results

All analysis results using the two MCEER ground motion bins are presented in Appendix B. The median response of the 16 models followed similar trends as those established for the SAC Steel Project ground motions. However, the differences between the two ground motion bins, discussed in Section 3.3.2, are also evident in the analysis results. The spectral acceleration demands of the MCEER ground motion bins are higher in the short period range than the demands from the SAC bins and vice versa at longer periods. Therefore, models with longer periods of vibration show a lower median maximum response for the MCEER bins than the SAC ground motion bins. Also, the two braced frames (Models M7 and M8), upon brace yielding, experience a greater reduction in acceleration demand in the MCEER ground motion bins than in the SAC bins. This trend is more obvious in the 2/50 bins. The dispersion in spectral acceleration values was smaller in the MCEER ground motion bins than in the corresponding SAC bins, which is also evident in the dispersion of the acceleration responses of each model.

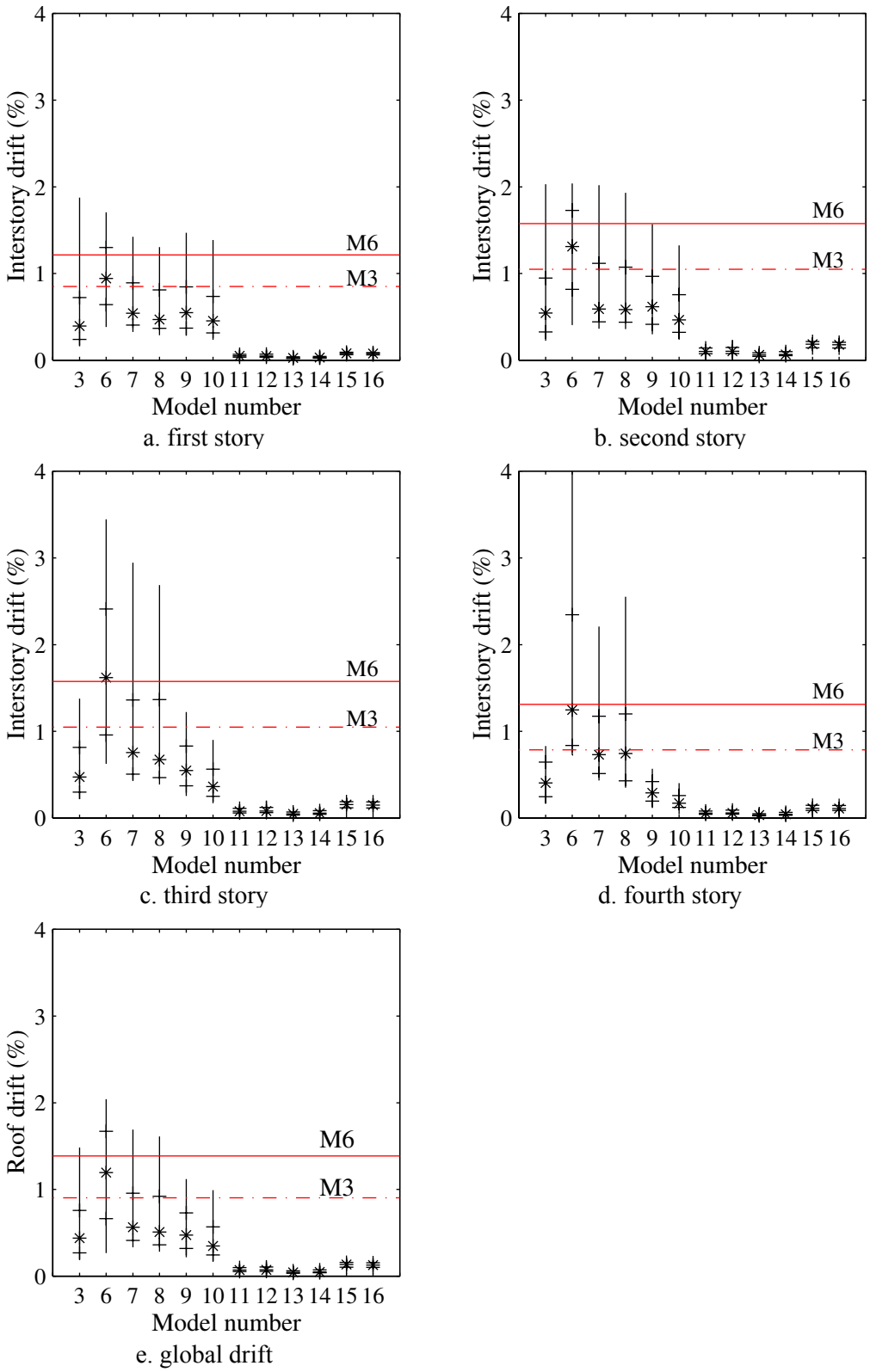

FIGURE 4-1: Distributions of Maximum Interstory and Roof Drift for the 50/50 Bin

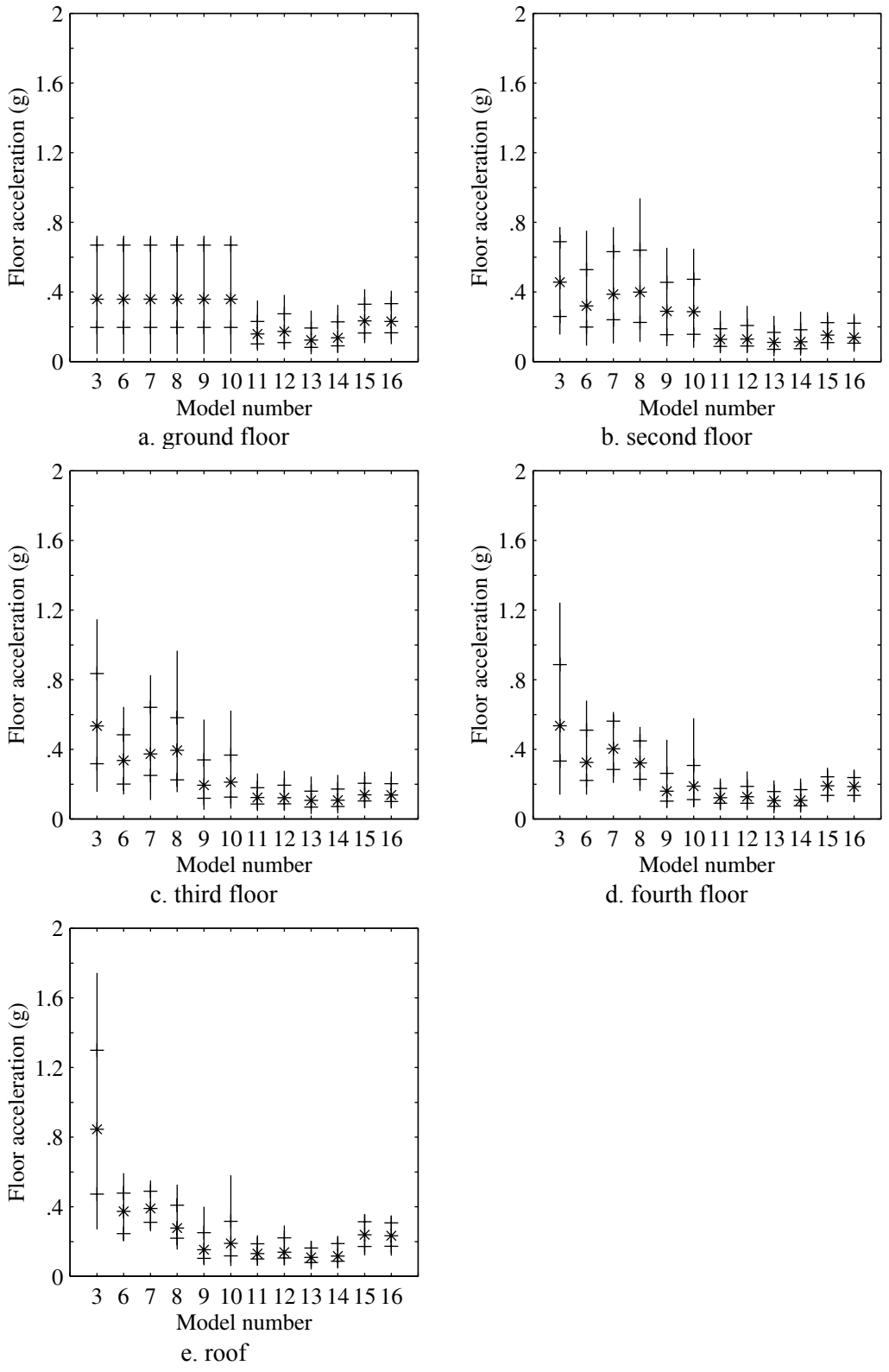

FIGURE 4-2: Distributions of Maximum Total Floor Acceleration for the 50/50 Bin

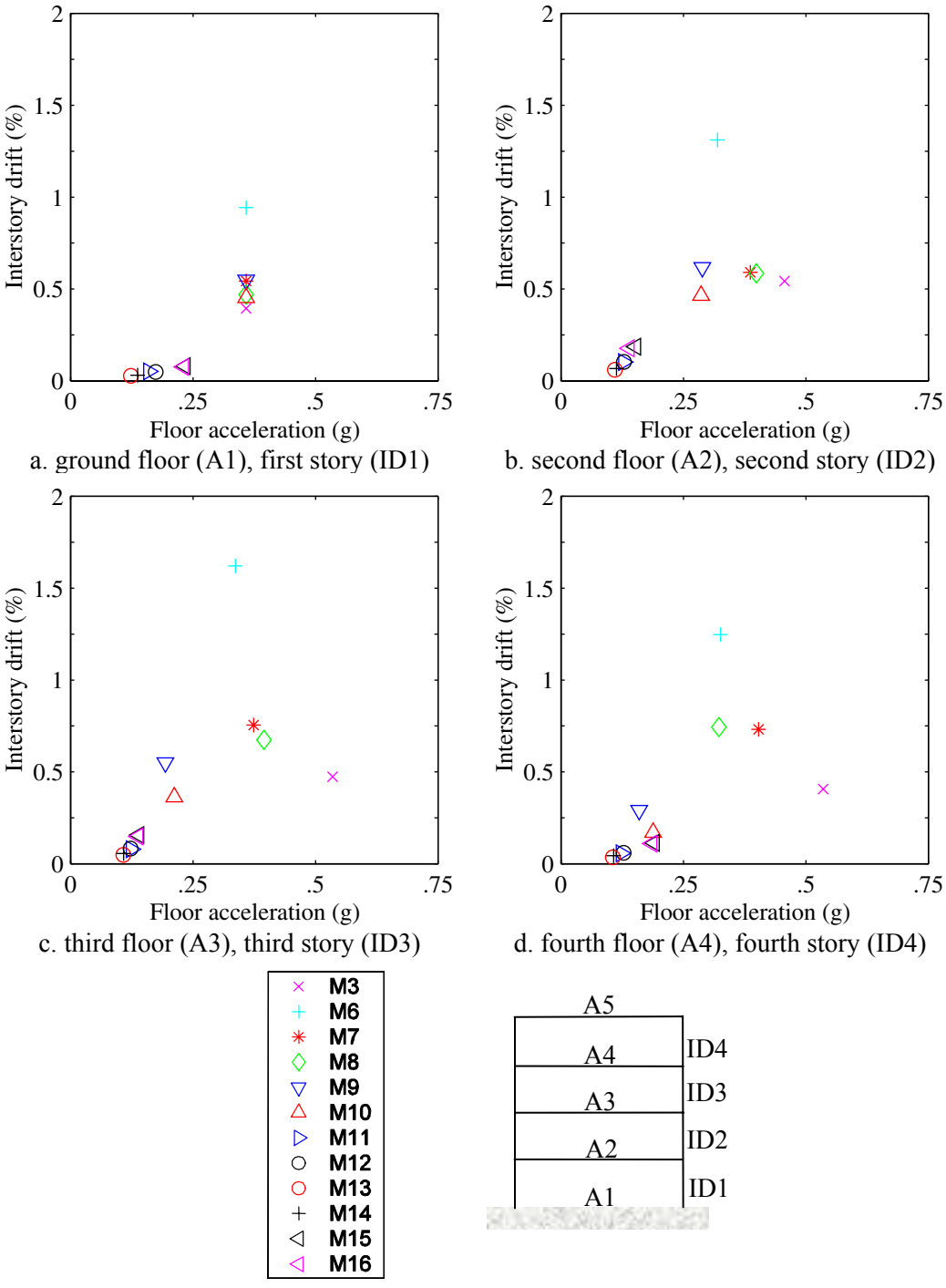

a. ground floor (A1), first story (ID1)

b. second floor (A2), second story (ID2)

c. third floor (A3), third story (ID3)

d. fourth floor (A4), fourth story (ID4)

e. legend and illustration of quantities

FIGURE 4-3: Performance Points for the 50/50 Bin

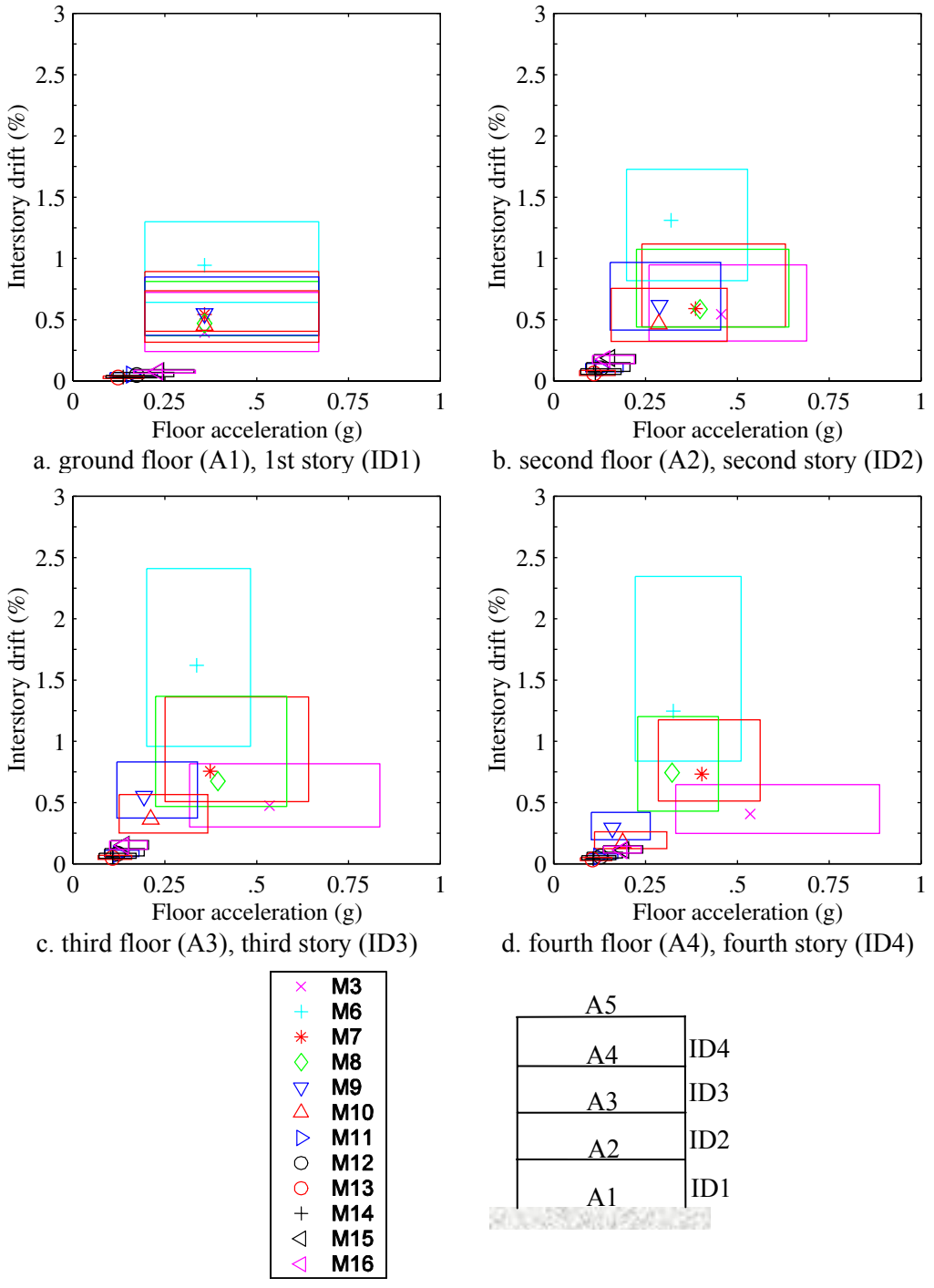

a. ground floor (A1), 1st story (ID1)

b. second floor (A2), second story (ID2)

c. third floor (A3), third story (ID3)

d. fourth floor (A4), fourth story (ID4)

e. legend and illustration of quantities

FIGURE 4-4: Performance Spaces for the 50/50 Bin

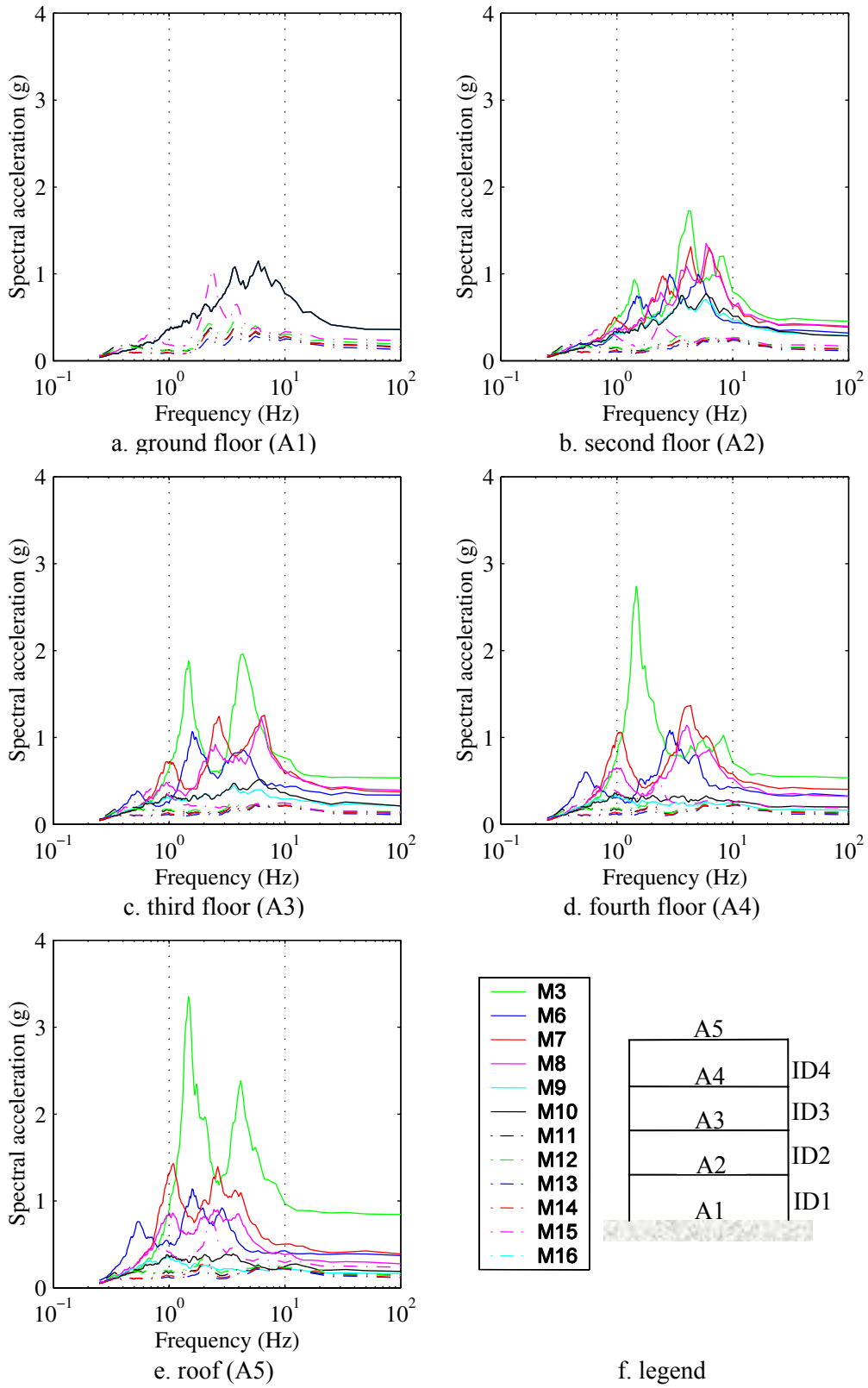

FIGURE 4-5: Total Floor Acceleration Response Spectra for the 50/50 Bin

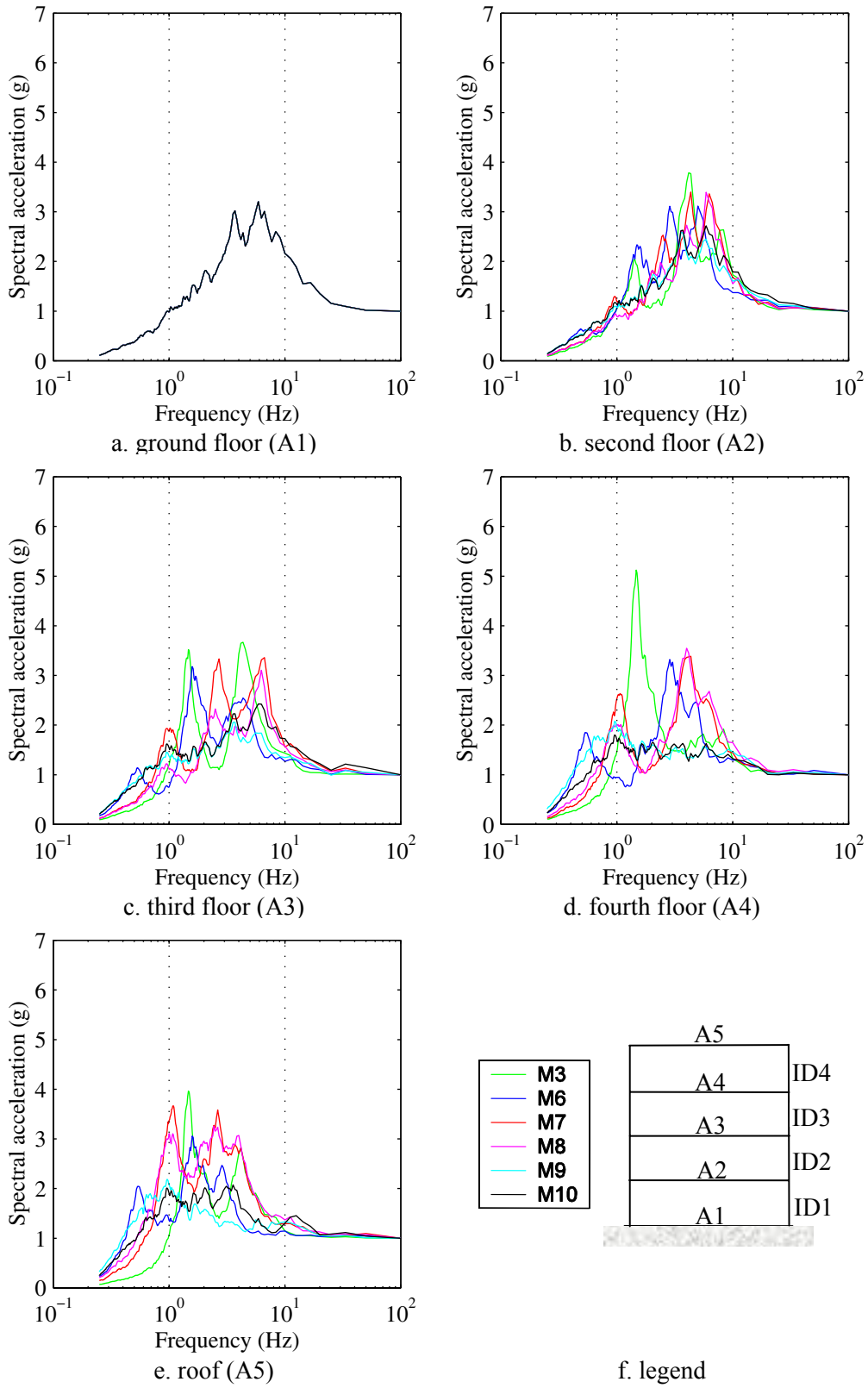

FIGURE 4-6: Normalized Floor Acceleration Response Spectra for the 50/50 Bin

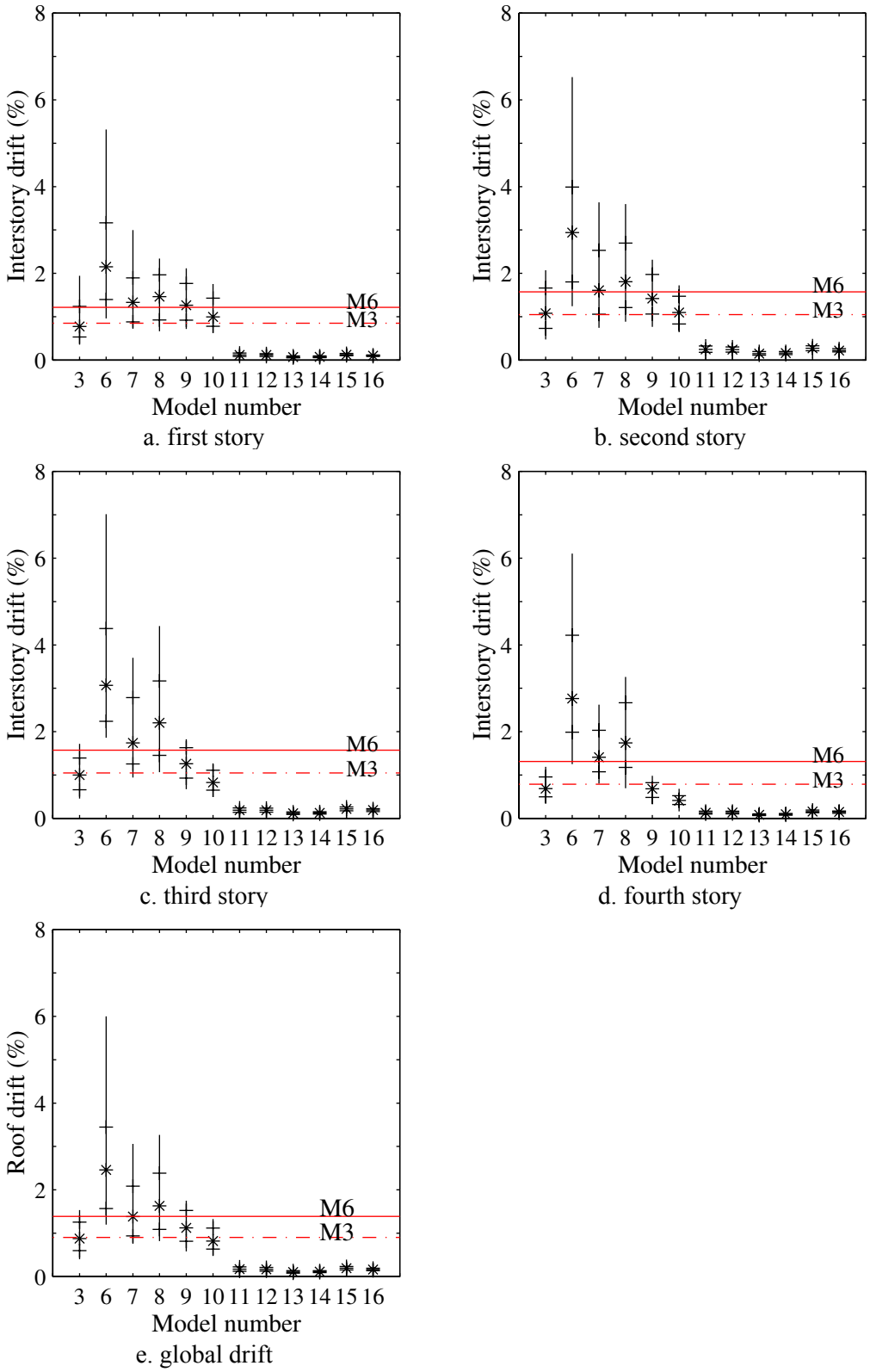

FIGURE 4-7: Distributions of Maximum Interstory and Roof Drift for the 10/50 Bin

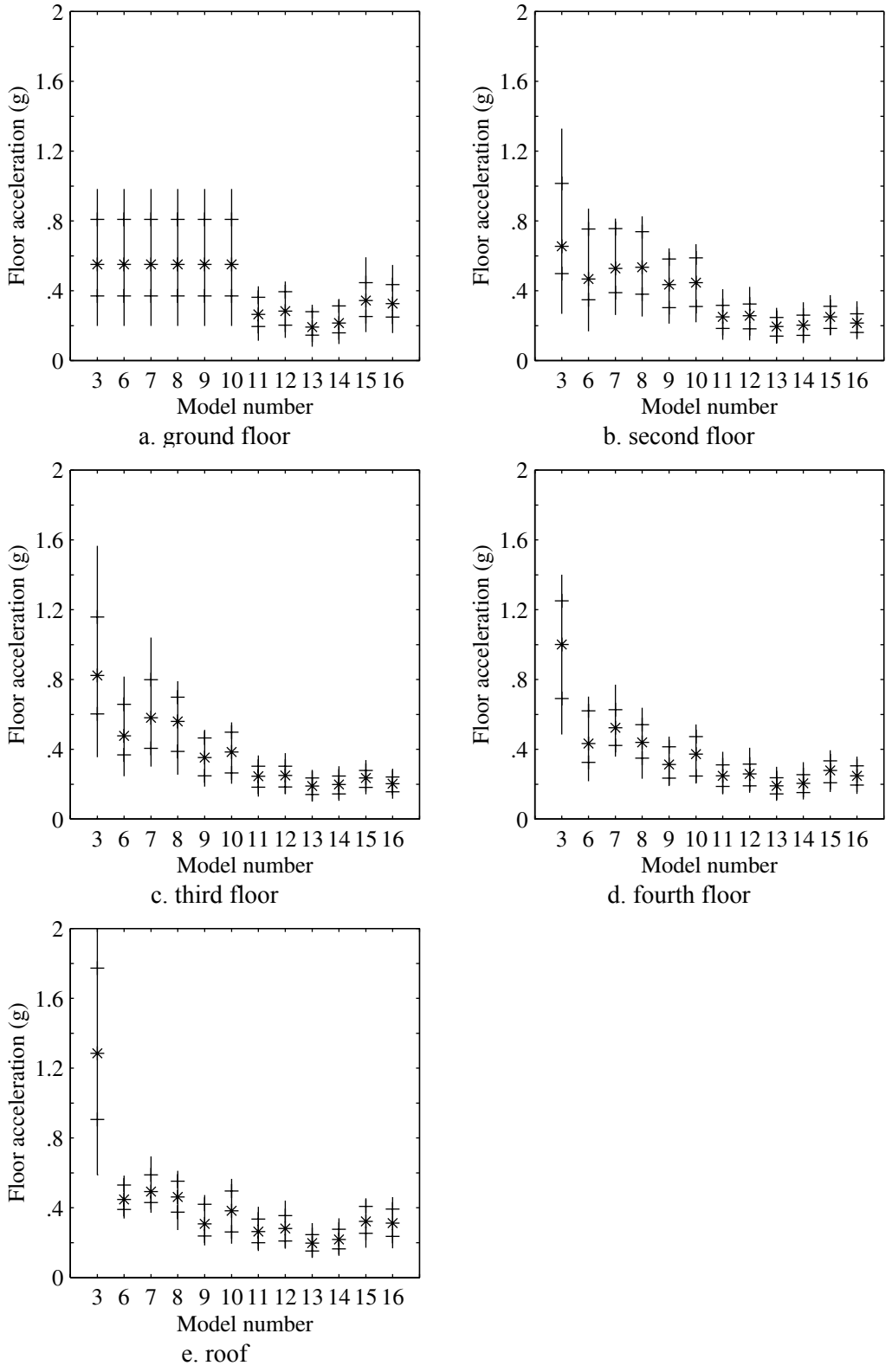

FIGURE 4-8: Distributions of Maximum Total Floor Acceleration for the 10/50 Bin

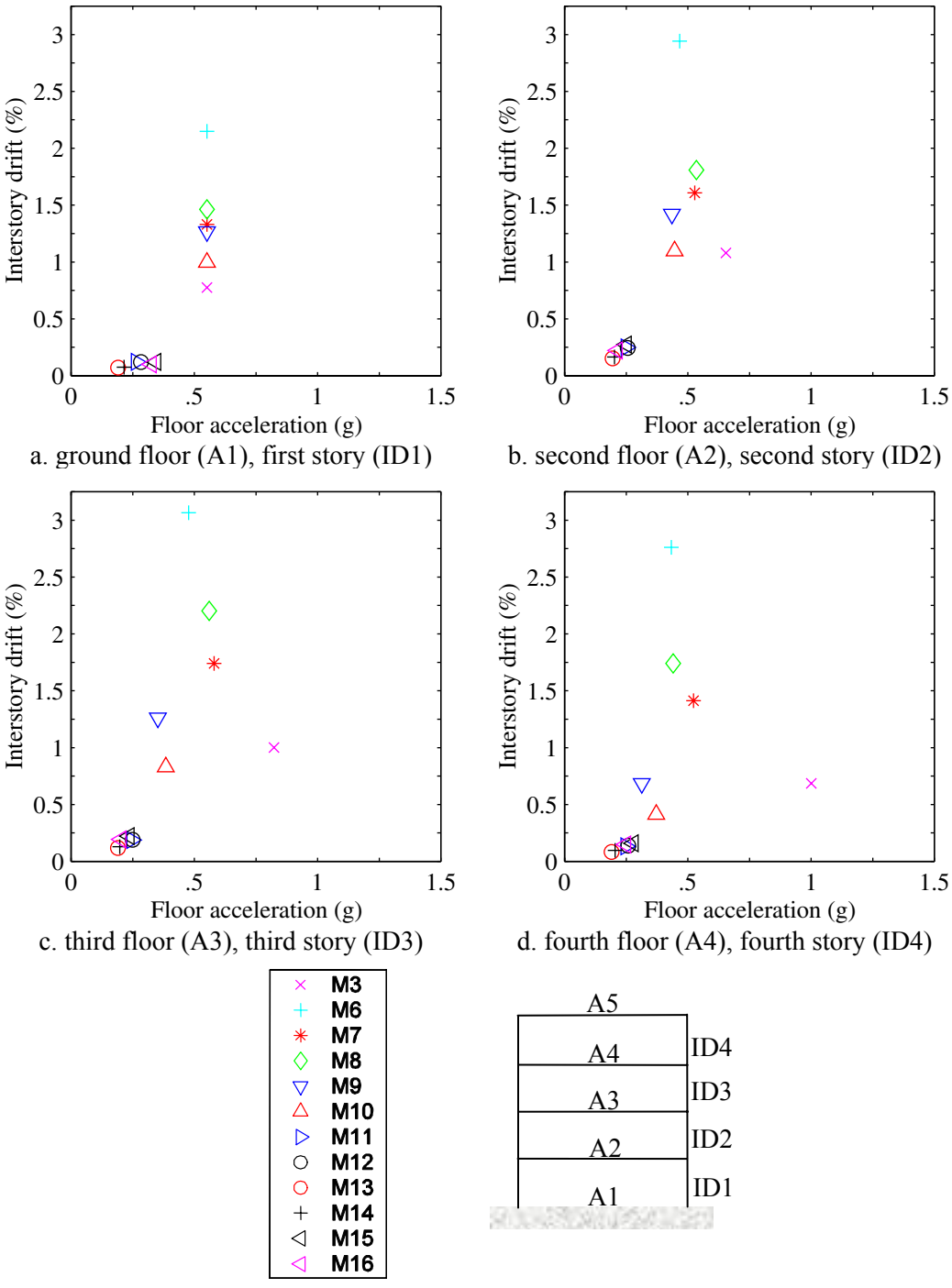

a. ground floor (A1), first story (ID1)

b. second floor (A2), second story (ID2)

c. third floor (A3), third story (ID3)

d. fourth floor (A4), fourth story (ID4)

e. legend and illustration of quantities

FIGURE 4-9: Performance Points for the 10/50 Bin

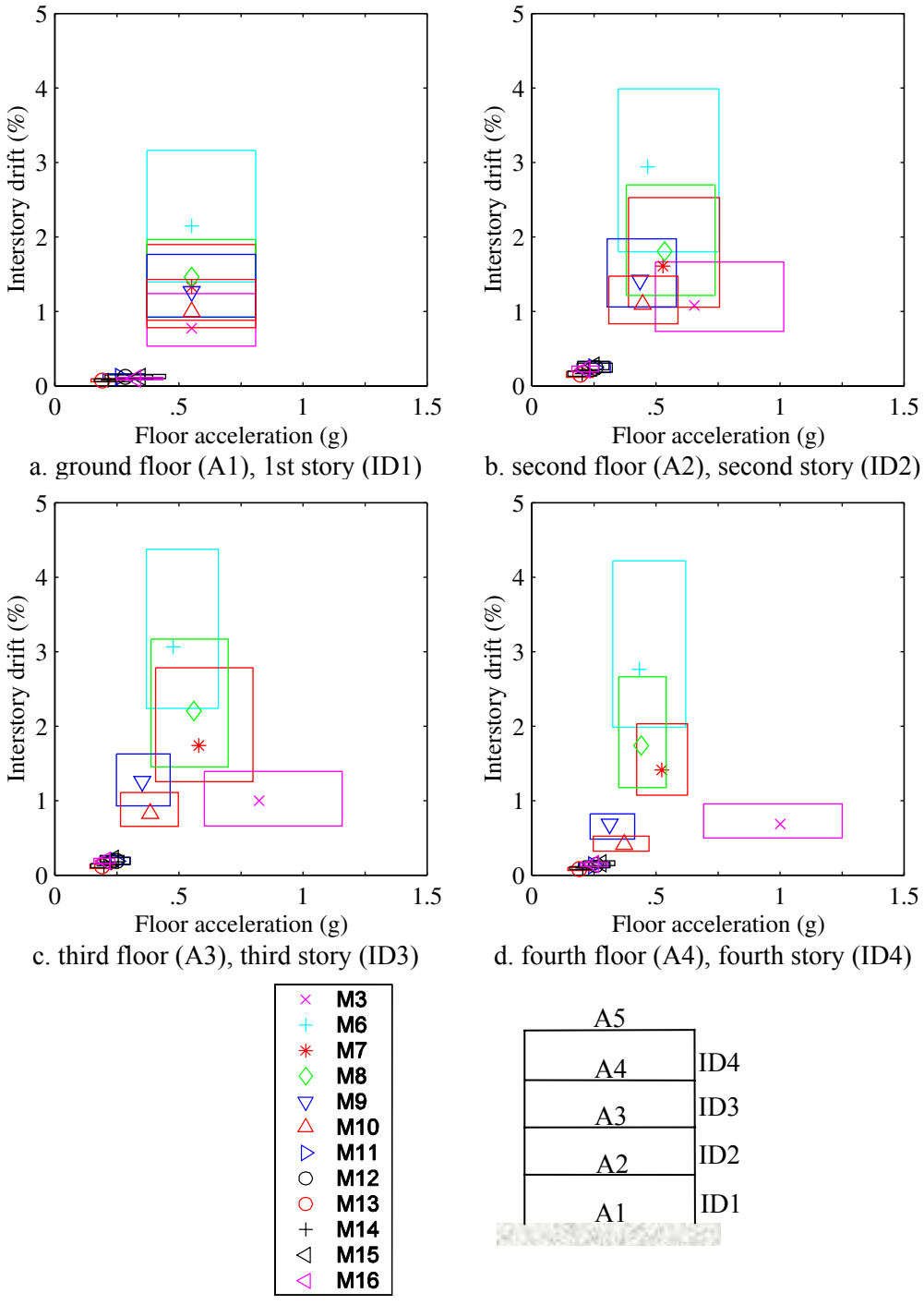

a. ground floor (A1), 1st story (ID1)

b. second floor (A2), second story (ID2)

c. third floor (A3), third story (ID3)

d. fourth floor (A4), fourth story (ID4)

e. legend and illustration of quantities

FIGURE 4-10: Performance Spaces for the 10/50 Bin

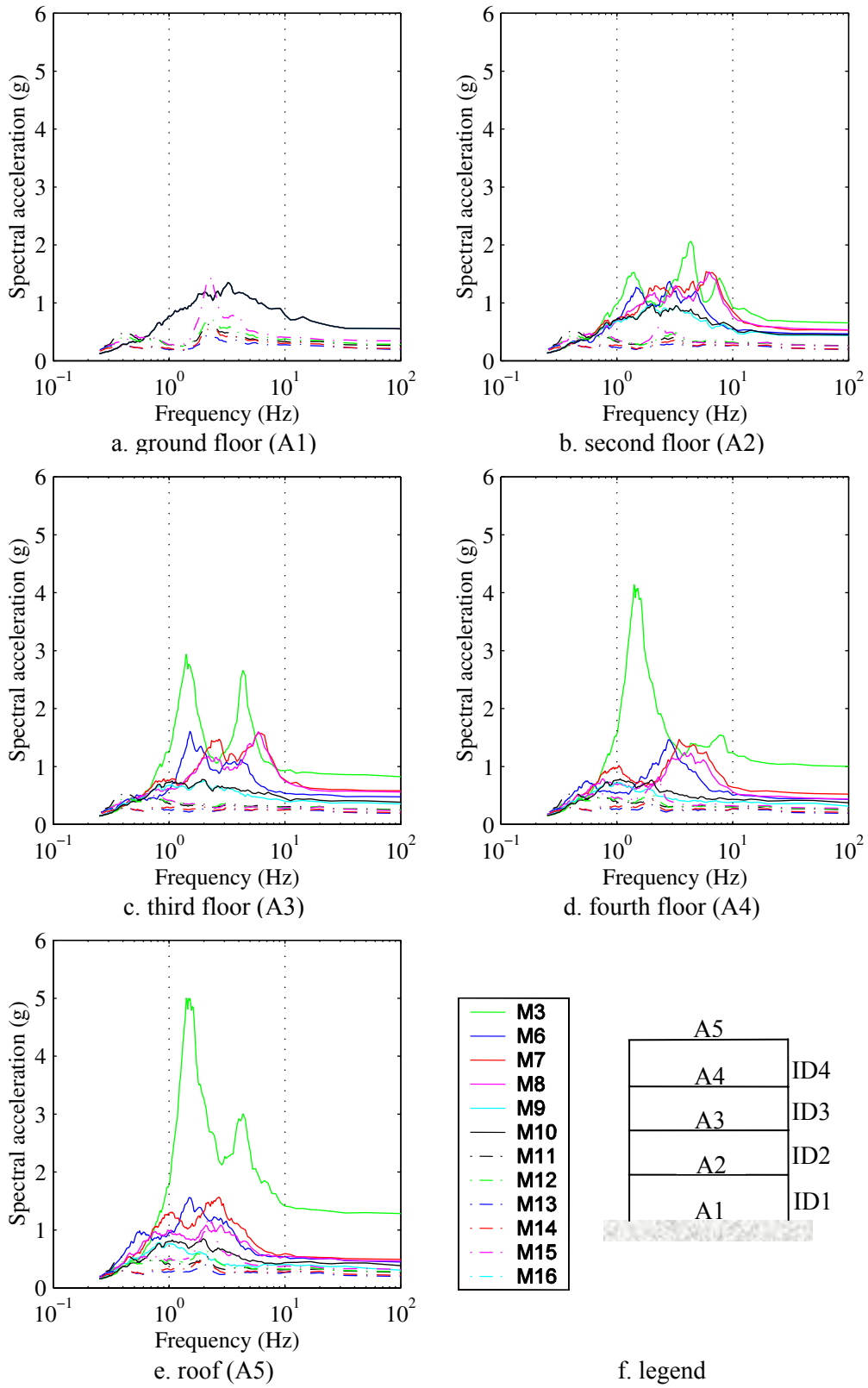

FIGURE 4-11: Total Floor Acceleration Response Spectra for the 10/50 Bin

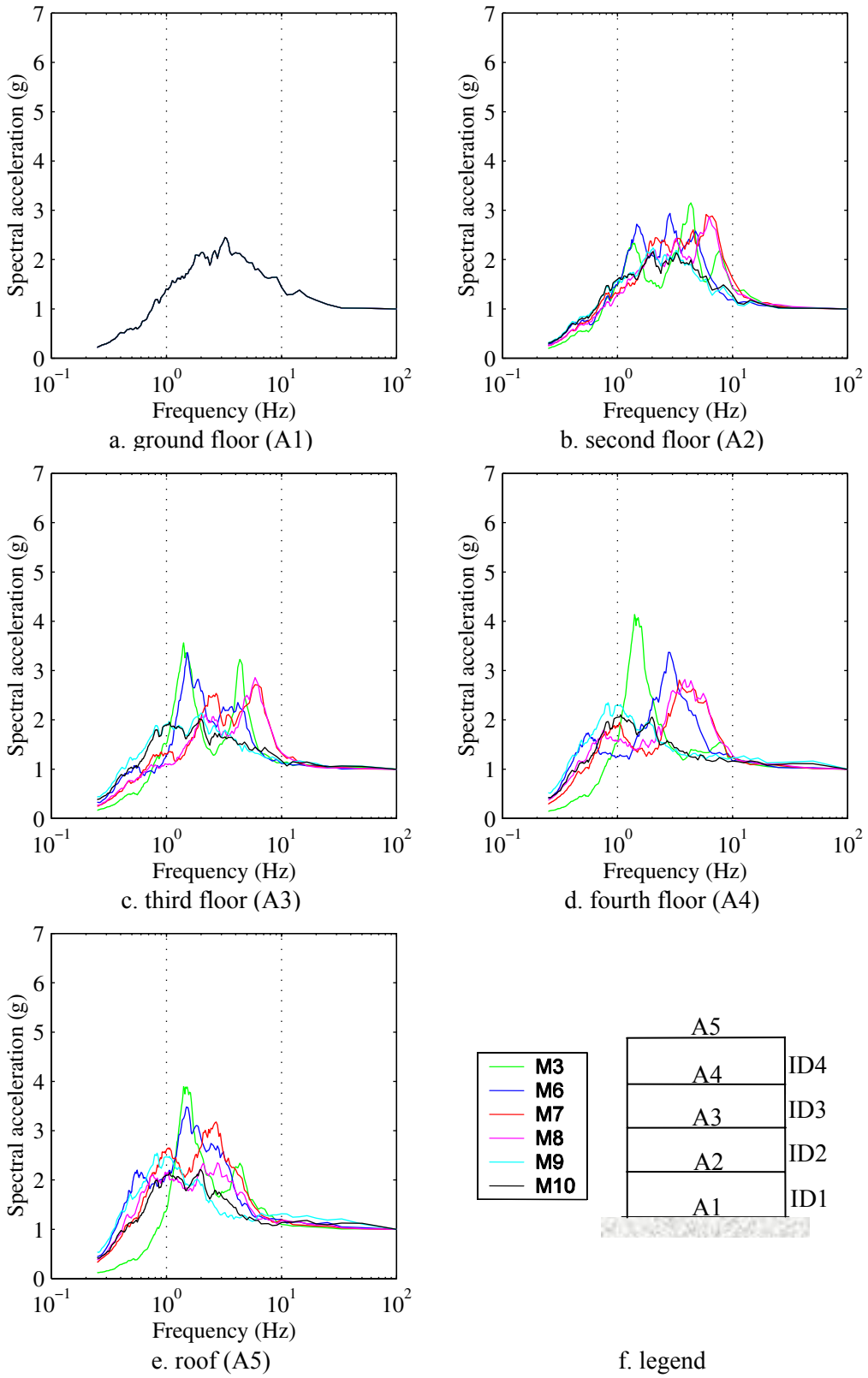

FIGURE 4-12: Normalized Floor Acceleration Response Spectra for the 10/50 Bin

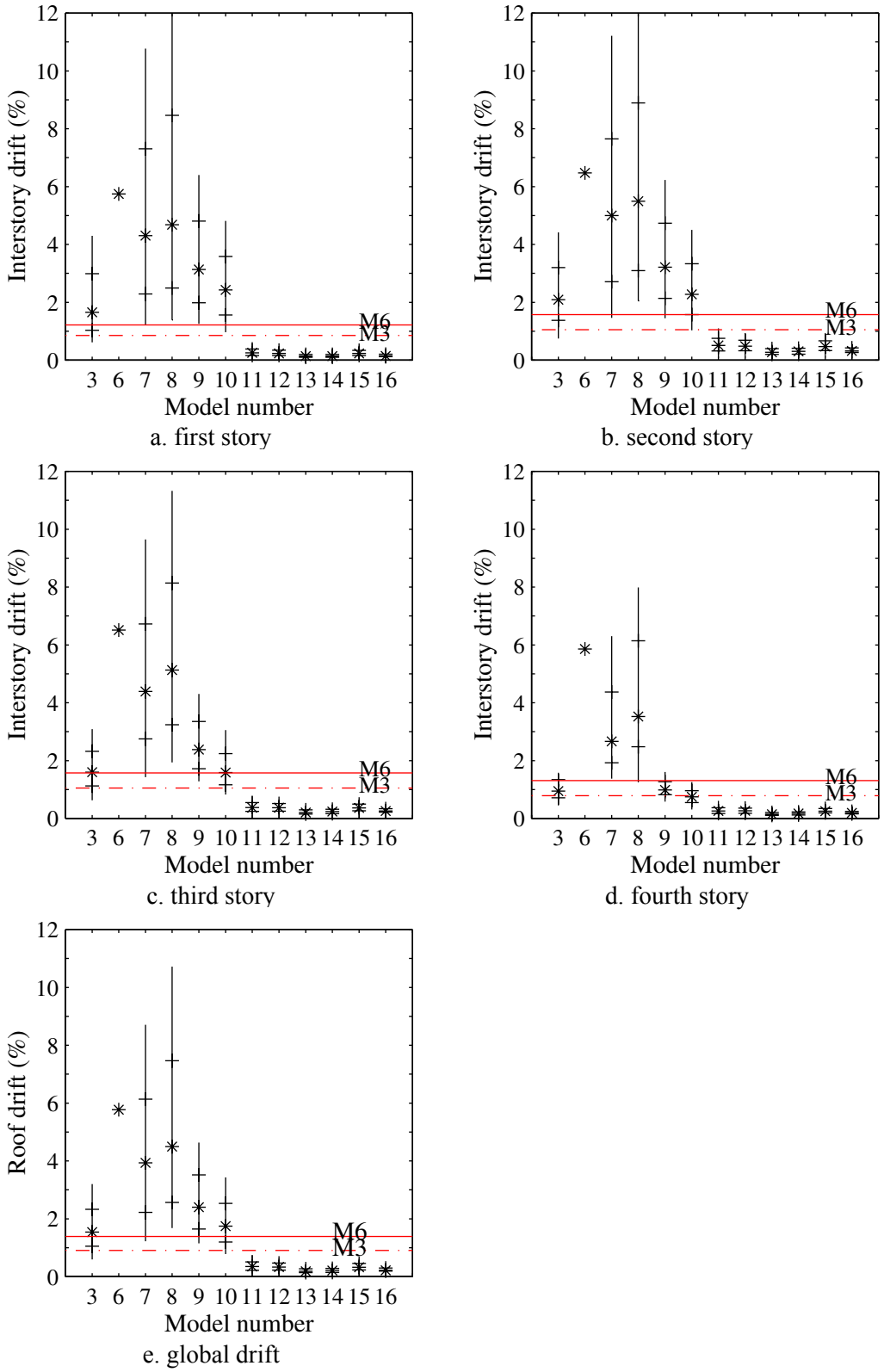

FIGURE 4-13: Distributions of Maximum Interstory and Roof Drift for the 2/50 Bin

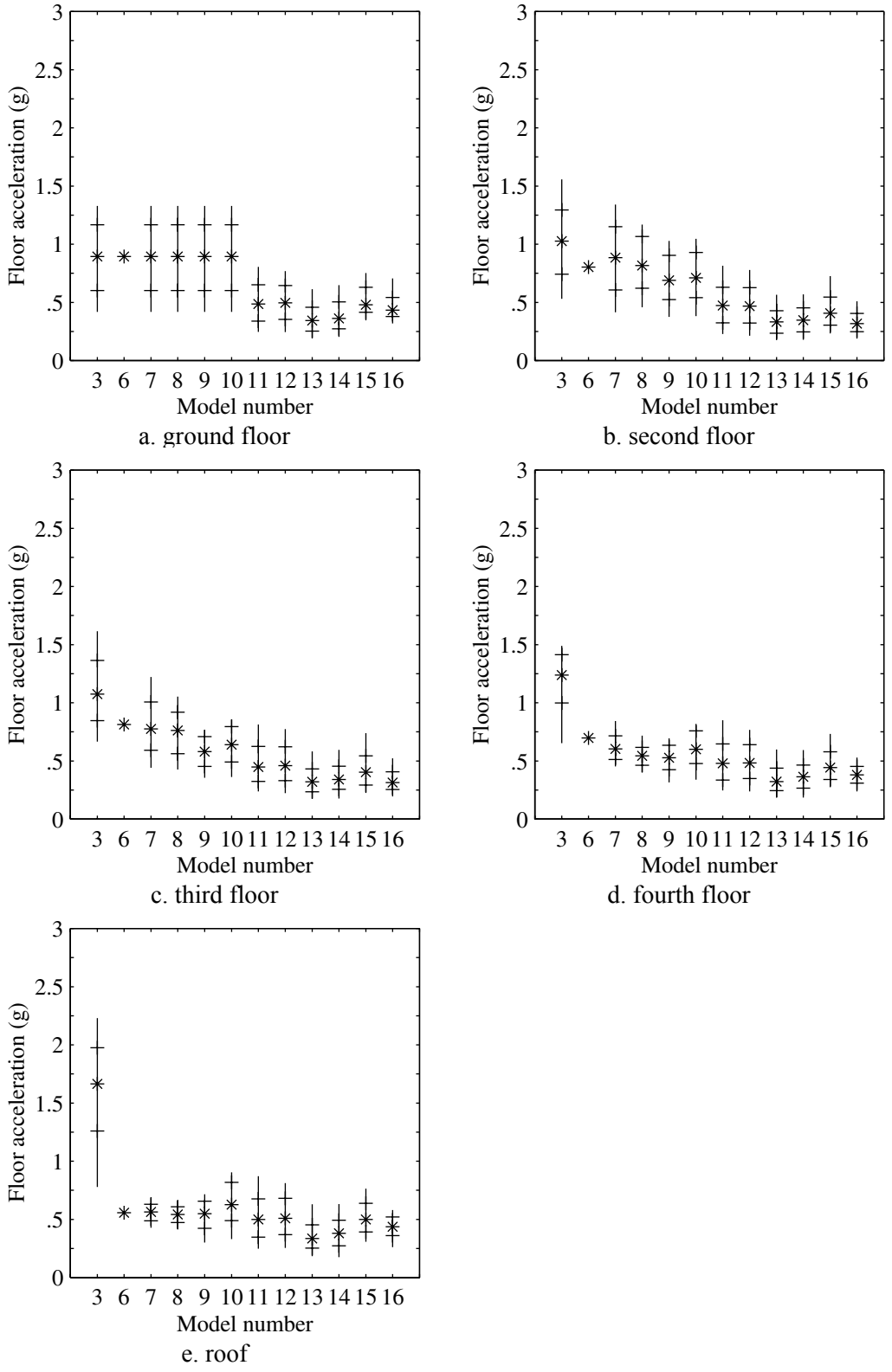

FIGURE 4-14: Distributions of Maximum Total Floor Acceleration for the 2/50 Bin

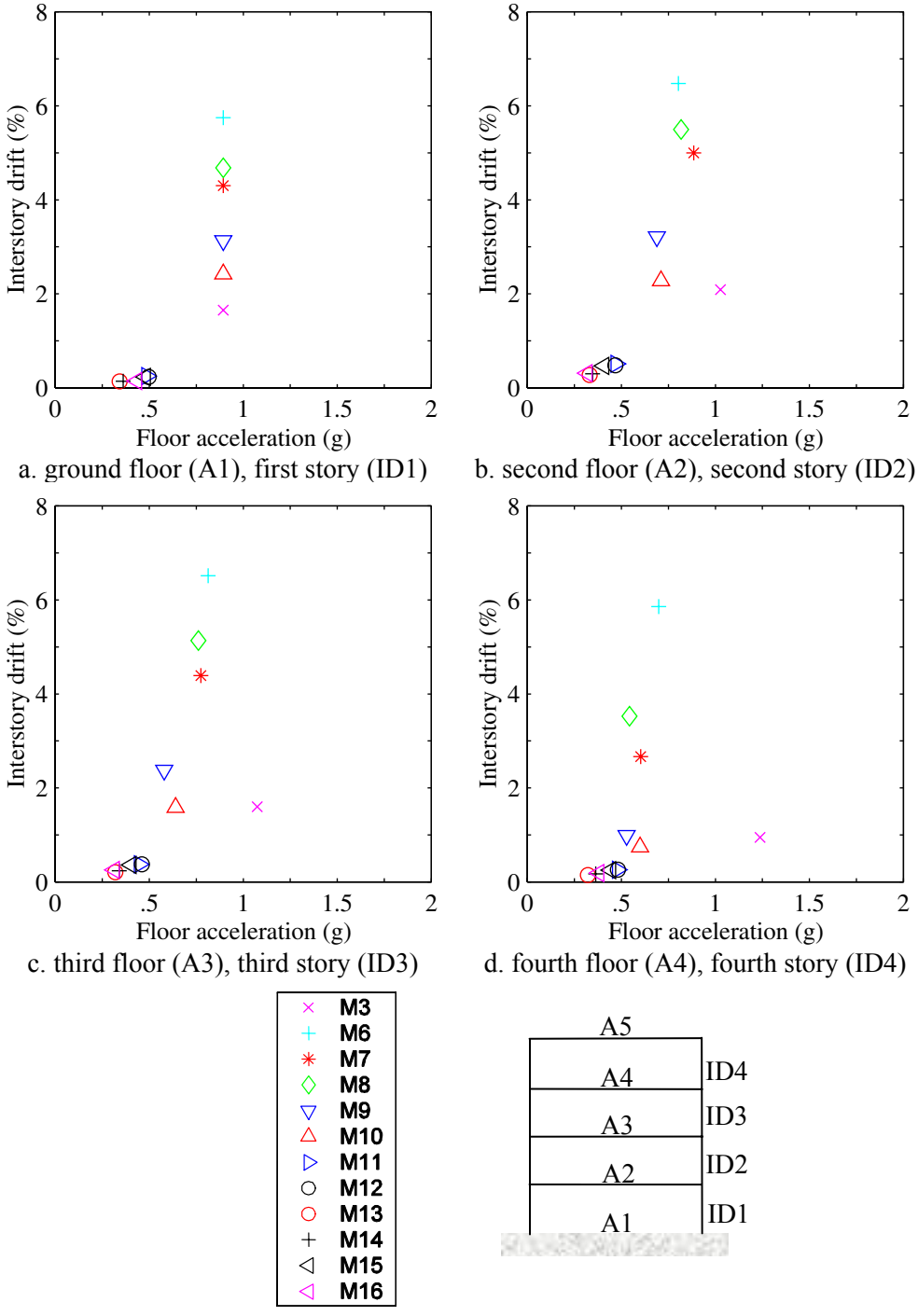

a. ground floor (A1), first story (ID1)

b. second floor (A2), second story (ID2)

c. third floor (A3), third story (ID3)

d. fourth floor (A4), fourth story (ID4)

e. legend and illustration of quantities

FIGURE 4-15: Performance Points for the 2/50 Bin

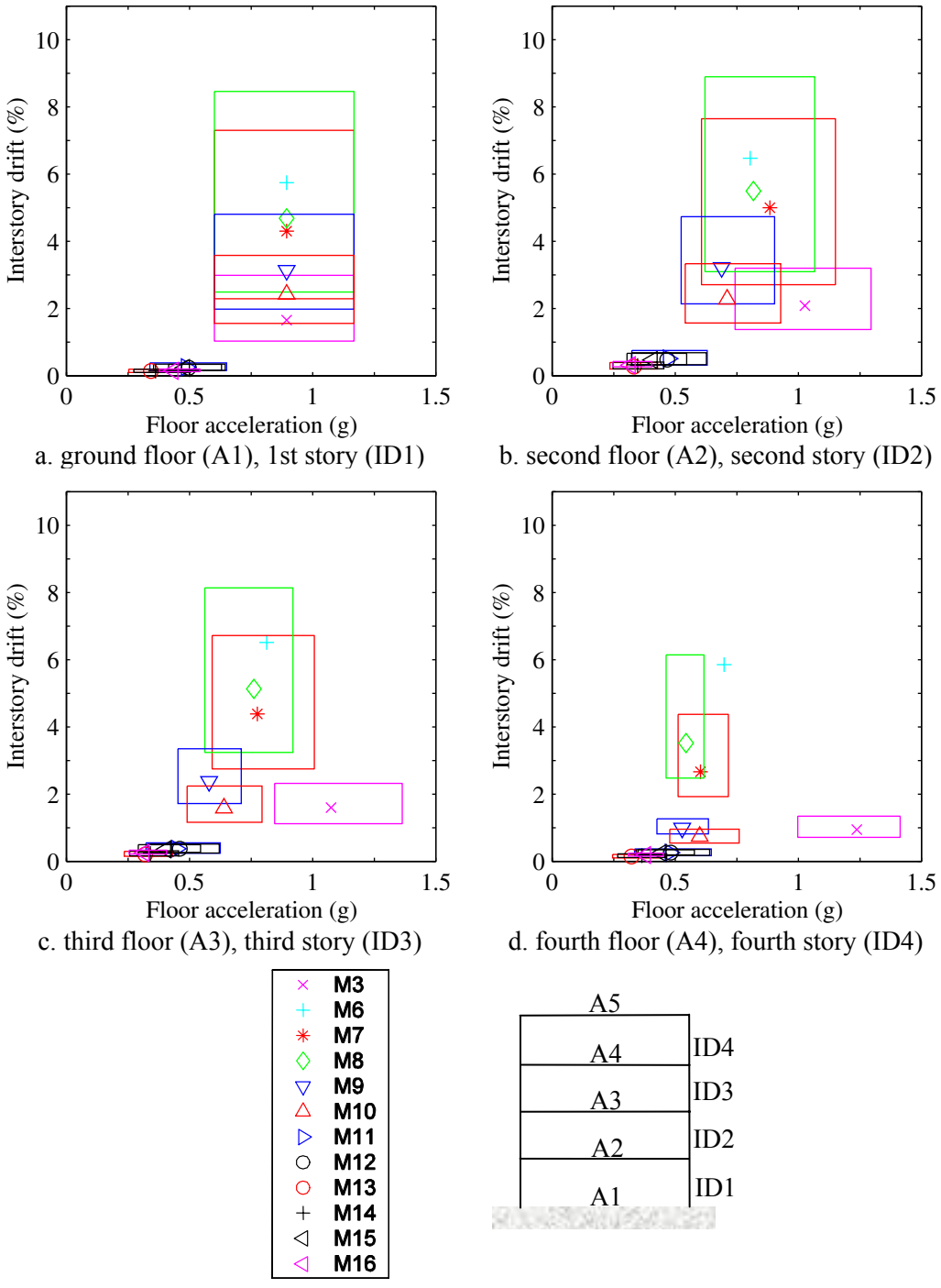

a. ground floor (A1), 1st story (ID1)

b. second floor (A2), second story (ID2)

c. third floor (A3), third story (ID3)

d. fourth floor (A4), fourth story (ID4)

e. legend and illustration of quantities

FIGURE 4-16: Performance Spaces for the 2/50 Bin

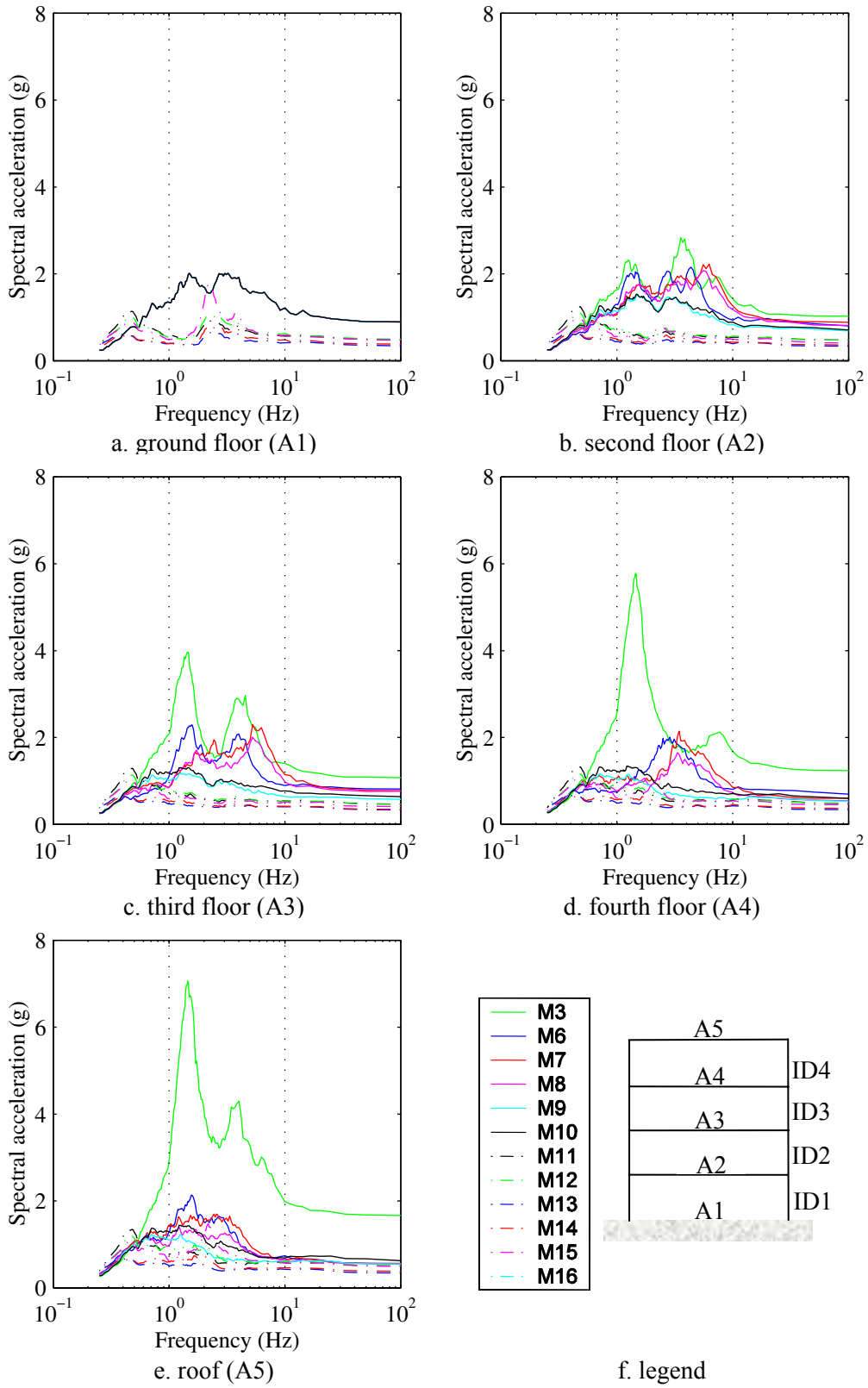

FIGURE 4-17: Total Floor Acceleration Response Spectra for the 2/50 Bin

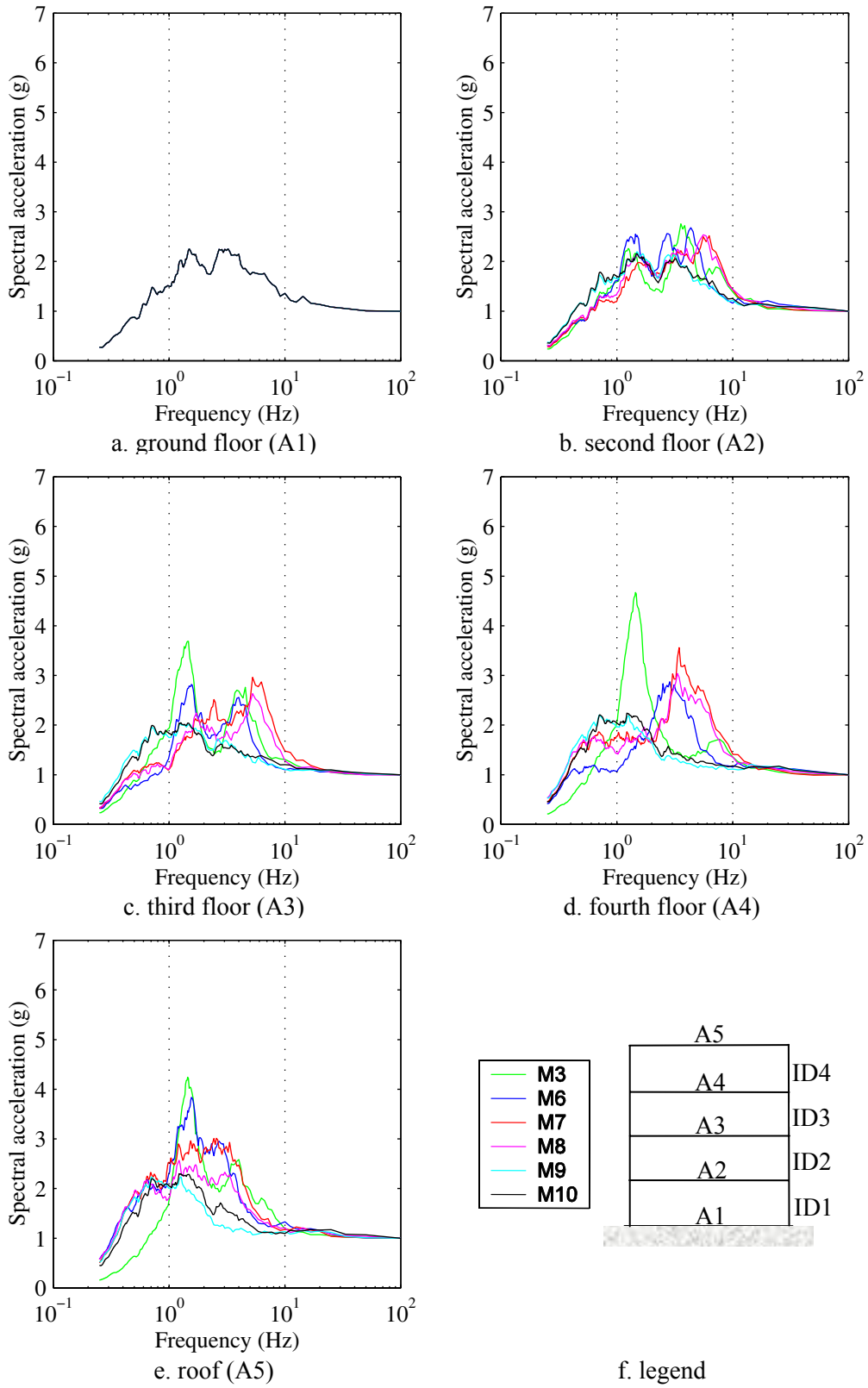

FIGURE 4-18: Normalized Floor Acceleration Response Spectra for the 2/50 Bin

CHAPTER 5

RESPONSE OF BASE-ISOLATED MODELS

5.1 Introduction

The data presented in Chapter 4 showed that the base-isolated models (M11 through M16) responded to each of the three bins of ground motions with the lowest accelerations and inter-story drifts. The isolated models also acted as the best filters of the ground motion considering the input to the nonstructural components and contents (NCCs), as evidenced by the flatter floor acceleration spectra (smaller peaks) and smaller performance spaces. Chapter 5 focuses on the response of the six base-isolated models, again with a concentration on NCC demands. This chapter compares responses of NCCs in base-isolated systems with longer periods (3.5 seconds) to systems with shorter periods (2.5 seconds), systems with lower levels of damping (10% of critical) to systems with higher levels of damping (20% of critical) and systems with viscoelastic isolators to systems with bilinear isolators.

The presentation of results in this section is similar to the presentation in Chapter 4, but focuses solely on the response of the base-isolated models[1]. A goal is to show the effect of isolation system choice on demands on NCCs. The measures of NCCs demand are maximum interstory drift, maximum floor acceleration, mean spectral acceleration over two frequency ranges (1 Hz to 10 Hz and 10 Hz to 20 Hz), performance spaces (discussed in Section 4.2), and total floor acceleration response spectra.

This chapter is organized in six sections. Section 5.2 discusses the dynamic properties of the six base-isolated models. Sections 5.3, 5.4 and 5.5 report the results of the response analysis using the SAC bins 1 (50/50), 2 (10/50) and 3 (2/50), respectively. Section 5.6 compares the

[1] The models discussed in this chapter were described in detail in Chapter 3.

performance of the isolation systems over the three levels of earthquake shaking in terms of the response of the superstructure and demands on NCCs.

The response of the base-isolated models is presented in three sets of tables and four sets of figures. Coefficients of variation of response are presented for roof drift (table 5-1) and 2nd floor peak total acceleration (table 5-2)[2]. Tables 5-3 through 5-8 present average median spectral acceleration values over two frequency ranges: 1 Hz to 10 Hz (tables 5-3, 5-5 and 5-7) and 10 Hz to 20 Hz (tables 5-4, 5-6 and 5-8). The median value of spectral acceleration over a range of frequencies could be used to identify demands on NCCs. Any frequency range of interest could be used to create this type of data.

TABLE 5-1: Effective Period of Each Isolation System[1]

	Model					
Bin	M11	M12	M13	M14	M15[2]	M16[2]
50/50	2.5	2.5	3.5	3.5	2.0 (88 mm)	2.28 (92 mm)
10/50	2.5	2.5	3.5	3.5	2.43 (244 mm)	2.92 (256 mm)
2/50	2.5	2.5	3.5	3.5	2.64 (551 mm)	3.31 (530 mm)

1. Calculated assuming a rigid superstructure.
2. Value in parentheses is the median peak isolator displacement for that bin. The effective period was calculated at this displacement.

TABLE 5-2: Effective Damping Ratio of Each Isolation System[1]

	Model					
Bin	M11	M12	M13	M14	M15[2]	M16[2]
50/50	0.10	0.20	0.10	0.20	0.38 (88 mm)	0.45 (92 mm)
10/50	0.10	0.20	0.10	0.20	0.20 (244 mm)	0.28 (256 mm)
2/50	0.10	0.20	0.10	0.20	0.10 (551 mm)	0.16 (530 mm)

1. Calculated assuming a rigid superstructure.
2. Value in parentheses is median peak isolator displacement for that bin. The effective damping ratio was calculated using this displacement.

[2] The 2nd floor data are representative of all floors in the building.

TABLE 5-3: Coefficient of Variation of Maximum Roof Drift

	Models					
Bin	M11	M12	M13	M14	M15	M16
50/50	0.606	0.616	0.619	0.606	0.495	0.484
10/50	0.579	0.531	0.540	0.483	0.474	0.434
2/50	0.727	0.668	0.643	0.633	0.640	0.506

TABLE 5-4: Coefficient of Variation of Maximum Total Floor Acceleration

	Models					
Bin	M11	M12	M13	M14	M15	M16
50/50	0.671	0.706	0.730	0.746	0.642	0.652
10/50	0.537	0.534	0.543	0.555	0.489	0.492
2/50	0.627	0.611	0.599	0.578	0.607	0.514

TABLE 5-5: Average Median Spectral Acceleration, 1 to 10 Hz, for the 50/50 Bin

	Model					
Floor	M11	M12	M13	M14	M15	M16
Ground	0.268	0.321	0.223	0.271	0.394	0.398
2nd	0.207	0.232	0.185	0.205	0.256	0.257
3rd	0.189	0.203	0.174	0.185	0.234	0.232
4th	0.193	0.198	0.172	0.179	0.283	0.282
Roof	0.212	0.239	0.182	0.204	0.359	0.361

TABLE 5-6: Average Median Spectral Acceleration, 10 to 20 Hz, for the 50/50 Bin

	Model					
Floor	M11	M12	M13	M14	M15	M16
Ground	0.231	0.257	0.209	0.228	0.300	0.295
2nd	0.201	0.217	0.189	0.203	0.225	0.218
3rd	0.182	0.189	0.179	0.185	0.203	0.203
4th	0.183	0.194	0.178	0.184	0.243	0.242
Roof	0.195	0.212	0.185	0.198	0.285	0.284

TABLE 5-7: Average Median Spectral Acceleration, 1 to 10 Hz, for the 10/50 Bin

	Model					
Floor	M11	M12	M13	M14	M15	M16
Ground	0.387	0.435	0.300	0.351	0.558	0.565
2nd	0.331	0.353	0.263	0.281	0.350	0.320
3rd	0.320	0.323	0.256	0.267	0.318	0.292
4th	0.333	0.336	0.262	0.281	0.383	0.368
Roof	0.356	0.387	0.274	0.306	0.499	0.495

TABLE 5-8: Average Median Spectral Acceleration, 10 to 20 Hz, for the 10/50 Bin

	Model					
Floor	M11	M12	M13	M14	M15	M16
Ground	0.332	0.360	0.273	0.305	0.392	0.385
2nd	0.311	0.317	0.262	0.276	0.307	0.272
3rd	0.304	0.296	0.258	0.261	0.294	0.271
4th	0.310	0.308	0.266	0.272	0.317	0.304
Roof	0.320	0.329	0.268	0.282	0.366	0.346

The four sets of six figures that are common to each of the three following sections (Section 5.2, Bin 1; Section 5.3, Bin 2; and Section 5.4, Bin 3) are discussed here. The first set (figures 5-1, 5-6 and 5-11) present interstory and roof drift data for the six models and the three bins. Data is presented as a distribution of maximum drifts resulting from the analysis with the 20 ground motion histories of that bin. The drifts are fitted with a lognormal distribution that is represented in the figure by five values, namely, the median, 16th and 84th percentile, minimum and maximum values. The dashed lines in figures 5-1, 5-6 and 5-11 represent the approximate yield drift in the story (see Chapter 4 for details). The second set of figures (figures 5-2, 5-7 and 5-12) present maximum total floor acceleration data. In the third set of figures (figures 5-3, 5-8 and 5-13) data is presented as a performance space. The performance spaces are adapted from the distributions presented in the first two sets of figures and are meant to be a very basic way of measuring the effectiveness of each system in reducing the input EDPs on all classes of NCCs (e.g., acceleration critical components, drift critical components and coupled components) by pairing the acceleration at a floor (A*) with the drift of the story immediately below (ID*). These spaces could easily be adapted to different acceleration and drift pairs (A* and ID*). Each performance space is bounded by the 16th and 84th percentile values of each metric. In the presentation of performance spaces in Chapter 4, those spaces created using the models equipped with base-isolation were tightly grouped near the origin (e.g., figure 4-4). In Chapter 5, the performance spaces of the isolated systems are shown at a larger scale, making it possible to compare the response of the different base-isolation systems. Figures 5-4, 5-9 and 5-14 present median total floor acceleration response spectra at each floor level in the model.

Figures 5-5, 5-10 and 5-15 present hysteresis loops for isolators from selected ground motions from Bin 1 (LA 42), Bin 2 (LA 1) and Bin 3 (LA 27) respectively. Hystereses from these three earthquake histories were presented because the peak displacements were close to the median peak displacement for the bin under consideration.

5.2 Dynamic properties of Models M11 through M16

Models M11 through M16 were described in Section 3.2. The viscoelastic isolation systems of Models M11 and M12 were assigned a period of 2.5 seconds and the isolation systems of Models M13 and M14 were assigned a period of 3.5 seconds, both assuming a rigid superstructure. Because the isolators in Models M11 through M14 are modeled as linear viscoelastic elements, the assigned period is constant for all levels of shaking. This is not true of the models equipped with bilinear isolators (M15 and M16). Models M15 and M16 were assigned second-slope (post-yield) periods of 2.5 seconds and 3.5 seconds, respectively. Because the isolator model is bilinear, the effective period of the isolation system depends on the magnitude of the isolator displacement. Table 5-1 presents the effective period (T_{eff}) of the different isolation systems for the three bins of shaking, calculated using the equation presented in FEMA 356 (FEMA, 2000):

$$T_{eff} = 2\pi\sqrt{\frac{m}{k_{eff}}} \tag{5.1}$$

where, k_{eff} is the secant stiffness of the isolation system at the median peak isolator displacement (Δ) for the bin under consideration, m is the total mass of the building; the superstructure is assumed to be rigid for the calculation. The flexibility of the superstructure increased the 1st mode period of Models M11 and M12, and Models M13 and M14, from 2.5 seconds and 3.5 seconds, to 2.6 seconds and 3.57, seconds respectively (as reported in table 3-2).

The viscoelastic isolator models were assigned levels of damping (10% of critical in Models M11 and M13 and 20% of critical in M12 and M14) that are independent of the isolator displacement. The hysteretic damping provided by the bilinear isolator model of Models M15 and M16 varies with isolator displacement. Table 5-12 presents the effective damping (β_{eff}) of each isolation system at each level of shaking, calculated using the equation presented in FEMA 356 (FEMA, 2000):

$$\beta_{eff} = \frac{1}{2\pi}\frac{W_D}{k_{eff}\Delta^2} \tag{5.2}$$

where W_D is the energy dissipated (area of a hysteresis loop) in one cycle to the median peak isolator displacement (Δ) and k_{eff} is the secant stiffness of the isolator at the median peak isolator displacement Δ.

5.3 Bin 1: 50% exceedence in 50 years (50/50)[3]

As described in Section 5.1, distributions of maximum interstory and roof drifts from analysis using models M11 through M16 and the 50/50 bin of ground motions are presented in figure 5-1. Figure 5-1f also presents information on the maximum isolator displacements for models M11 through M16. Figure 5-2 presents maximum floor accelerations. Figure 5-2f presents peak base shear data, normalized by the total supported weight. Figure 5-3 combines the distributions of story drifts and floor accelerations into performance spaces. The coefficients of variation were calculated for each model for the 50/50 bin using the roof drift and the 2nd floor acceleration; the results are presented in table 5-3 and 5-4, respectively. Figure 5-4 presents averaged median floor acceleration spectra for the six base-isolated models analyzed using the 50/50 bin. Tables 5-5 and 5-6 present median spectral accelerations over the frequency ranges of 1 Hz to 10 Hz and 10 Hz to 20 Hz, respectively.

Based on the information presented a number of trends can be identified regarding the impact of isolation-system choice on demands on NCCs. Trends are presented below as a numbered list for organization and reference later in this chapter.

1. Smaller story drifts and floor accelerations develop in the models with the most flexible isolation systems. This is an expected result because 1) spectral acceleration demands are lower at longer periods; and 2) the superstructure acts more like a rigid block when the stiffness of the isolation system is lower (Naeim and Kelly, 1999). The maximum story drifts and floor accelerations are highest in the models with bilinear isolators (Models M15 and M16) because they have the shortest effective periods (see table 5-1).

[3] Descriptions of the SAC Los Angeles bins of ground motions are provided in Chapter 3 of this report.

2. Adding viscous damping decreases the displacement across the isolators but increases the demands on NCCs because damping forces contribute to the shear force in the super-structure.
3. The values of effective period (T_{eff}) presented in table 5-1 for the bilinear models (M15 and M16) were calculated using median peak displacements (established in figure 5-1). For the isolator hysteresis of figure 5-5, the isolator attains values close to the peak displacement only once in the history and displacements in most cycles are substantially less than 50% of the maximum value. This observation explains the location of the significant peak in figure 5-4 at a frequency of approximately 0.7 Hz (corresponding to a period of about 1.4 seconds): the vibration frequency of the bilinear isolation system based on its pre-yield stiffness.
4. The ordinates of the total floor acceleration response spectra from Models M15 and M16 are higher, and in some cases substantially higher, than those for the linear viscoelastic systems across the frequency range of 0.5 Hz to 100 Hz.
5. The increase in damping (10% to 20%) in the linear viscoelastic isolators (Model M11 to M12 and M13 to M14) has little effect on the median spectral accelerations averaged over the frequency ranges of 1 to 10 Hz and 10 Hz to 20 Hz, although median spectral accelerations are lowest for the 10% damped isolation systems. The increase in second-slope period from 2.5 seconds to 3.5 seconds (Model M15 to M16) has little effect on the median spectral accelerations.
6. The coefficients of variation in maximum roof drift and maximum total floor acceleration are smallest for the bilinear isolators (Models M15 and M16).

5.4 Bin 2: 10% exceedence in 50 years (10/50)

The results of analysis of models M11 through M16 subjected to the earthquake histories of the 10/50 bin are presented in this section. The distributions of maximum interstory and roof drifts are presented in figure 5-6; figure 5-6f presents information on the maximum isolator displacements for Models M11 through M16. The distributions of maximum total floor accelerations over the height of the models are shown in figure 5-7. Figure 5-7f presents peak

base shear data, normalized by the total supported weight. Figure 5-8 combines the distributions from figures 5-6 and 5-7 into performance spaces. The coefficients of variation were calculated for each model for the 10/50 bin using the roof drift and the 2nd floor acceleration; results are presented in table 5-3 and 5-4, respectively. Figure 5-9 presents the floor total acceleration spectra. Tables 5-7 and 5-8 present averaged median spectral accelerations over the frequency ranges of 1 Hz to 10 Hz, and 10 Hz to 20 Hz, respectively. Figure 5-10 presents isolator hysteresis for one of the 10/50 earthquake histories. From these data some trends can be observed, namely,

1. Consistent with the results of analysis with Bin 1, peak story drifts and peak floor accelerations are smallest in the isolated models with the longest effective period (Models M13 and M14).
2. Increasing the viscous damping (10% to 20%) in the models equipped with viscous isolators (Model M11 to M12 and M13 to M14) reduced the isolator displacement and increased the normalized base shear, story drifts and peak total floor accelerations very slightly.
3. The peak in the floor spectra in figure 5-4 at 1.4 seconds for the bilinear isolators at 50/50 shaking is substantially diminished, in a relative sense, for the more severe 10/50 shaking as seen in figure 5-9 because the 10/50 shaking produces 2- to 3-fold increases in isolator displacement. The increase in isolator displacement reduces the effective stiffness of the isolation system and increases the effective period of the isolated building.
4. In the frequency range of 10 to 20 Hz, the ordinates of the total floor acceleration response spectra from Models M15 and M16 are comparable to or less than those of Models M11 and M12 (2.5-second effective period isolators) but are greater than those of Models M13 and M14 (3.5-second effective period isolators).
5. The increase in second-slope period of the bilinear isolators from 2.5 seconds to 3.5 seconds (M15 to M16) results in only modest (<10%) reductions in the median spectral accelerations.
6. The coefficients of variation in maximum roof drift and maximum total floor acceleration are smallest for the bilinear isolators (Models M15 and M16).

5.5 Bin 3: 2% exceedence in 50 years (2/50)

This section presents results from analysis using the 2/50 bin of earthquake histories. Figures 5-11 and 5-12 illustrate the distributions of maximum drift and acceleration response. Figure 5-13 combines the distributions of drift and acceleration into performance spaces. The coefficients of variation were calculated for each model for the 2/50 bin using the roof drift and the 2nd floor acceleration; results are presented in table 5-3 and 5-4, respectively. Floor acceleration spectra are presented in figure 5-14. Averaged median values of spectral acceleration over the frequency ranges 1 Hz to 10 Hz, and 10 Hz to 20 Hz, are presented in tables 5-9 and 5-10, respectively. Figure 5-15 presents isolator hysteresis for one of the 2/50 earthquake histories. A number of trends can be identified from this data.

1. Peak story drifts and peak floor accelerations are smallest in the isolated models with the longest effective period (Models M13 and M14).
2. Increasing the viscous damping (10% to 20%) in the models equipped with linear viscous isolators (Model M11 to M12 and M13 to M14) reduced the isolator deformation but resulted in a slight increase in the normalized base shear, story drifts and peak total floor accelerations.
3. The ordinates of the total floor acceleration response spectra from Models M14 and M15 are comparable to or less than those of Models M11 and M12 (2.5-second effective period isolators) but are greater than those of Models M13 and M14 (3.5-second effective period isolators) across a broad frequency range.
4. The increase in second-slope period of the bilinear isolators from 2.5 seconds to 3.5 seconds (M15 to M16) produces significant reductions in median spectral accelerations.
5. For the 2/50 bin, the coefficients of variation in maximum roof drift and maximum total floor acceleration for the bilinear isolators (Models M14 and M15) are comparable to those for the linear viscous models.

TABLE 5-9: Average Median Spectral Acceleration,1 to 10 Hz, for the 2/50 Bin

	Model					
Floor	M11	M12	M13	M14	M15	M16
Ground	0.658	0.704	0.474	0.545	0.759	0.719
2nd	0.584	0.607	0.425	0.460	0.546	0.461
3rd	0.567	0.585	0.419	0.443	0.528	0.435
4th	0.579	0.609	0.429	0.459	0.581	0.497
Roof	0.622	0.667	0.447	0.495	0.703	0.620

TABLE 5-10: Average Median Spectral Acceleration, 10 to 20 Hz, for the 2/50 Bin

	Model					
Floor	M11	M12	M13	M14	M15	M16
Ground	0.573	0.593	0.424	0.464	0.561	0.517
2^{nd}	0.546	0.559	0.413	0.424	0.507	0.416
3^{rd}	0.537	0.549	0.412	0.416	0.512	0.412
4^{th}	0.563	0.568	0.421	0.430	0.532	0.433
Roof	0.579	0.600	0.428	0.453	0.577	0.489

5.6 Performance of isolated Models M11 through M16 across three levels of shaking

The influence of three basic seismic isolator characteristics, namely, effective stiffness, equivalent viscous damping and model type, on both the response of a hospital building frame and the demands on NCCs in the building was studied. Broad conclusions cannot be drawn from the study because a) no seismic isolator in the marketplace today displays the exact characteristics of any of the models (M11 through M16), b) only one building was studied, and c) earthquake histories for only one site were used for the analysis. However, on the basis of the results presented in this section:

1. No single isolator type appears to offer superior performance across all levels of earthquake shaking, where superior performance here is measured in terms of lowest interstory drift, lowest peak total floor acceleration, and lowest floor acceleration spectral demands across a range of frequencies that would include most NCCs.
2. The addition of viscous damping to an isolation system will reduce isolator displacements but might increase story drifts, peak total floor accelerations and peak spectral accelerations.

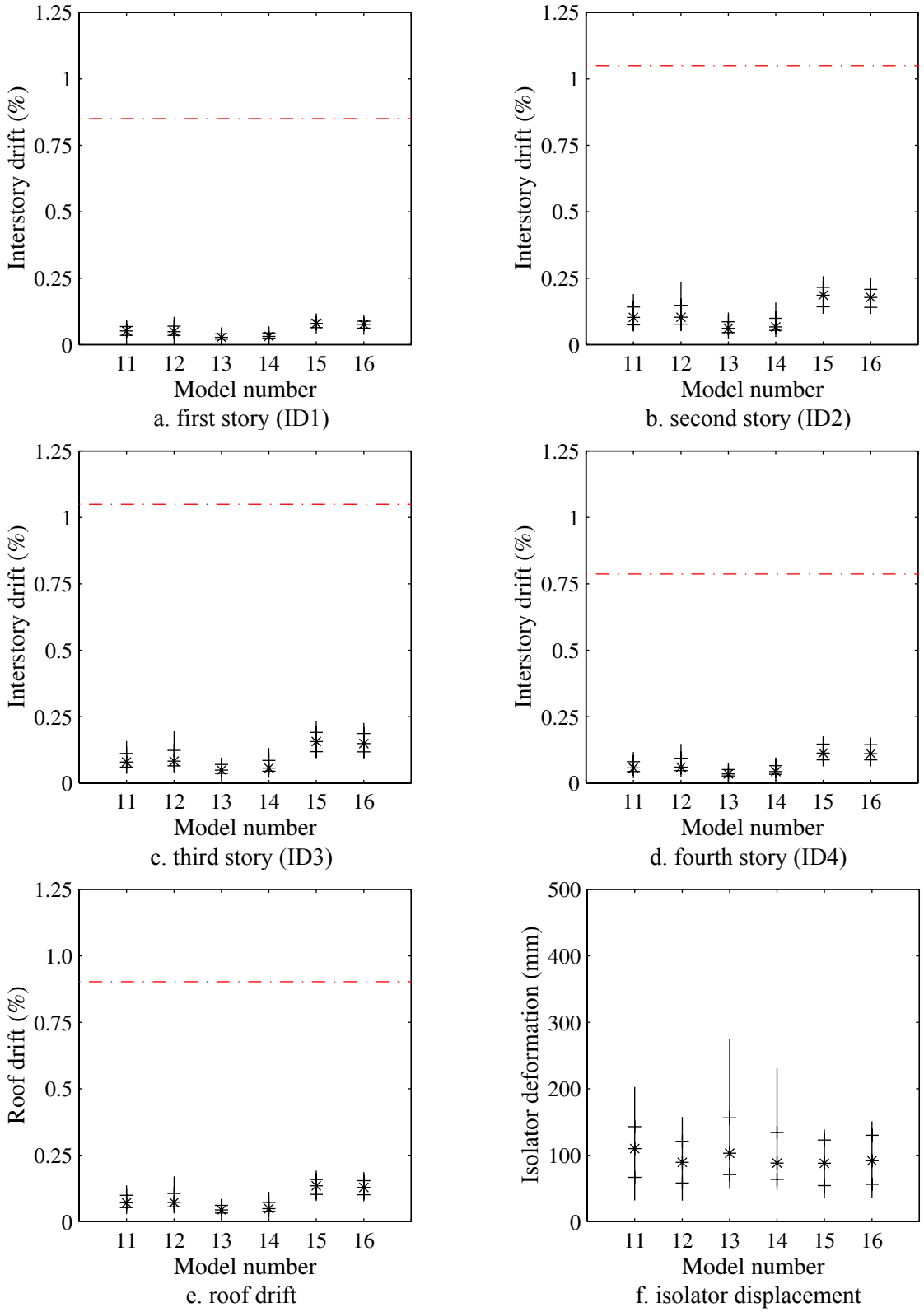

FIGURE 5-1: Interstory and Roof Drifts for the 50/50 Bin

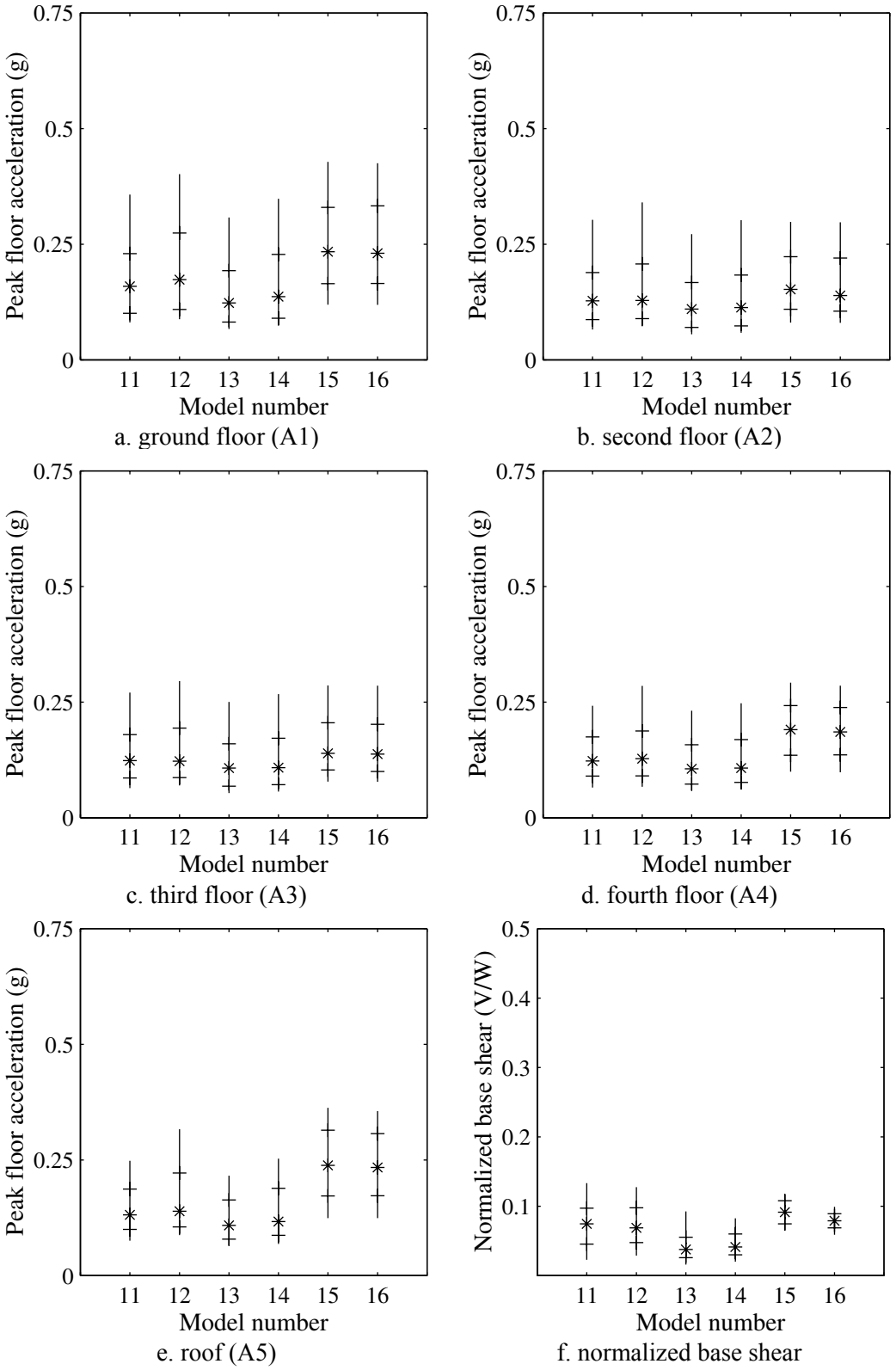

FIGURE 5-2: Maximum Total Floor Accelerations for the 50/50 Bin

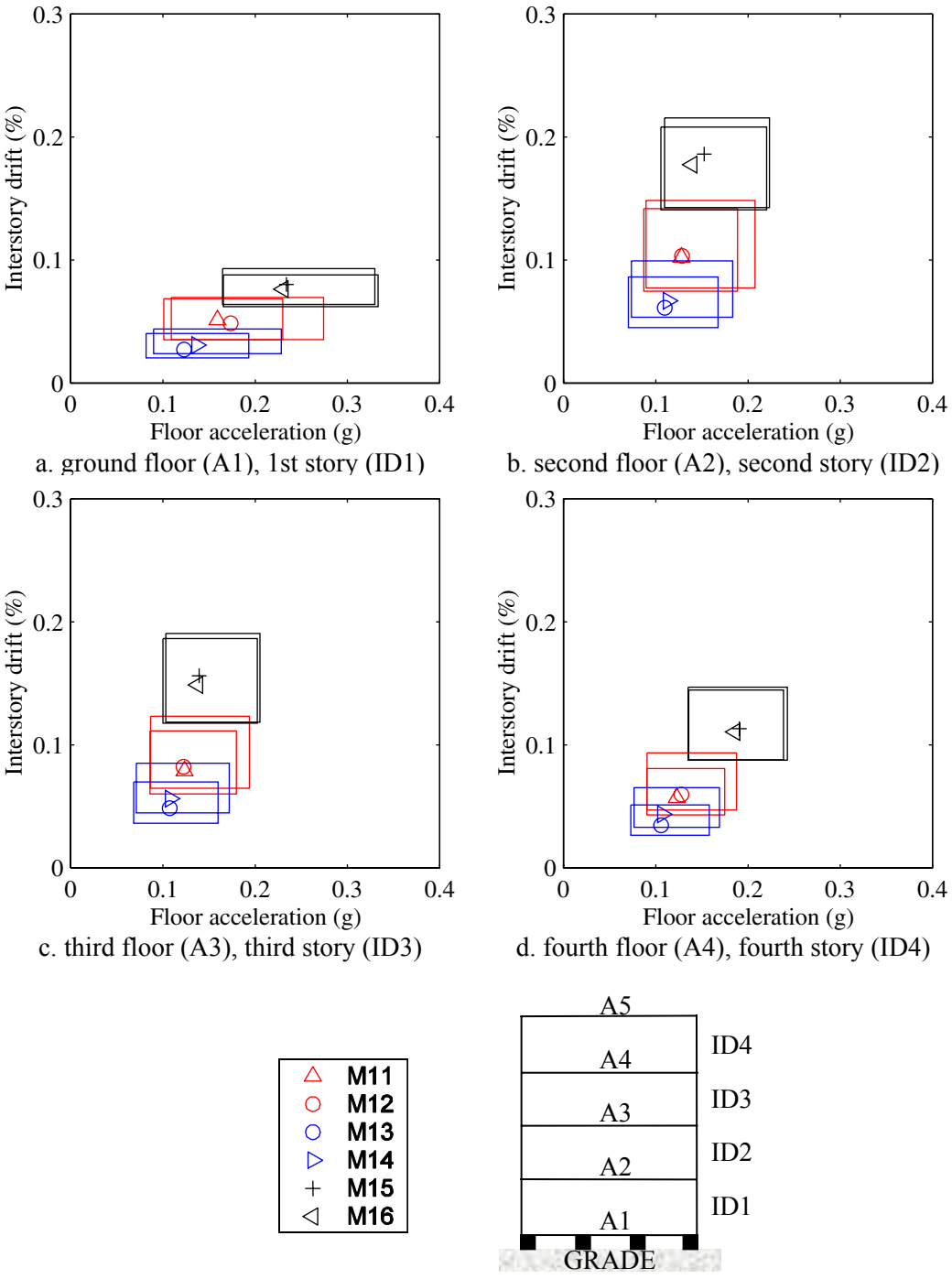

a. ground floor (A1), 1st story (ID1)

b. second floor (A2), second story (ID2)

c. third floor (A3), third story (ID3)

d. fourth floor (A4), fourth story (ID4)

e. legend and illustration of quantities

FIGURE 5-3: Performance Spaces for the 50/50 Bin

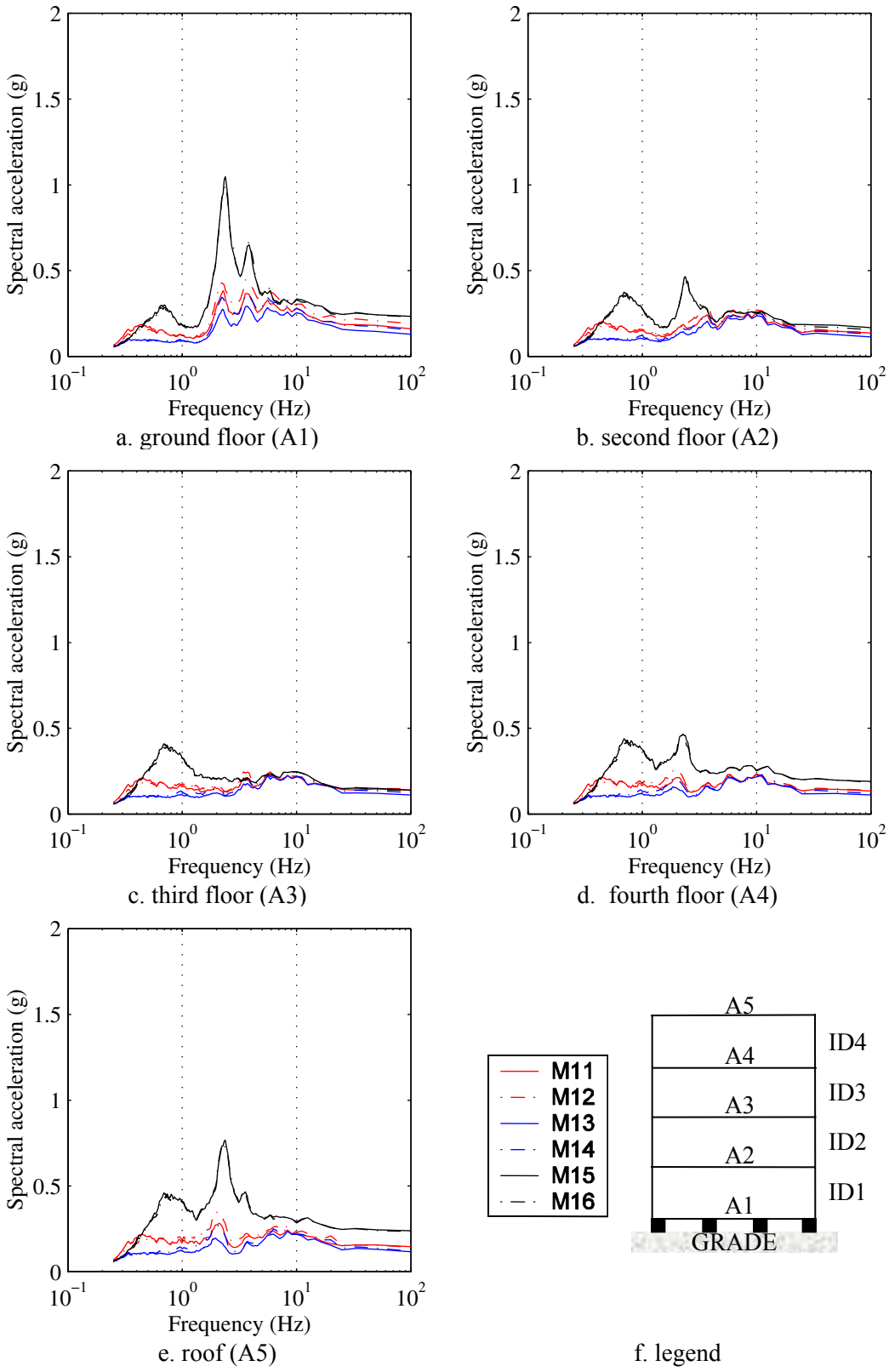

FIGURE 5-4: Total Floor Acceleration Response Spectra for the 50/50 Bin

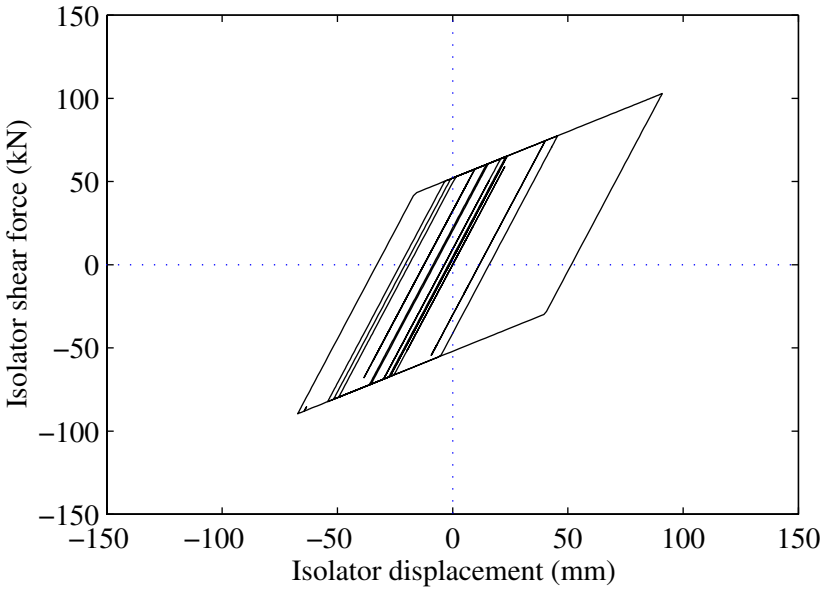

a. Model M15

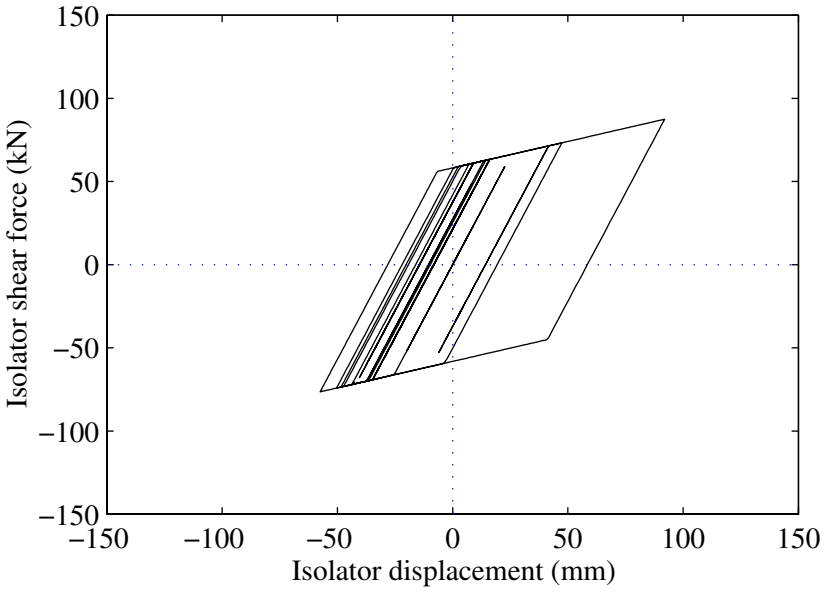

b. Model M16

FIGURE 5-5: Typical Isolator Hysteresis for LA 42 (from the 50/50 bin)

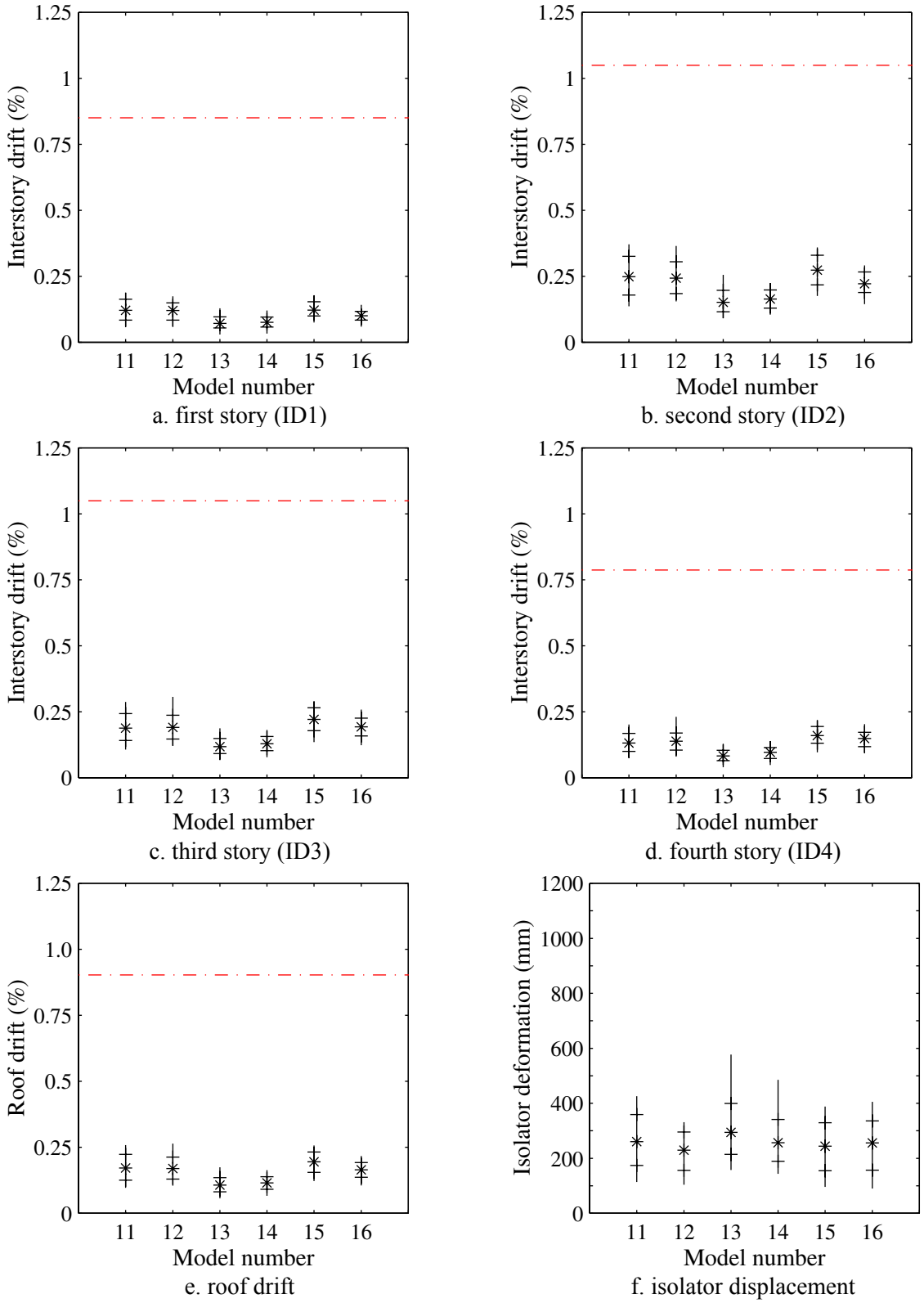

FIGURE 5-6: Interstory and Roof Drifts for the 10/50 Bin

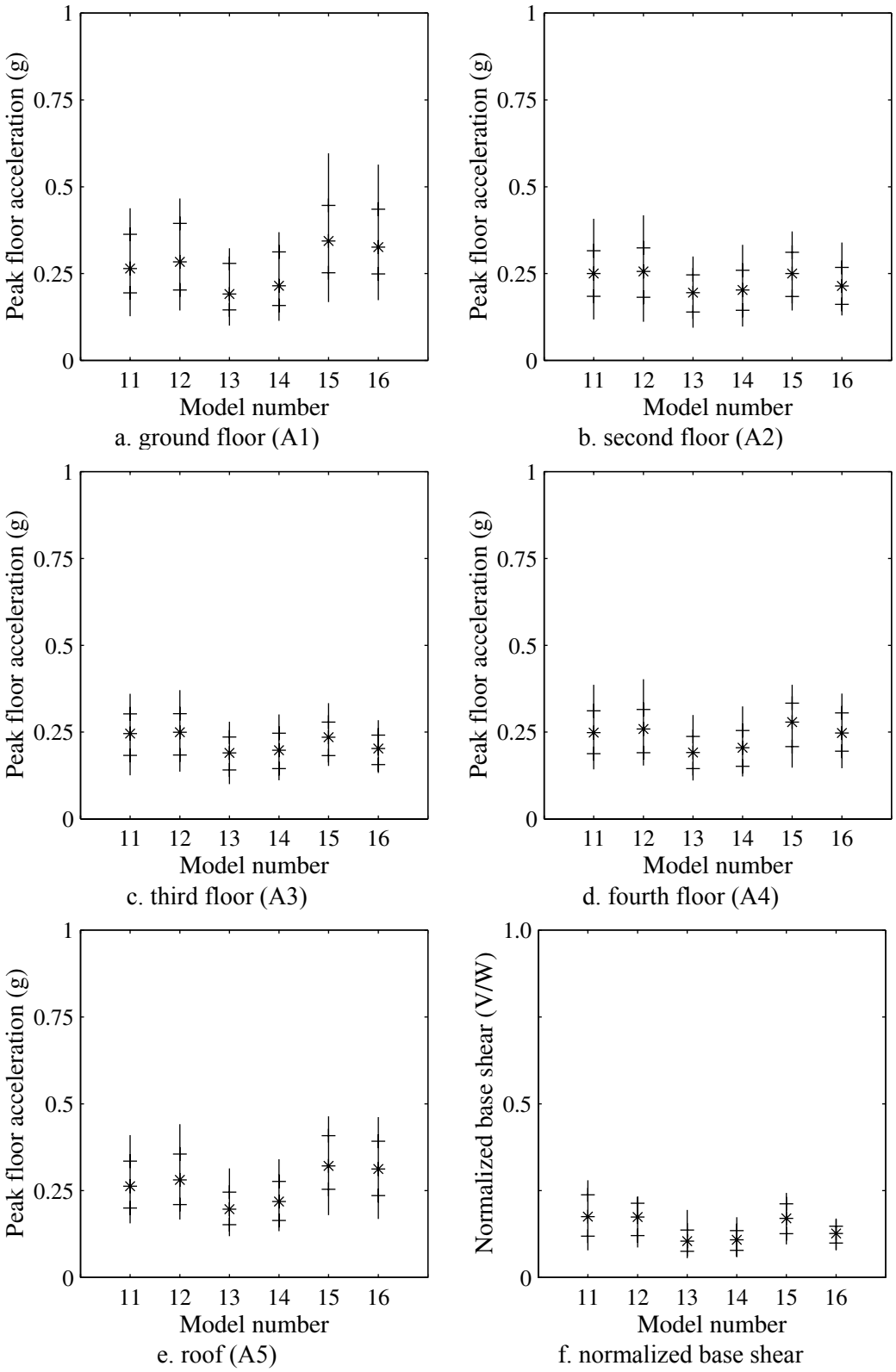

FIGURE 5.7: Maximum Total Floor Accelerations for the 10/50 Bin

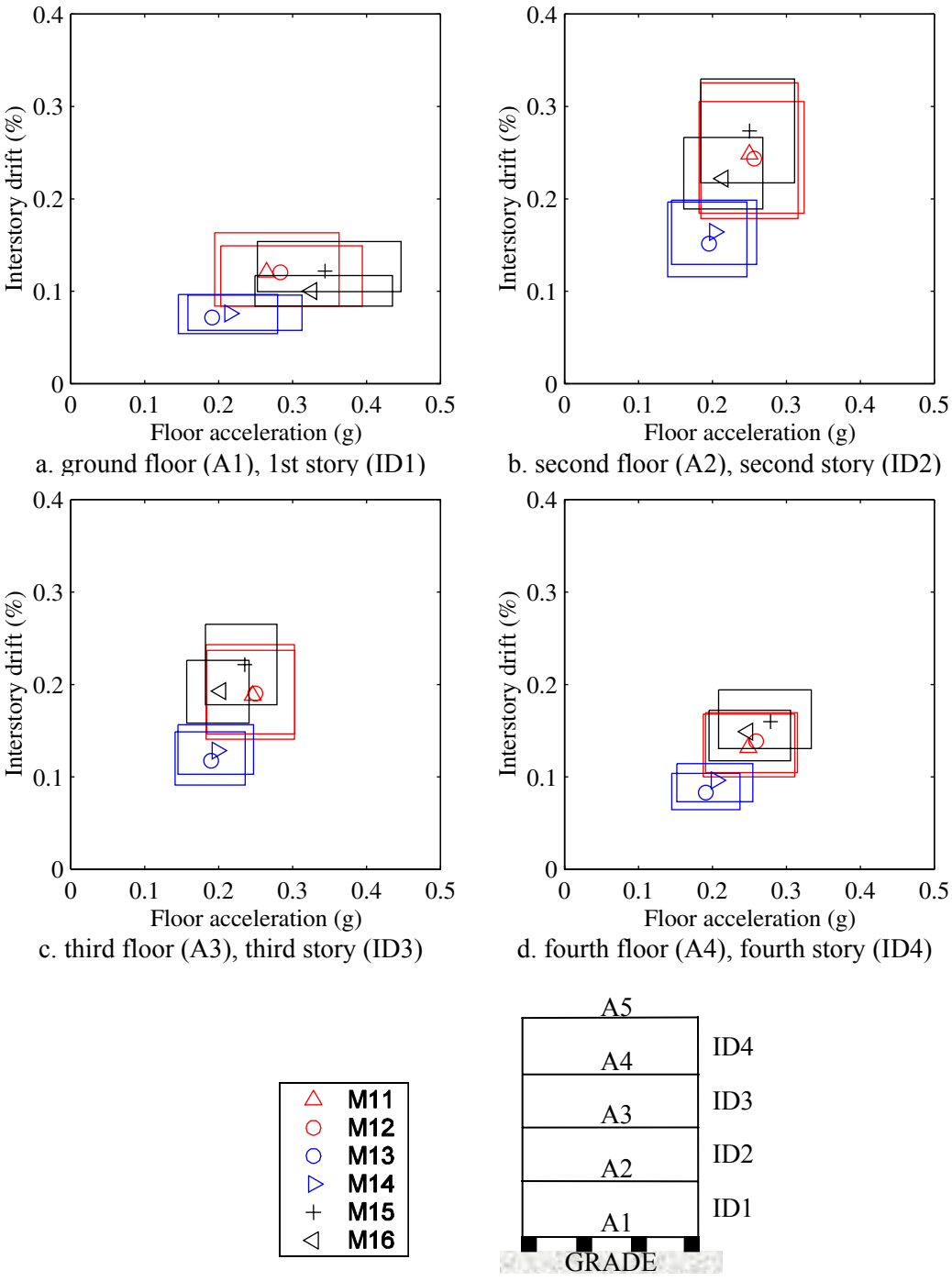

a. ground floor (A1), 1st story (ID1)

b. second floor (A2), second story (ID2)

c. third floor (A3), third story (ID3)

d. fourth floor (A4), fourth story (ID4)

e. legend and illustration of quantities

FIGURE 5-8: Performance Spaces for the 10/50 Bin

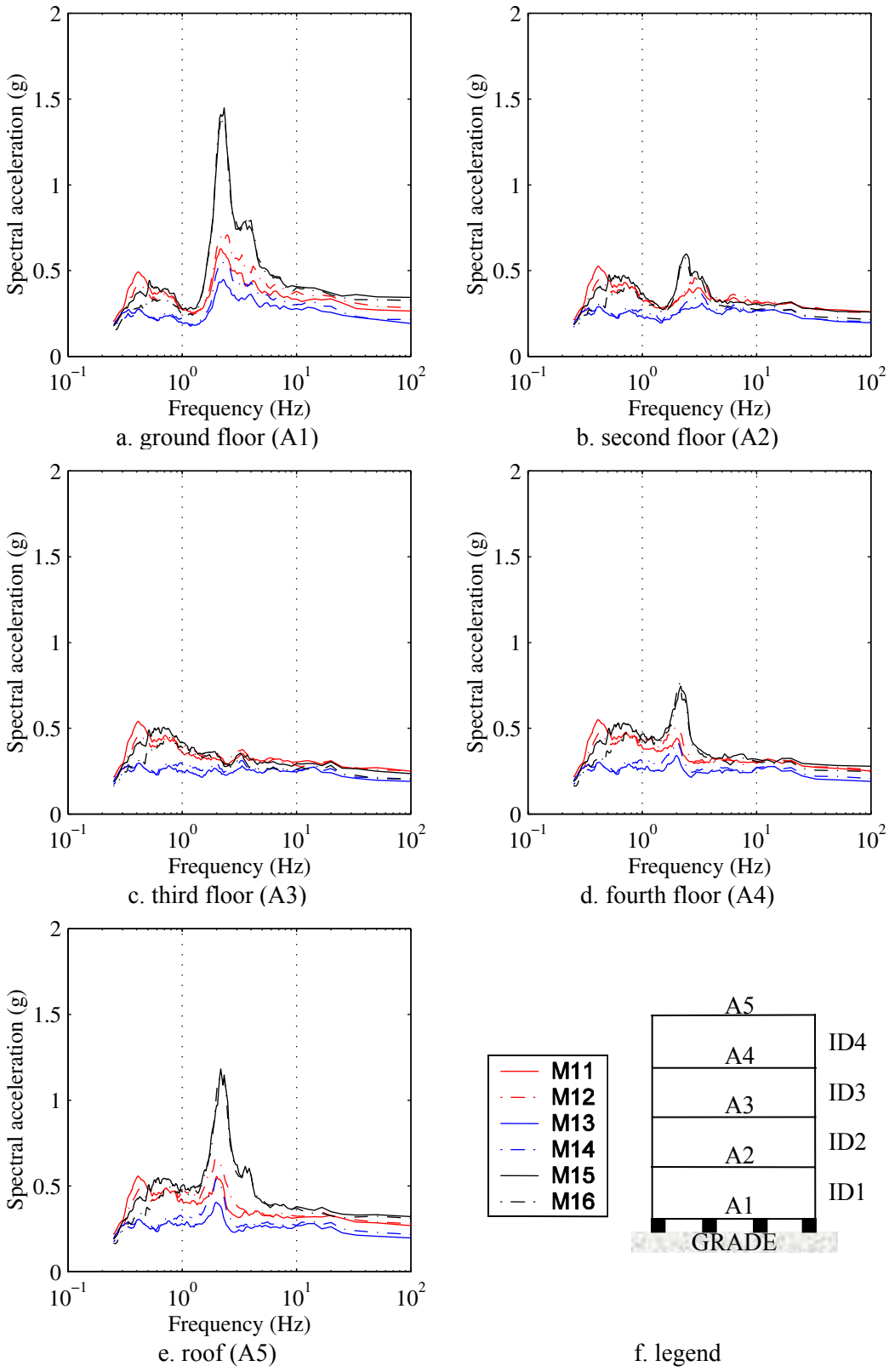

FIGURE 5-9: Floor Total Acceleration Response Spectra for the 10/50 Bin

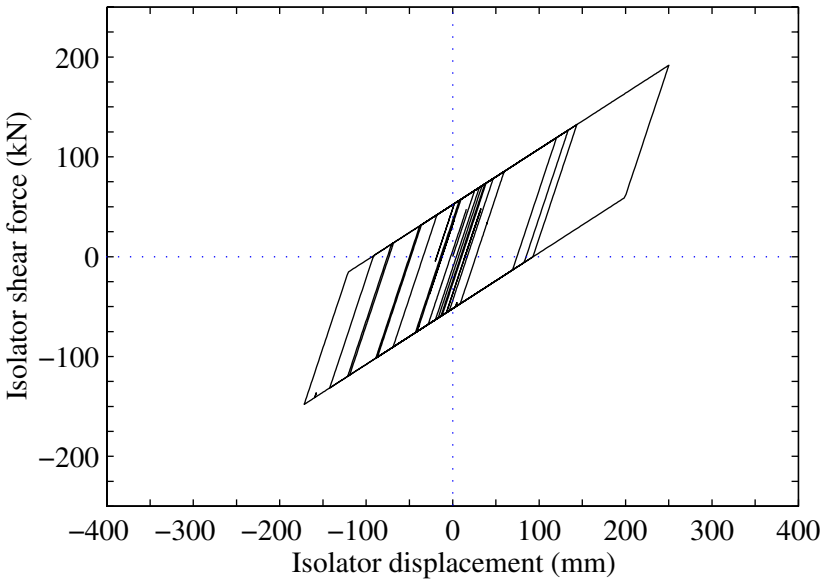

a. Model M15

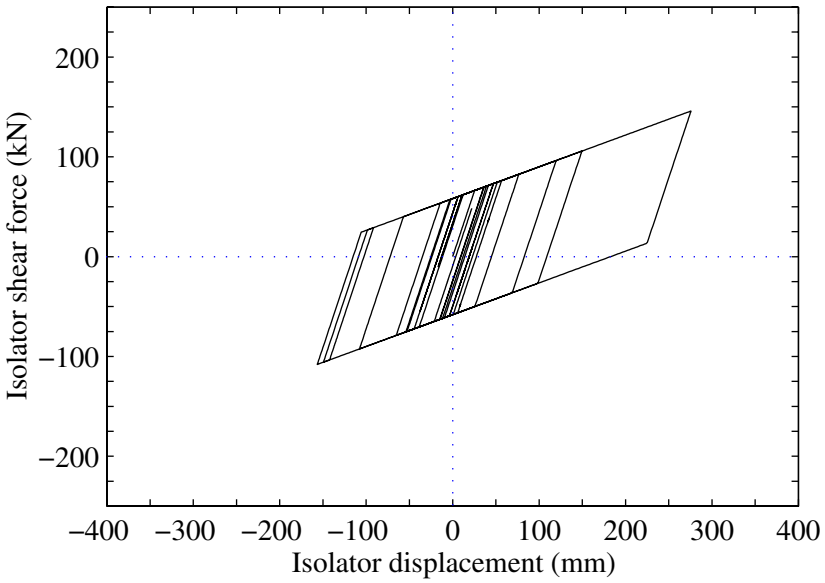

b. Model M16

FIGURE 5-10: Typical Isolator Hysteresis for LA 1 (from the 10/50 bin)

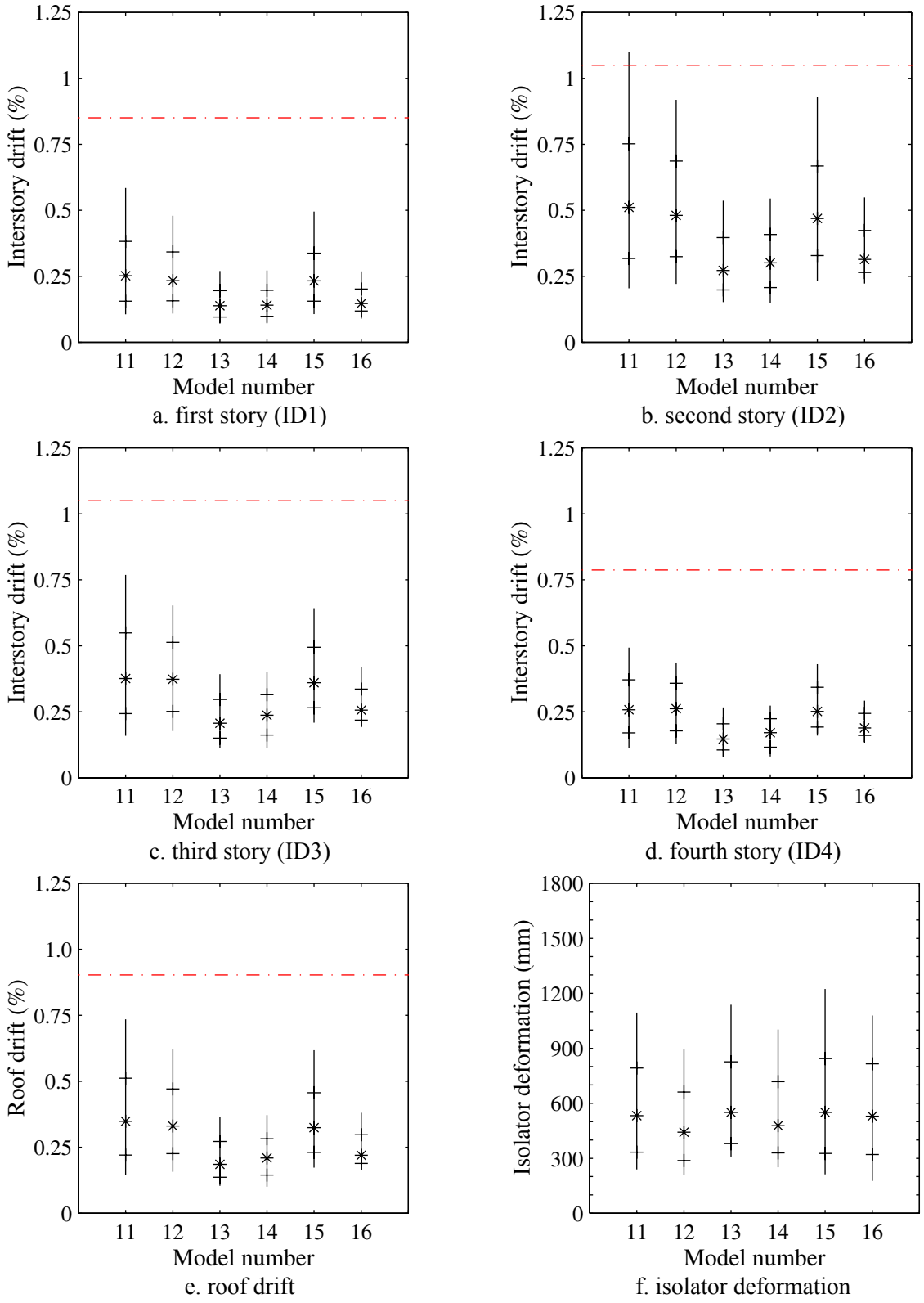

FIGURE 5-11: Interstory and Roof Drifts for the 2/50 Bin

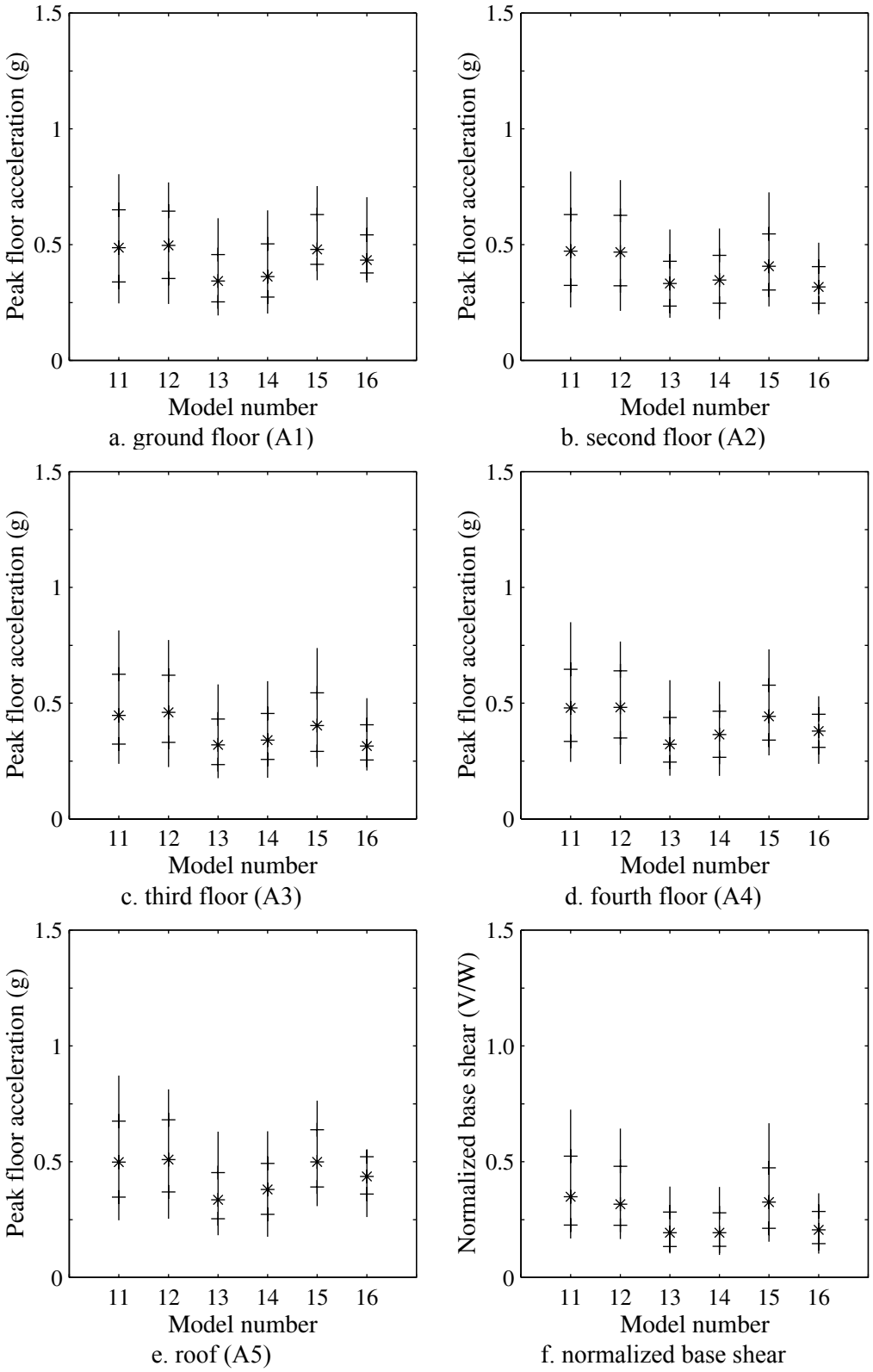

FIGURE 5-12: Maximum Total Floor Accelerations for the 2/50 Bin

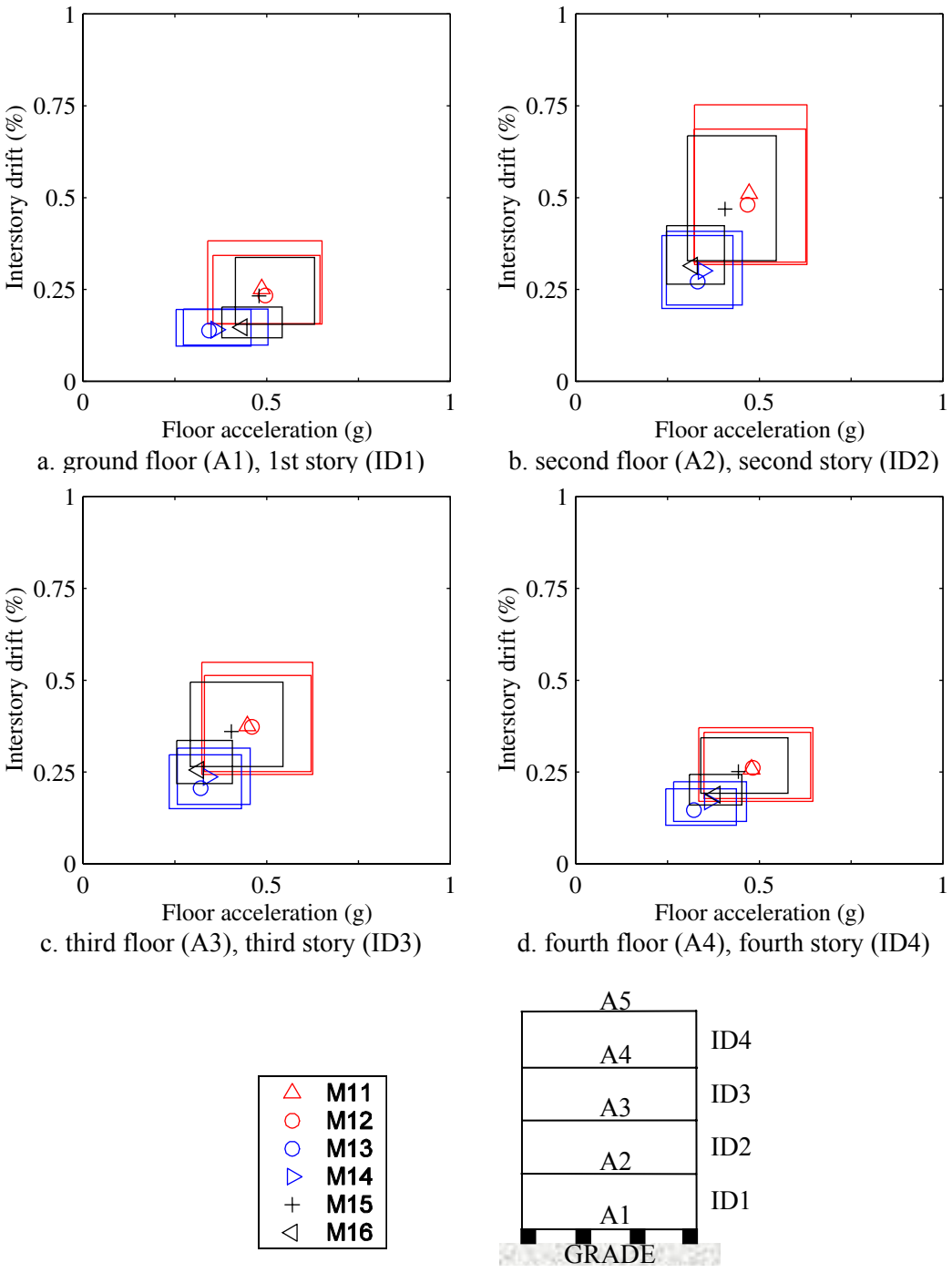

a. ground floor (A1), 1st story (ID1)

b. second floor (A2), second story (ID2)

c. third floor (A3), third story (ID3)

d. fourth floor (A4), fourth story (ID4)

e. legend and illustration of quantities

FIGURE 5-13: Performance Spaces for the 2/50 Bin

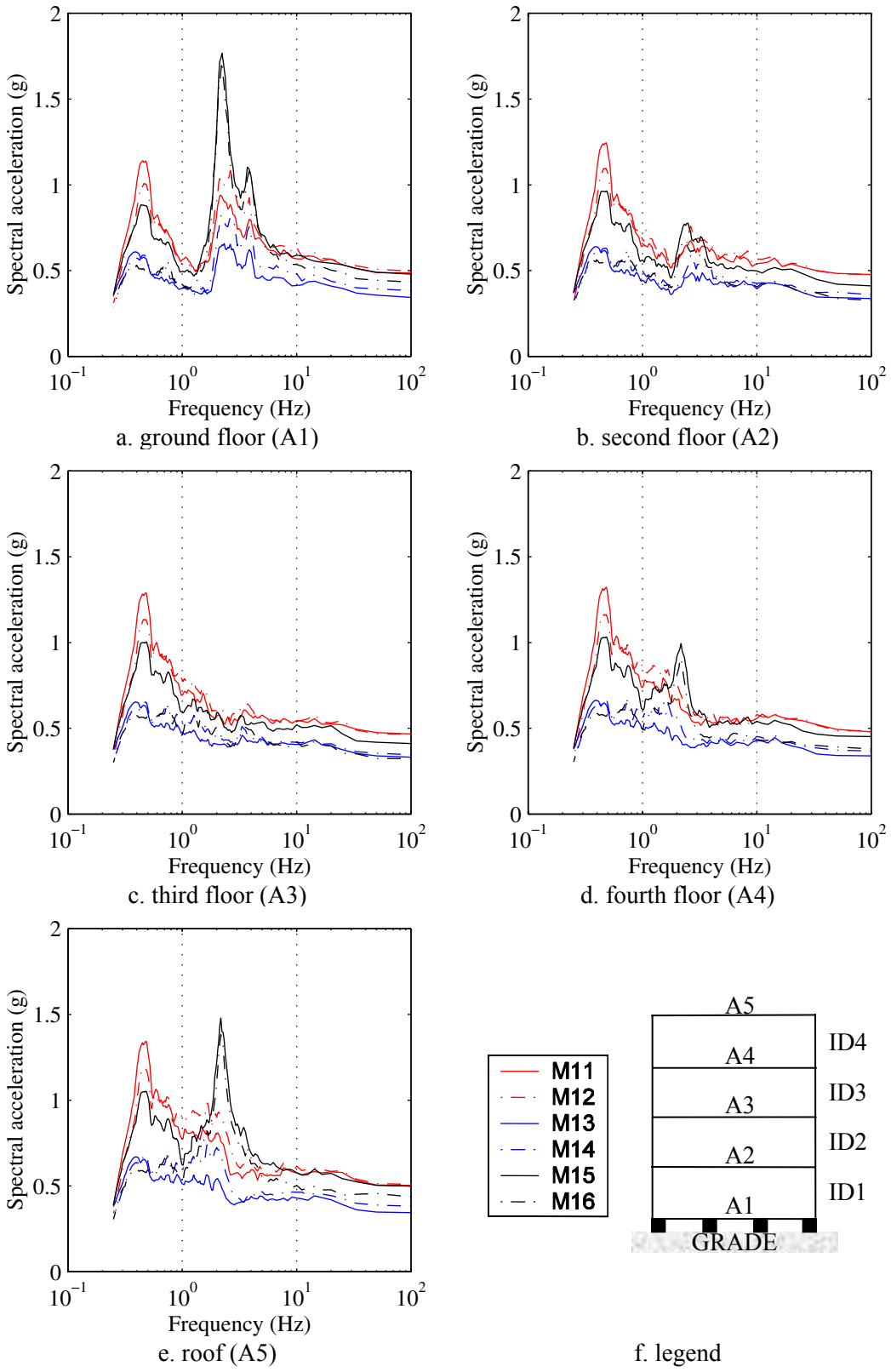

FIGURE 5-14: Floor Total Acceleration Response Spectra for the 2/50 Bin

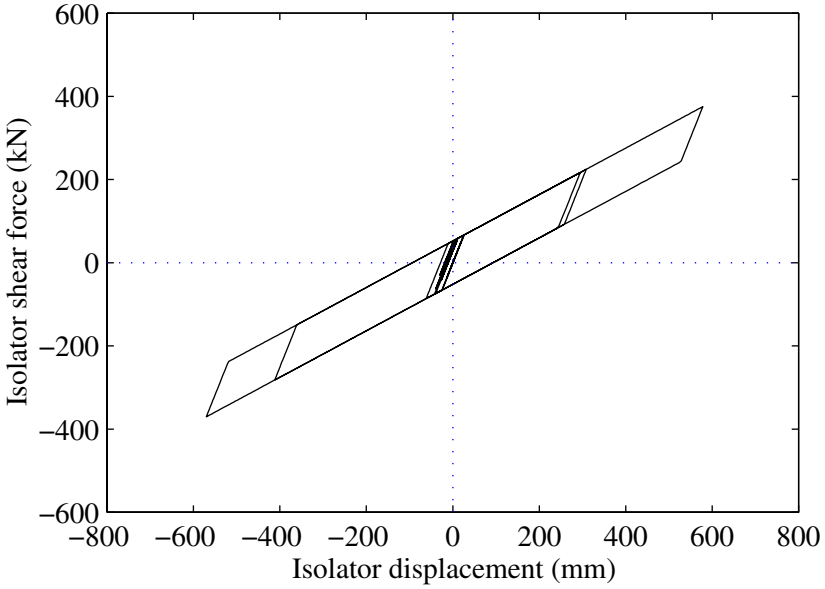

a. Model M15

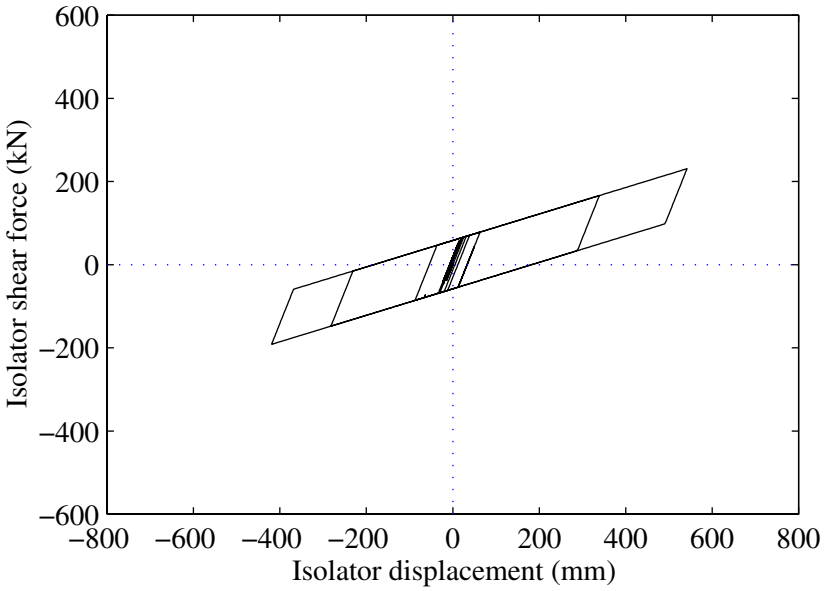

b. Model M16

FIGURE 5-15: Typical Isolator Hysteresis for LA 27 (from 2/50 bin)

CHAPTER 6

SUMMARY AND CONCLUSIONS

6.1 Summary

New tools for performance-based earthquake engineering of buildings are being developed by Multidisciplinary Center for Earthquake Engineering Research (MCEER), the Pacific Earthquake Engineering Research (PEER) center and the ATC-58 project. To date, these next-generation tools have focused on assessing the performance of buildings whose components, both structural and nonstructural, have been fully defined. New probability-based performance assessment procedures have been developed to predict damage and economic loss.

The next step in preparing the next-generation tools for performance-based earthquake engineering is the development of performance-based design tools that will enable the structural engineer to design a building (from a blank sheet of paper) to achieve, albeit approximately, specific levels of performance (and likely loss). The development of design tools is necessary to prevent a large number of performance-assessment and re-design iterations. To date, little work has been completed on performance-based design, outside of the SAC Steel Project, which focused solely on steel moment frames and did not address nonstructural components and contents (NCCs). The study described in this report sought to lay some of the ground work for performance-based design by assessing a) the response of different seismic framing systems to a broad range of earthquake shaking intensity, and b) the impact of framing-system choice on the demands on NCCs.

Assessment of demands on NCCs was the focus of the work described herein. In most building structures, less than 20% of the total expenditure is related to structural framing. More than 80% of the total investment in a new building is in the NCCs. Because performance-based earthquake

engineering tools must facilitate the calculation of direct and indirect economic losses, all sources of potential loss must be considered in the design process. Paying scant attention to more than 80% of the total investment in performance-based design, by not considering the NCCs, would make no sense.

The traditional design process that focuses 95% of the structural-engineering design effort on less than 20% of the total expenditure (i.e., the structural framing) is inadequate in a performance-oriented design environment. *A new design paradigm is proposed for performance-based earthquake engineering*, where the choice of framing system is driven by the goal to minimize direct and indirect losses from earthquake shaking. In most cases, these losses will be best controlled by minimizing the seismic demands (drifts, velocity and acceleration) on NCCs. Because the choice of seismic framing system, together with the earthquake hazard, will determine the demands on NCCs, *superior* seismic framing systems must be identified. Two questions arise from this proposal, namely,

1. What performance metrics can and should be used to define a *superior* system?
2. What are the *superior* framing systems for those performance metrics?

To provide insight into the relationship between framing system choice and demands on NCCs, the MCEER Demonstration Hospital was selected for detailed analysis. A hospital building was chosen for evaluation because the investment in NCCs in hospital buildings generally exceeds 90% of the total construction cost, and losses following earthquake shaking will depend to a large degree on the performance of the NCCs. This four-story steel-framed hospital building is located in Northridge, California: a region prone to severe earthquake shaking. The baseline building was constructed as a steel moment-resisting frame in the early 1970s.

A total of 16 mathematical models were prepared for response-history analysis using three levels of earthquake shaking. Models were prepared for weak and strong moment-resisting frames, a braced frame, two frames equipped with fluid viscous dampers and six frames equipped with a total of three types of seismic isolators. These types of framing systems represent those used for

hospital construction in California at the time of this writing. Each model was analyzed using three bins of earthquake histories, each representing a distinct hazard level, namely, 50% exceedence in 50 years, 10% exceedence in 50 years and 2% exceedence in 50 years. The ground-motion histories were developed for the Los Angeles basin by others for the SAC Steel Project. Demands on NCCs were presented in the form of maximum story drifts, maximum peak total floor accelerations, performance points, performance spaces and total floor acceleration response spectra. Some preliminary observations and conclusions about the performance of the different framing systems are presented in the following section.

The performances of the twelve models analyzed in this report are compared in Tables 6.1 through 6.4 by ranking the maximum response of each model (1 = best; 11 = poorest). Rankings are presented for 2nd story and roof drift (Table 6.1), 2nd floor and roof peak total acceleration (Table 6.2), averaged median floor spectral acceleration over the frequency range of 1 to 10 Hz for the 2nd floor and roof (Table 6.3) and averaged median floor spectral acceleration over the frequency range of 10 to 20 Hz for the 2nd floor and roof (Table 6.4). Although the rankings vary slightly if other floors and story levels are used to compare responses, the differences in ranking are minor and the trends are unchanged.

Table 6.1: Rank based on drift response[1]

	50/50	10/50	2/50	50/50	10/50	2/50
Model	2nd story drift			Roof drift		
M3	8	7	7	8	8	8
M6	11	11	11	11	11	11
M7	10	9	9	10	10	10
M8	9	10	10	9	9	9
M9	7	8	8	7	7	8
M10	4	6	6	4	6	6
M11	3	4	5	3	4	5
M12	1	2	2	1	1	2
M13	2	1	1	2	2	1
M14	6	5	4	6	5	4
M15	5	3	3	5	3	3

1. 1 = best; 11 = poorest.

Table 6.2: Rank based on peak total floor acceleration[1]

	50/50	10/50	2/50	50/50	10/50	2/50
Model	2nd floor			Roof		
M3	11	11	11	11	11	11
M6	9	9	9	9	9	4
M7	10	10	10	10	10	10
M8	7	7	7	5	5	7
M9	8	8	8	6	8	9
M10	3	6	6	3	4	8
M11	4	5	5	4	3	6
M12	1	1	2	1	1	2
M13	2	1	2	2	2	1
M14	6	4	4	7	7	5
M15	5	3	1	8	6	3

1. 1 = best; 11 = poorest.

Table 6.3: Rank based on average median floor spectral acceleration, 1 to 10 Hz[1]

	50/50	10/50	2/50	50/50	10/50	2/50
Model	2nd floor			Roof		
M3	11	11	10	11	11	11
M6	8	9	8	9	9	8
M7	10	10	11	10	10	10
M8	7	7	7	5	5	5
M9	9	8	9	6	8	9
M10	3	6	6	3	4	6
M11	4	4	5	4	3	4
M12	1	1	2	1	1	1
M13	2	2	1	2	2	2
M14	6	5	4	7	7	7
M15	5	3	3	8	6	3

1. 1= best; 11 = poorest

Table 6.4: Rank based on average median floor spectral acceleration, 10 to 20 Hz[1]

	50/50	10/50	2/50	50/50	10/50	2/50
Model	2nd floor			Roof		
M3	11	11	11	11	11	11
M6	7	7	8	9	9	4
M7	10	10	10	10	10	10
M8	8	8	7	3	7	7
M9	9	9	9	6	8	9
M10	3	6	6	5	5	8
M11	4	5	5	4	3	6
M12	1	3	3	1	2	2
M13	2	1	1	2	1	1
M14	6	4	4	7	6	5
M15	5	2	2	8	4	3

1. 1= best; 11 = poorest

6.2 Conclusions

Conclusions are drawn below regarding the influence of framing-system choice on the demands on NCCs. Strictly speaking, these conclusions are only valid for the building studied, the site in Southern California and response to three levels of earthquake shaking. Other framing systems should be considered (e.g., M7 with much larger braces; M9 with more damping; M3 with greater strength and stiffness) in a more extensive study. Alternate building geometries should be considered similar to those evaluated in the SAC Steel Project. Different bins of earthquake histories representative of shaking in other cities in the United States should be used for the analysis. These issues aside, the important conclusions from this study are:

1. Performance spaces are a most useful tool for comparing the performance of different framing systems and demands on different NCCs. Performance-spaces should be defined for all major classes of NCCs.
2. The three levels of earthquake shaking (Bin 1: 50/50; Bin 2: 10/50; and Bin 3: 2/50) used in this study cover a broad range of earthquake shaking, from *frequent* to *very rare* (SEAOC, 1995). Framing systems that perform well for all levels of earthquake shaking are likely *superior* framing systems.
3. For the 50/50 shaking, all framing systems equipped with protective hardware (unbonded braces, fluid viscous dampers and seismic isolators) suffer no structural damage. The base-isolated models performed best in terms of the smallest demands on the NCCs. Of the non-isolated models (Models M3, M6, M7, M8, M9 and M10), the buildings equipped with fluid viscous dampers (Models M9 and M10) show superior performance; story drifts, peak total floor accelerations, and averaged median floor spectral accelerations are generally minimized in Models M9 and M10.
4. For the 10/50 shaking, damage is sustained by both traditional (conventional) moment frames (Models M3 and M6). Large story drifts are sustained by the weak and flexible 1960s-vintage moment frame (Model M6). The protective devices reduce substantially or eliminate structural damage in these conventional moment frames. The base-isolated

models performed best with the smallest demands on the NCCs. Of the non-isolated models (Models M3, M6, M7, M8, M9 and M10), the buildings equipped with fluid viscous dampers (Models M9 and M10) show superior performance.

5. For the 2/50 shaking, only the base-isolated frames (Models M11 through M16) suffer no structural damage. Demands on the NCCs are minimized in the base-isolated buildings. The range of peak floor accelerations across all models is smaller for the 2/50 shaking than the 10/50 and 50/50 shaking because yielding in the non-isolated frames limits the peak floor accelerations. The addition of fluid viscous dampers to the weak and flexible moment frame (Model M6) led to substantial reductions in story drifts and modest reductions in floor accelerations.
6. Across all three levels of earthquake shaking, the base-isolated models offer *superior* performance as measured by smallest story drifts, peak total floor accelerations, and floor acceleration response spectral ordinates. Tables 6.1 through 6.4 rank the 6 base-isolated models in the top 6 of 11 in nearly all categories for each bin of earthquake shaking. Of the non-isolated models, the frames equipped with fluid viscous dampers offer *superior* performance.
7. No single base-isolated frame offers superior performance across all three levels of earthquake shaking. The smallest demands on NCCs are recorded for the frames equipped with 3.5-second effective-period seismic isolators. (Whether such an isolation system is feasible is matter for debate.) Of the four remaining base-isolated frames, the 2.5-second effective period isolators (Models M10 and M11) outperform the bilinear isolators (Models M14 and M15) for the frequent 50/50 shaking and vice-versa for the very rare 2/50 shaking.

CHAPTER 7

REFERENCES

Astrella, M. and A. S. Whittaker, 2004, "Changing the paradigm for performance-based seismic design," *Proceedings*, International Workshop on Performance Based Seismic Design, Report PEER 2004/05, Pacific Earthquake Engineering Research Center, Bled, Slovenia.

Badillo-Almaraz, H., 2003, "Seismic Fragility Testing of Suspended Ceiling Systems," Master's Thesis, Department of Civil, Structural and Environmental Engineering, University at Buffalo, NY.

Badillo, H., A. S. Whittaker and A. M. Reinhorn, 2004, "Seismic qualification and fragility testing of suspended ceiling systems," *Proceedings*, 13th World Conference on Earthquake Engineering, Paper 1053, Vancouver, B.C., Canada.

Borzorgnia, Y. and V. V. Bertero (Eds.), 2004, *Earthquake Engineering,* CRC Press, Boca Raton, FL.

Bruneau, M., S. Chang, R. Eguchi, G. Lee, T. O'Rourke, A. Reinhorn, M. Shinozuka, K. Tierney, W. Wallace, D. von Winterfelt, 2003, "A framework to quantitatively assess and enhance the seismic resilience of communities," *Earthquake Spectra*, EERI, 19(4), pp.733-752.

Chopra, A. K., 1995, *Dynamics of Structures: Theory and Application to Earthquake Engineering*, Prentice Hall, Upper Saddle River, NJ.

Constantinou, M. C., T. T. Soong, and G. F. Dargush, 1998, *Passive Energy Dissipation Systems or Structural Design and Retrofit*, Monograph, Multidisciplinary Center for Earthquake Engineering Research, Buffalo, NY.

Constantinou, M. C., P. Tsopelas, A. Kasalanati and E. D. Wolff, 1999, "Property Modification Factors for Seismic Isolation Bearings," *Report No. MCEER-99-0012*, Multidisciplinary Center for Earthquake Engineering Research, University at Buffalo, Buffalo, NY.

Cornell, C. Allin, F. Jalayer, R. Hamburger, and D. A. Foutch, 2002, "Probabilistic basis for 2000 SAC Federal Emergency Management Agency steel moment frame guidelines," *Journal of Structural Engineering*, ASCE, 128(4), pp. 526-533.

FEMA, 1994, "Performance Based Seismic Design of Buildings," *Report no. FEMA 283*, Federal Emergency Management Agency, Washington D.C.

FEMA, 1997, "NEHRP Guidelines for the Seismic Rehabilitation of Buildings," *Reports Nos. 273 (Guidelines) and 274 (Commentary)*, Federal Emergency Management Agency, Washington D.C.

FEMA, 2000a, "Action Plan for Performance Based Seismic Design," *Report No. FEMA 349*, Federal Emergency Management Agency, Washington D.C.

FEMA 2000b, "Prestandard and Commentary for the Seismic Rehabilitation of Buildings," *Report No. FEMA 356*, Federal Emergency Management Agency, Washington D.C.

FEMA, 2001, "NEHRP Recommended Provisions for Seismic Regulations for New Buildings and Other Structures," *Report FEMA 368*, Federal Emergency Management Agency, Washington D.C.

FEMA, 2005, "Program Plan for Development of Next-Generation Performance-Based Seismic Design Guidelines for New and Existing Buildings," To be published as *Report No. FEMA 445*, Federal Emergency Management Agency, Washington, D.C.

Filiatrault, A., S. Kuan and R. Tremblay, 2004, "Shake table testing of bookcase-partition wall systems," *Canadian Journal of Civil Engineering*, 31(4), pp. 664-676.

Frank, K. H., 1996, "The physical and metallurgical properties of structural steels," *Technical Report No. SAC/BD-95/09*, SAC Joint Venture, Sacramento, CA.

Hamburger, R. O., 2003, "A Vision of the ATC-58 Project, Development of Performance-Based Seismic Guidelines," *Proceedings,* Programming Workshop on Performance-Based Design, Applied Technology Council, Redwood City, CA.

Hanson, R. D. and T. T. Soong, 2001, *Seismic Design with Supplemental Energy Dissipation Devices*, EERI Monograph No. 8, Oakland, CA.

Hutchinson, T. C. and S. R. Chaudhuri, 2003, "Bench- and shelf-mounted equipment and contents: shake table experiments," *Proceedings*, ATC-29-2 Seminar on the Seismic Design, Performance and Retrofit of Nonstructural Components in Critical Facilities, Irvine, CA.

ICBO, 1970, *Uniform Building Code, 1970 Edition*, International Conference of Building Officials, Whittier, CA.

ICC, 2003, *International Building Code, 2003 Edition*, International Code Council, Whittier, CA.

Lopez-Garcia, D. and T. T. Soong, 2003, "Sliding fragility of block-type non-structural components, part 1: Unrestrained components," *Earthquake Engineering and Structural Dynamics*, 32(1), pp. 111–129.

Moehle, J., 2003, "A framework for performance-based earthquake engineering," *Proceedings*, Tenth U.S.-Japan Workshop on Improvement of Building Seismic Design and Construction Practices, Report No. ATC-15-9, Applied Technology Council, Redwood City, CA.

Miranda, E. and S. Taghavi, 2003, "Response Assessment of Nonstructural Building Elements," *PEER Report 2002/03,* Pacific Earthquake Engineering Research Center, University of California, Berkeley, CA.

Naeim, F. and J. M. Kelly, 1999, *Design of Seismic Isolated Structures*, John Wiley & Sons, New York, NY.

Nakashima, M., 1995, "Strain-hardening behavior of shear panels made of low-yield steel," *Journal of Structural Engineering*, ASCE, 121(12), pp. 1742-1749.

NIBS, 1997, "Earthquake loss estimation technology – HAZUS; user's manual," National Institute of Building Sciences, Washington, D.C.

Nishkian, M. A., 1937, "Earthquakes and Some Practical Aspects of Earthquake Resistant Design," Bachelor of Science Thesis, Department of Civil Engineering, University of California, Berkeley, CA.

Papageorgiou, A. S. and Aki, K., 1983, A Specific Barrier Model for the Quantitative Description of Inhomogeneous Faulting and the Prediction of Strong Ground Motion, Bulletin of the Seismological Society of America, 73, pp. 693-722.

Park, Y. J. and A. H-S. Ang, 1985, "Mechanistic seismic damage model for reinforced concrete," *Journal of Structural Engineering*, ASCE, 111, pp. 722-739.

Pavlou, E. and M. C. Constantinou, 2004, "Response of nonstructural components in structures with damping systems," Paper submitted for review, *Journal of Structural Engineering*, ASCE.

Ramirez, O. M., M. C. Constantinou, C. A. Kircher, A. S. Whittaker, M. W. Johnson and J. D. Gomez, 2000, "Development and Evaluation of Simplified Procedures for Analysis and Design of Buildings with Passive Energy Dissipation Systems" *Report No. MCEER-00-0010*, Multidisciplinary Center for Earthquake Engineering Research, University at Buffalo, Buffalo, NY.

Restrepo, J., 2004, Personal Communication.

Somerville, P., N. Smith, S. Punyamurthula and J. Sun, 1997, "Development of Ground Motion Time Histories for Phase 2 of the FEMA/SAC Steel Project," *Technical Report SAC/BD-97/04*, SAC Joint Venture, Sacramento, CA.

SEAOC, 1995, *Vision 2000 - A Framework for Performance Based Design,* Volumes I, II, III, Structural Engineers Association of California, Sacramento, CA.

Wanitkorkul, A. and A. Filiatrault, 2005, "Simulation of Strong Ground Motions for Seismic Fragility Evaluation of Nonstructural Components in Hospitals," *Report No. MCEER-05-0005*, Multidisciplinary Center for Earthquake Engineering Research, University at Buffalo, Buffalo, NY.

Whittaker, A. S. and T. T. Soong, 2003, "An overview of nonstructural components research at three U.S. Earthquake Engineering Research Centers," *Proceedings,* ATC-29-2 Seminar on Seismic Design, Performance, and Retrofit of Nonstructural Components in Critical Facilities, Applied Technology Council, Redwood City, CA.

APPENDIX A

STRUCTURAL FRAMING DATA FOR MODELS M3 AND M6

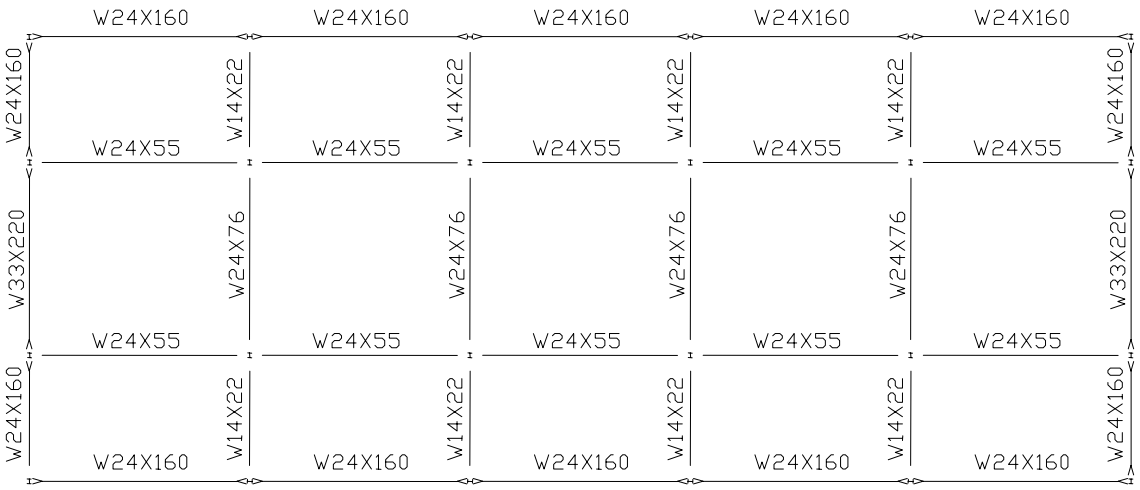

FIGURE A-1: Plan View of Second Floor of M3

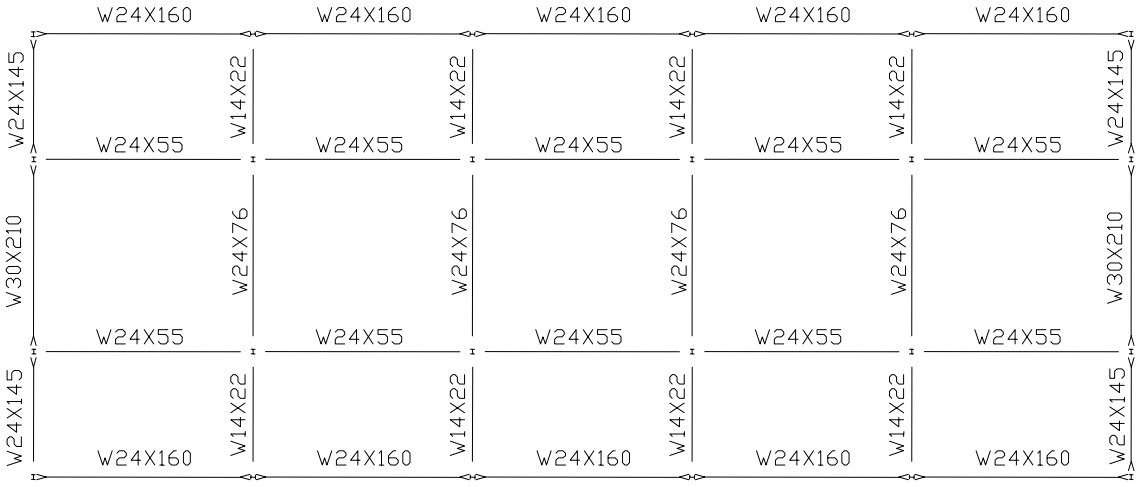

FIGURE A-2: Plan View of Third Floor of M3

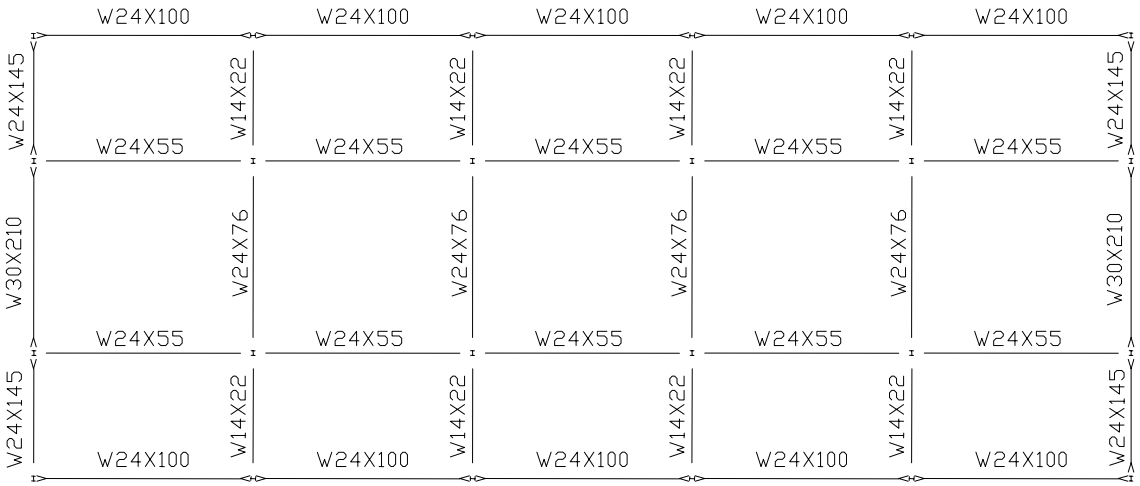

FIGURE A-3: Plan View of Fourth Floor of M3

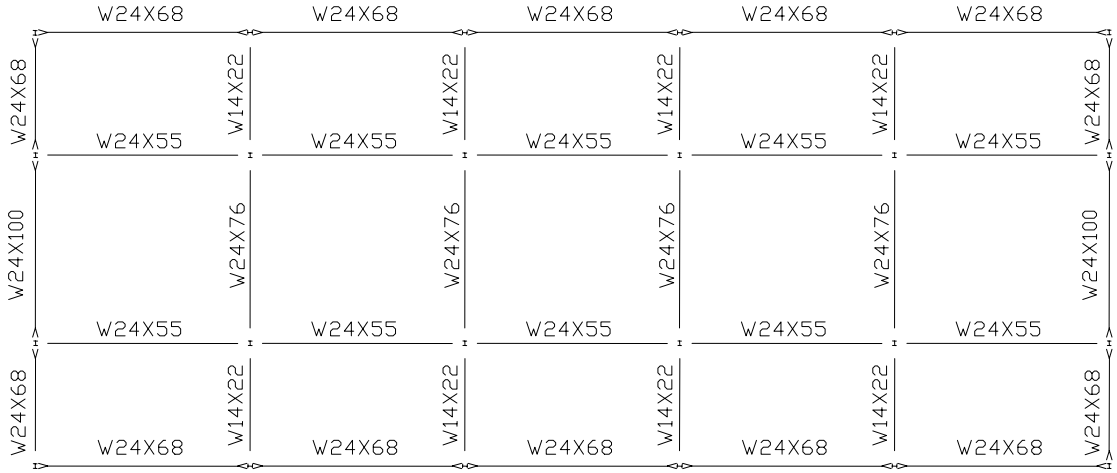

FIGURE A-4: Plan View of Roof of M3

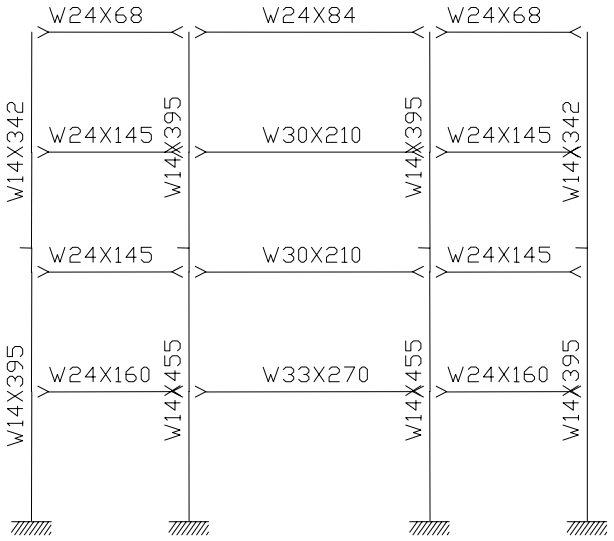

FIGURE A-5: Typical N-S Moment Resisting Frame of M3

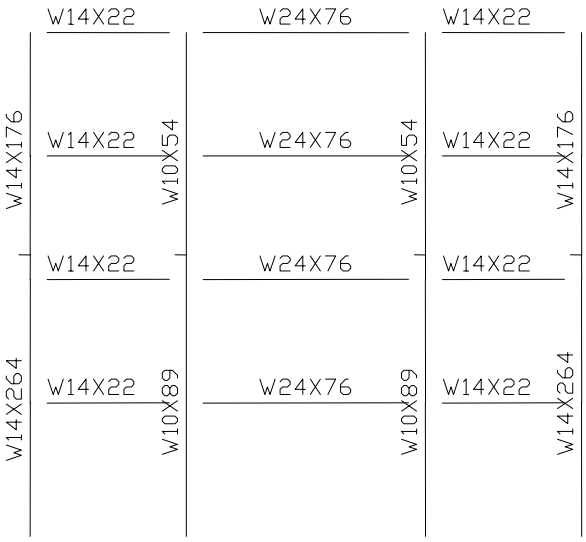

FIGURE A-6: Typical N-S Non-Moment Resisting Frame of M3

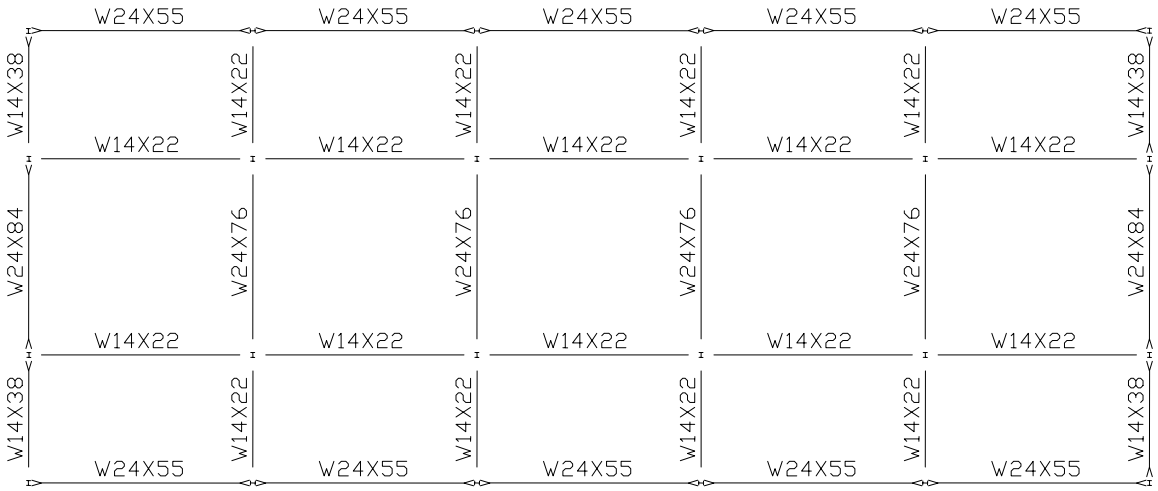

FIGURE A-7: Plan View of Typical Floor of M6

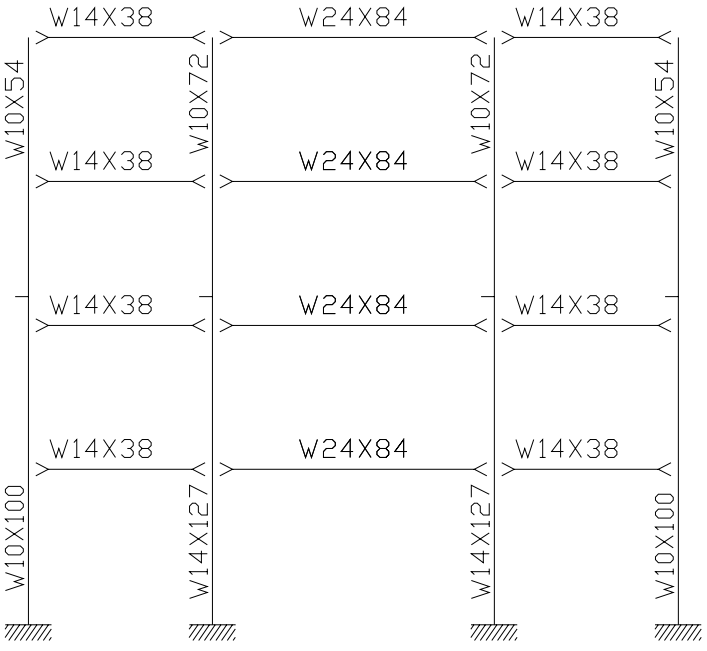

FIGURE A-8: Typical N-S Moment-Resisting Frame of M6

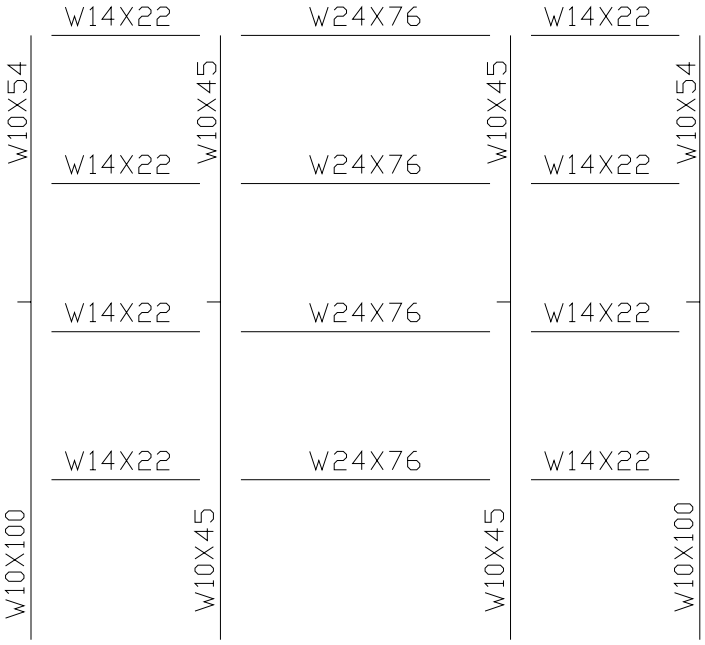

FIGURE A-9: Typical N-S Non-Moment-Resisting Frame of M6

APPENDIX B

GROUND MOTION DATA AND ANALYSIS RESULTS FOR THE MCEER 10/50 AND 2/50 GROUND MOTION BINS

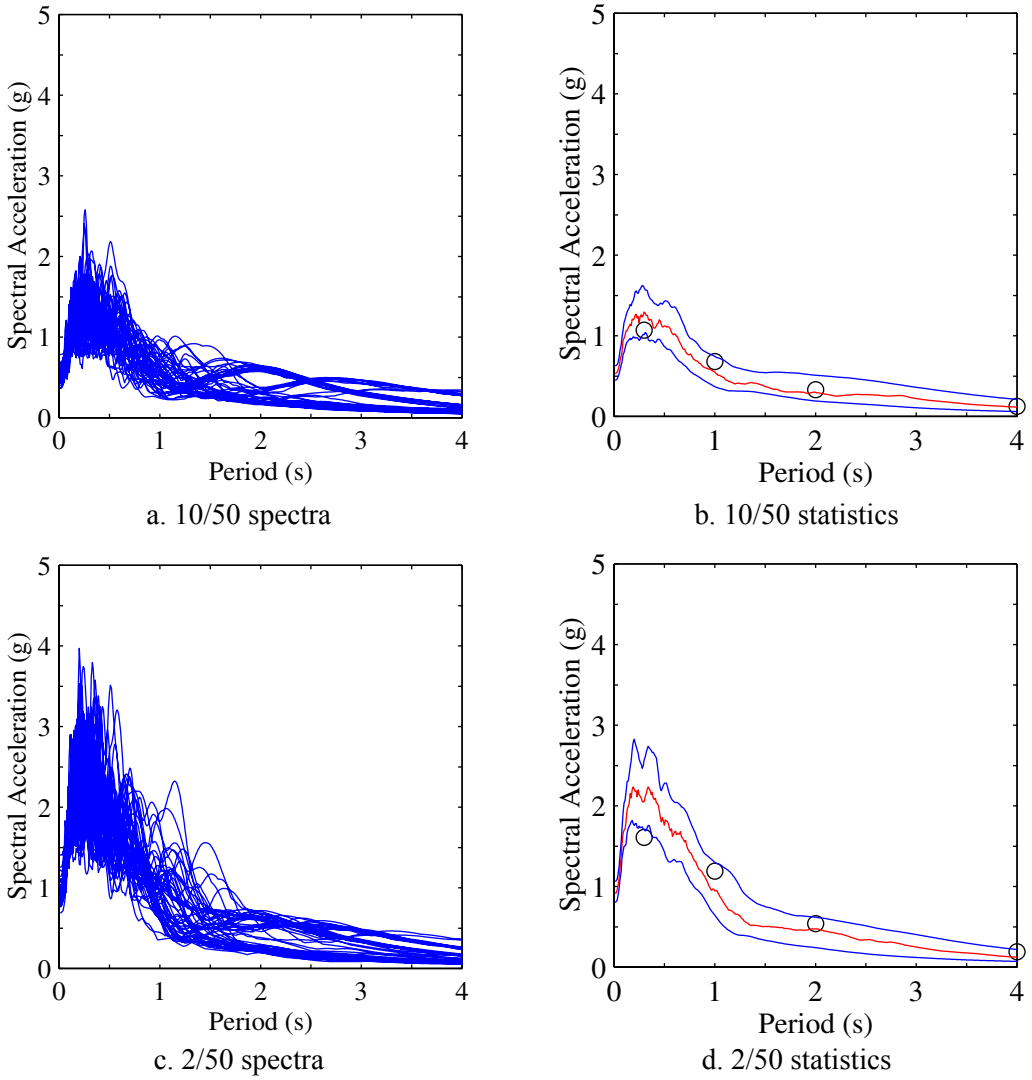

FIGURE B-1: Acceleration Spectra and Spectra Distribution for MCEER Ground Motion Bins for Northridge, CA (Wanitkorkul and Filiatrault, 2005)

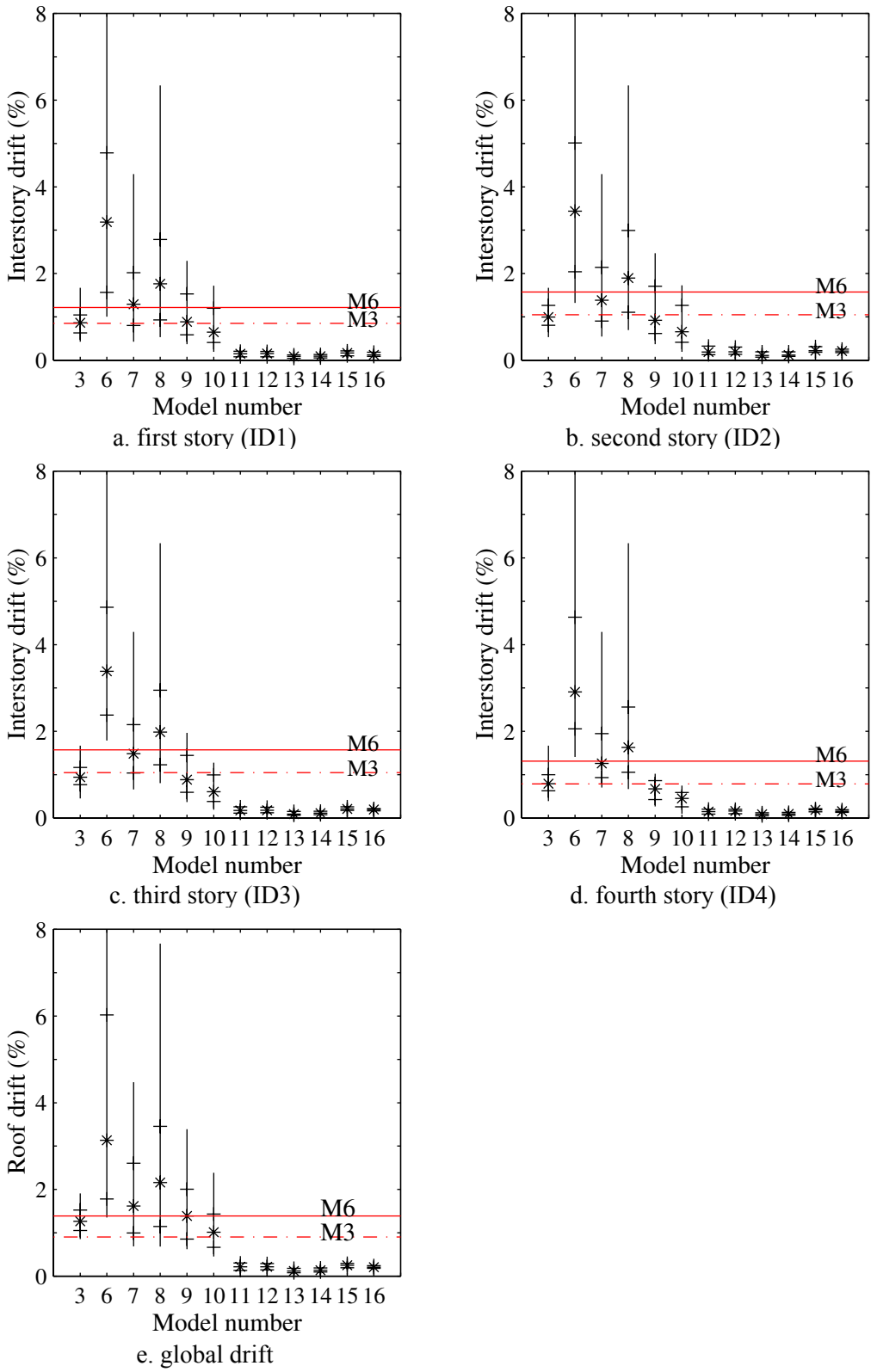

FIGURE B-2: Distributions of Maximum Interstory and Roof Drift for the 10/50 Bin

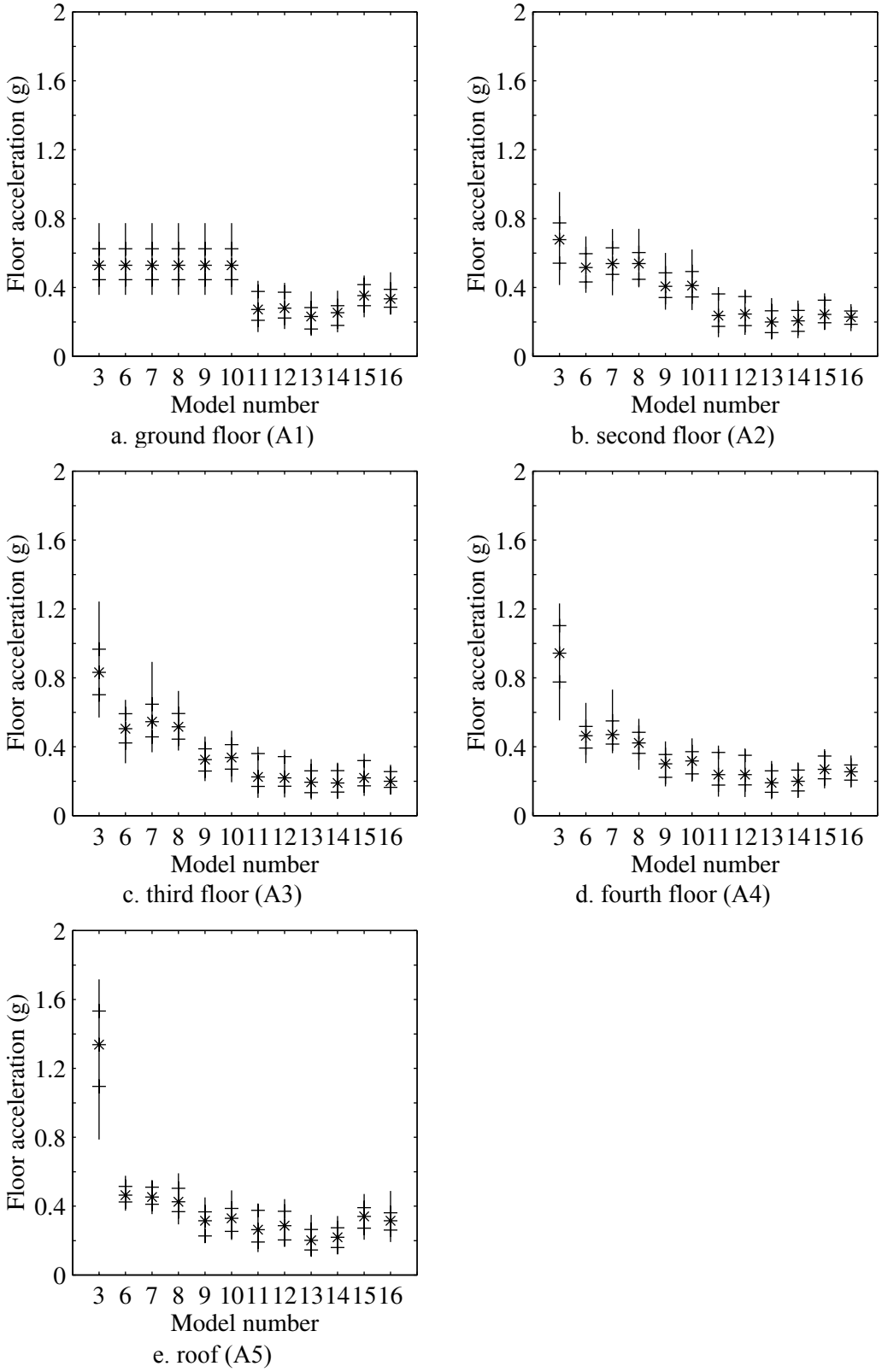

FIGURE B-3: Distributions of Maximum Total Floor Acceleration for the 10/50 Bin

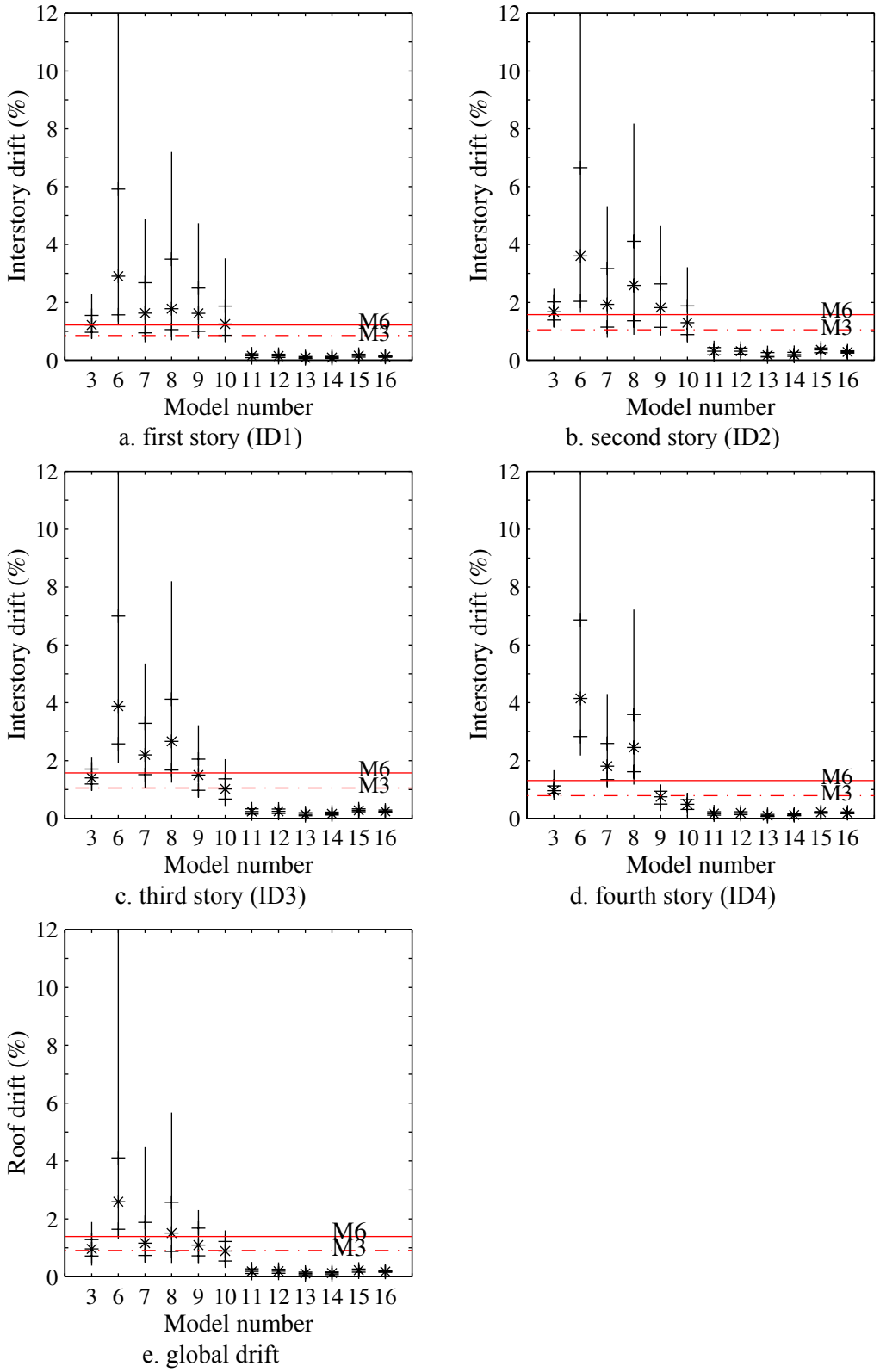

FIGURE B-4: Distributions of Maximum Interstory and Roof Drift for the 2/50 Bin

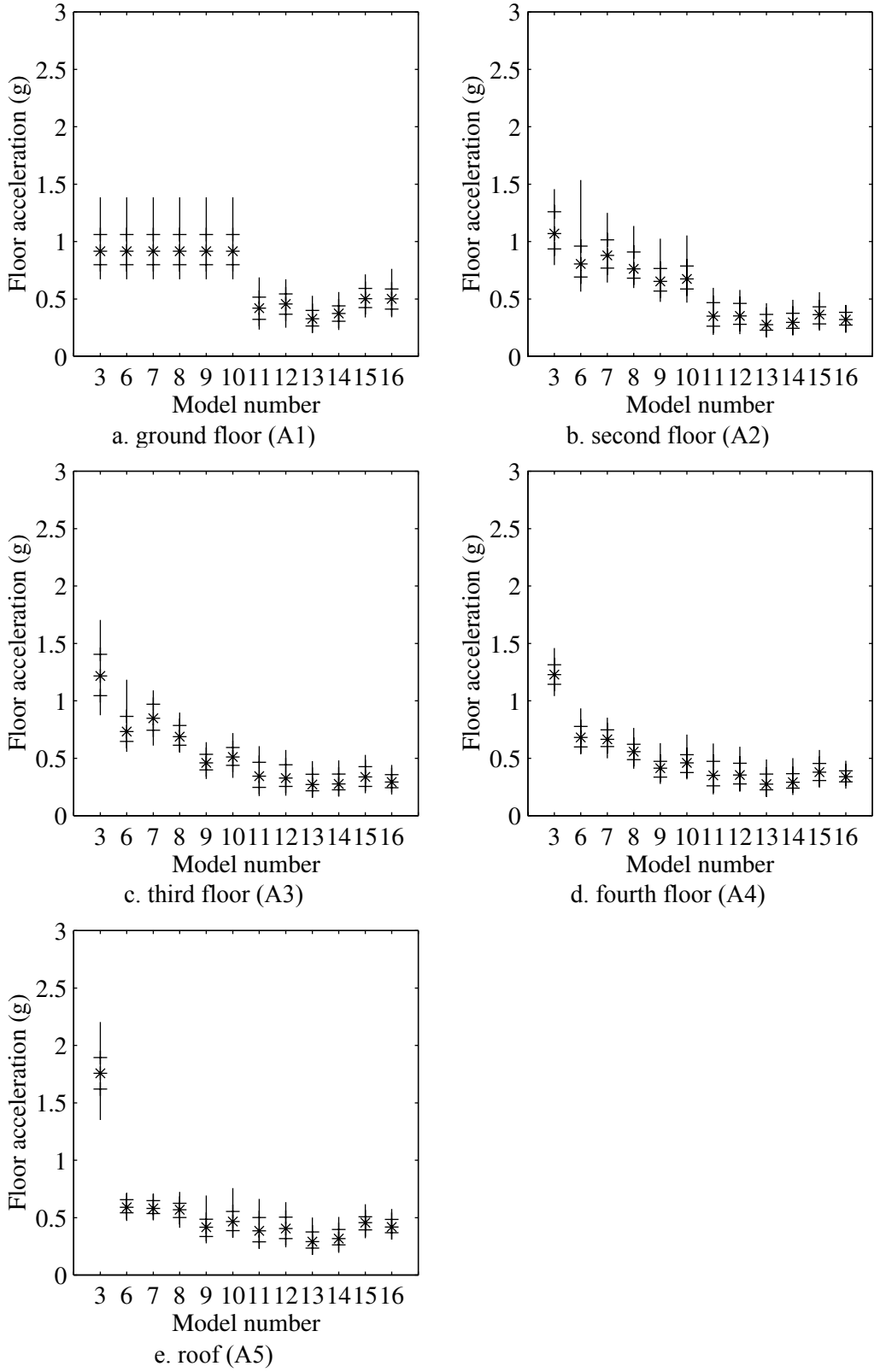

FIGURE B-5: Distributions of Maximum Total Floor Acceleration for the 2/50 Bin

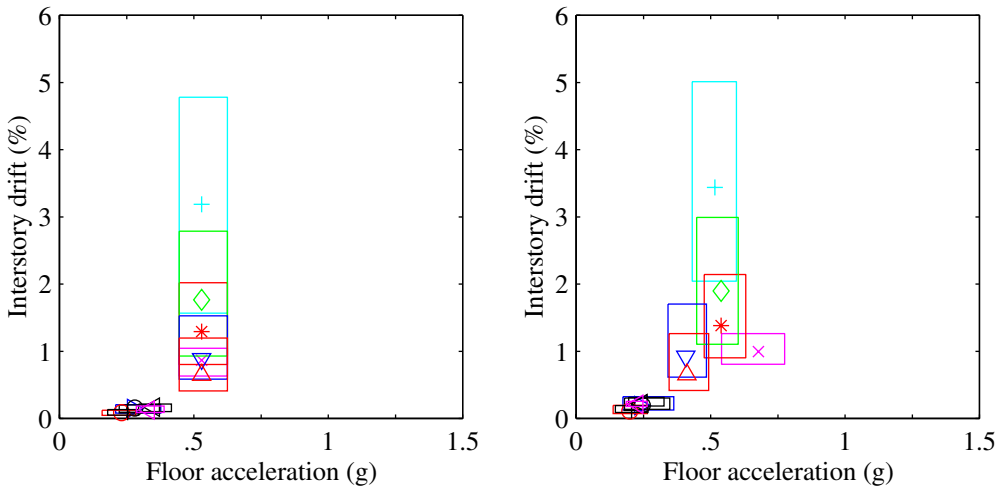

a. ground floor (A1), 1st story (ID1)

b. second floor (A2), second story (ID2)

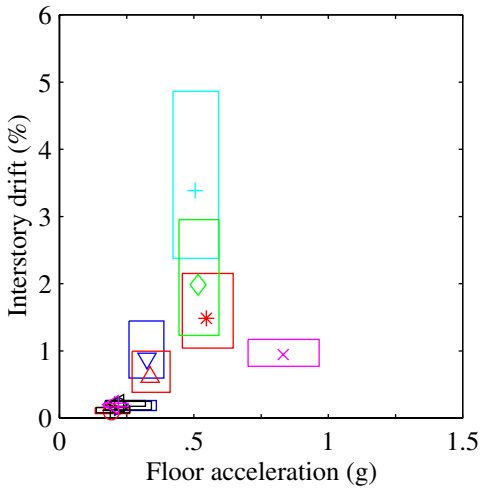

c. third floor (A3), third story (ID3)

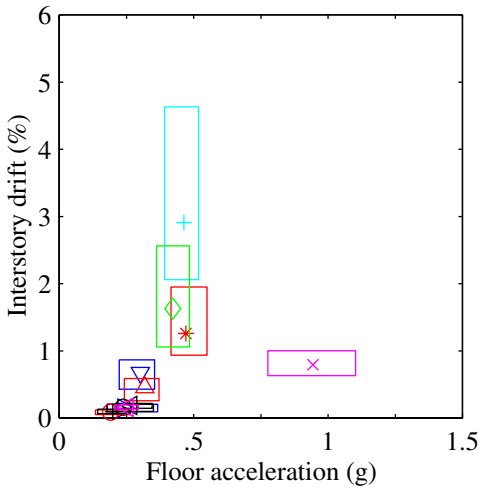

d. fourth floor (A4), fourth story (ID4)

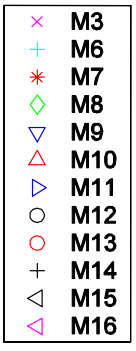

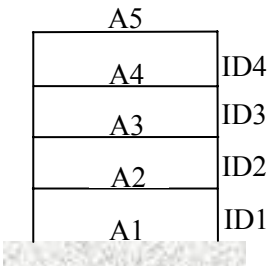

e. legend and illustration of quantities

FIGURE B-6: Performance Spaces for the 10/50 Bin

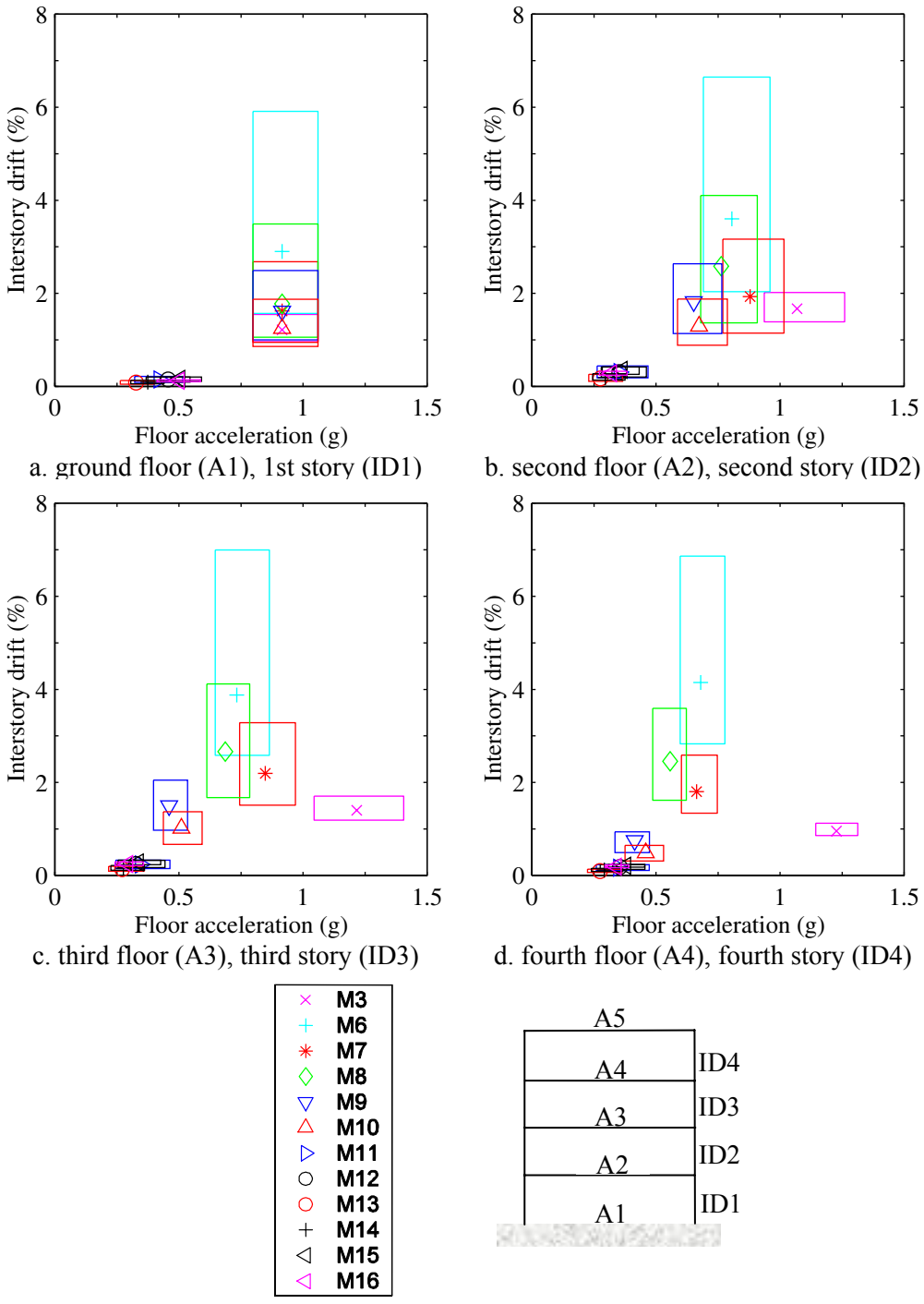

a. ground floor (A1), 1st story (ID1)

b. second floor (A2), second story (ID2)

c. third floor (A3), third story (ID3)

d. fourth floor (A4), fourth story (ID4)

e. legend and illustration of quantities

FIGURE B-7: Performance Spaces for the 2/50 Bin

Multidisciplinary Center for Earthquake Engineering Research
List of Technical Reports

The Multidisciplinary Center for Earthquake Engineering Research (MCEER) publishes technical reports on a variety of subjects related to earthquake engineering written by authors funded through MCEER. These reports are available from both MCEER Publications and the National Technical Information Service (NTIS). Requests for reports should be directed to MCEER Publications, Multidisciplinary Center for Earthquake Engineering Research, State University of New York at Buffalo, Red Jacket Quadrangle, Buffalo, New York 14261. Reports can also be requested through NTIS, 5285 Port Royal Road, Springfield, Virginia 22161. NTIS accession numbers are shown in parenthesis, if available.

NCEER-87-0001 "First-Year Program in Research, Education and Technology Transfer," 3/5/87, (PB88-134275, A04, MF-A01).

NCEER-87-0002 "Experimental Evaluation of Instantaneous Optimal Algorithms for Structural Control," by R.C. Lin, T.T. Soong and A.M. Reinhorn, 4/20/87, (PB88-134341, A04, MF-A01).

NCEER-87-0003 "Experimentation Using the Earthquake Simulation Facilities at University at Buffalo," by A.M. Reinhorn and R.L. Ketter, to be published.

NCEER-87-0004 "The System Characteristics and Performance of a Shaking Table," by J.S. Hwang, K.C. Chang and G.C. Lee, 6/1/87, (PB88-134259, A03, MF-A01). This report is available only through NTIS (see address given above).

NCEER-87-0005 "A Finite Element Formulation for Nonlinear Viscoplastic Material Using a Q Model," by O. Gyebi and G. Dasgupta, 11/2/87, (PB88-213764, A08, MF-A01).

NCEER-87-0006 "Symbolic Manipulation Program (SMP) - Algebraic Codes for Two and Three Dimensional Finite Element Formulations," by X. Lee and G. Dasgupta, 11/9/87, (PB88-218522, A05, MF-A01).

NCEER-87-0007 "Instantaneous Optimal Control Laws for Tall Buildings Under Seismic Excitations," by J.N. Yang, A. Akbarpour and P. Ghaemmaghami, 6/10/87, (PB88-134333, A06, MF-A01). This report is only available through NTIS (see address given above).

NCEER-87-0008 "IDARC: Inelastic Damage Analysis of Reinforced Concrete Frame - Shear-Wall Structures," by Y.J. Park, A.M. Reinhorn and S.K. Kunnath, 7/20/87, (PB88-134325, A09, MF-A01). This report is only available through NTIS (see address given above).

NCEER-87-0009 "Liquefaction Potential for New York State: A Preliminary Report on Sites in Manhattan and Buffalo," by M. Budhu, V. Vijayakumar, R.F. Giese and L. Baumgras, 8/31/87, (PB88-163704, A03, MF-A01). This report is available only through NTIS (see address given above).

NCEER-87-0010 "Vertical and Torsional Vibration of Foundations in Inhomogeneous Media," by A.S. Veletsos and K.W. Dotson, 6/1/87, (PB88-134291, A03, MF-A01). This report is only available through NTIS (see address given above).

NCEER-87-0011 "Seismic Probabilistic Risk Assessment and Seismic Margins Studies for Nuclear Power Plants," by Howard H.M. Hwang, 6/15/87, (PB88-134267, A03, MF-A01). This report is only available through NTIS (see address given above).

NCEER-87-0012 "Parametric Studies of Frequency Response of Secondary Systems Under Ground-Acceleration Excitations," by Y. Yong and Y.K. Lin, 6/10/87, (PB88-134309, A03, MF-A01). This report is only available through NTIS (see address given above).

NCEER-87-0013 "Frequency Response of Secondary Systems Under Seismic Excitation," by J.A. HoLung, J. Cai and Y.K. Lin, 7/31/87, (PB88-134317, A05, MF-A01). This report is only available through NTIS (see address given above).

NCEER-87-0014 "Modelling Earthquake Ground Motions in Seismically Active Regions Using Parametric Time Series Methods," by G.W. Ellis and A.S. Cakmak, 8/25/87, (PB88-134283, A08, MF-A01). This report is only available through NTIS (see address given above).

NCEER-87-0015 "Detection and Assessment of Seismic Structural Damage," by E. DiPasquale and A.S. Cakmak, 8/25/87, (PB88-163712, A05, MF-A01). This report is only available through NTIS (see address given above).

NCEER-87-0016 "Pipeline Experiment at Parkfield, California," by J. Isenberg and E. Richardson, 9/15/87, (PB88-163720, A03, MF-A01). This report is available only through NTIS (see address given above).

NCEER-87-0017 "Digital Simulation of Seismic Ground Motion," by M. Shinozuka, G. Deodatis and T. Harada, 8/31/87, (PB88-155197, A04, MF-A01). This report is available only through NTIS (see address given above).

NCEER-87-0018 "Practical Considerations for Structural Control: System Uncertainty, System Time Delay and Truncation of Small Control Forces," J.N. Yang and A. Akbarpour, 8/10/87, (PB88-163738, A08, MF-A01). This report is only available through NTIS (see address given above).

NCEER-87-0019 "Modal Analysis of Nonclassically Damped Structural Systems Using Canonical Transformation," by J.N. Yang, S. Sarkani and F.X. Long, 9/27/87, (PB88-187851, A04, MF-A01).

NCEER-87-0020 "A Nonstationary Solution in Random Vibration Theory," by J.R. Red-Horse and P.D. Spanos, 11/3/87, (PB88-163746, A03, MF-A01).

NCEER-87-0021 "Horizontal Impedances for Radially Inhomogeneous Viscoelastic Soil Layers," by A.S. Veletsos and K.W. Dotson, 10/15/87, (PB88-150859, A04, MF-A01).

NCEER-87-0022 "Seismic Damage Assessment of Reinforced Concrete Members," by Y.S. Chung, C. Meyer and M. Shinozuka, 10/9/87, (PB88-150867, A05, MF-A01). This report is available only through NTIS (see address given above).

NCEER-87-0023 "Active Structural Control in Civil Engineering," by T.T. Soong, 11/11/87, (PB88-187778, A03, MF-A01).

NCEER-87-0024 "Vertical and Torsional Impedances for Radially Inhomogeneous Viscoelastic Soil Layers," by K.W. Dotson and A.S. Veletsos, 12/87, (PB88-187786, A03, MF-A01).

NCEER-87-0025 "Proceedings from the Symposium on Seismic Hazards, Ground Motions, Soil-Liquefaction and Engineering Practice in Eastern North America," October 20-22, 1987, edited by K.H. Jacob, 12/87, (PB88-188115, A23, MF-A01). This report is available only through NTIS (see address given above).

NCEER-87-0026 "Report on the Whittier-Narrows, California, Earthquake of October 1, 1987," by J. Pantelic and A. Reinhorn, 11/87, (PB88-187752, A03, MF-A01). This report is available only through NTIS (see address given above).

NCEER-87-0027 "Design of a Modular Program for Transient Nonlinear Analysis of Large 3-D Building Structures," by S. Srivastav and J.F. Abel, 12/30/87, (PB88-187950, A05, MF-A01). This report is only available through NTIS (see address given above).

NCEER-87-0028 "Second-Year Program in Research, Education and Technology Transfer," 3/8/88, (PB88-219480, A04, MF-A01).

NCEER-88-0001 "Workshop on Seismic Computer Analysis and Design of Buildings With Interactive Graphics," by W. McGuire, J.F. Abel and C.H. Conley, 1/18/88, (PB88-187760, A03, MF-A01). This report is only available through NTIS (see address given above).

NCEER-88-0002 "Optimal Control of Nonlinear Flexible Structures," by J.N. Yang, F.X. Long and D. Wong, 1/22/88, (PB88-213772, A06, MF-A01).

NCEER-88-0003 "Substructuring Techniques in the Time Domain for Primary-Secondary Structural Systems," by G.D. Manolis and G. Juhn, 2/10/88, (PB88-213780, A04, MF-A01).

NCEER-88-0004 "Iterative Seismic Analysis of Primary-Secondary Systems," by A. Singhal, L.D. Lutes and P.D. Spanos, 2/23/88, (PB88-213798, A04, MF-A01).

NCEER-88-0005 "Stochastic Finite Element Expansion for Random Media," by P.D. Spanos and R. Ghanem, 3/14/88, (PB88-213806, A03, MF-A01).

NCEER-88-0006 "Combining Structural Optimization and Structural Control," by F.Y. Cheng and C.P. Pantelides, 1/10/88, (PB88-213814, A05, MF-A01).

NCEER-88-0007 "Seismic Performance Assessment of Code-Designed Structures," by H.H-M. Hwang, J-W. Jaw and H-J. Shau, 3/20/88, (PB88-219423, A04, MF-A01). This report is only available through NTIS (see address given above).

NCEER-88-0008 "Reliability Analysis of Code-Designed Structures Under Natural Hazards," by H.H-M. Hwang, H. Ushiba and M. Shinozuka, 2/29/88, (PB88-229471, A07, MF-A01). This report is only available through NTIS (see address given above).

NCEER-88-0009 "Seismic Fragility Analysis of Shear Wall Structures," by J-W Jaw and H.H-M. Hwang, 4/30/88, (PB89-102867, A04, MF-A01).

NCEER-88-0010 "Base Isolation of a Multi-Story Building Under a Harmonic Ground Motion - A Comparison of Performances of Various Systems," by F-G Fan, G. Ahmadi and I.G. Tadjbakhsh, 5/18/88, (PB89-122238, A06, MF-A01). This report is only available through NTIS (see address given above).

NCEER-88-0011 "Seismic Floor Response Spectra for a Combined System by Green's Functions," by F.M. Lavelle, L.A. Bergman and P.D. Spanos, 5/1/88, (PB89-102875, A03, MF-A01).

NCEER-88-0012 "A New Solution Technique for Randomly Excited Hysteretic Structures," by G.Q. Cai and Y.K. Lin, 5/16/88, (PB89-102883, A03, MF-A01).

NCEER-88-0013 "A Study of Radiation Damping and Soil-Structure Interaction Effects in the Centrifuge," by K. Weissman, supervised by J.H. Prevost, 5/24/88, (PB89-144703, A06, MF-A01).

NCEER-88-0014 "Parameter Identification and Implementation of a Kinematic Plasticity Model for Frictional Soils," by J.H. Prevost and D.V. Griffiths, to be published.

NCEER-88-0015 "Two- and Three- Dimensional Dynamic Finite Element Analyses of the Long Valley Dam," by D.V. Griffiths and J.H. Prevost, 6/17/88, (PB89-144711, A04, MF-A01).

NCEER-88-0016 "Damage Assessment of Reinforced Concrete Structures in Eastern United States," by A.M. Reinhorn, M.J. Seidel, S.K. Kunnath and Y.J. Park, 6/15/88, (PB89-122220, A04, MF-A01). This report is only available through NTIS (see address given above).

NCEER-88-0017 "Dynamic Compliance of Vertically Loaded Strip Foundations in Multilayered Viscoelastic Soils," by S. Ahmad and A.S.M. Israil, 6/17/88, (PB89-102891, A04, MF-A01).

NCEER-88-0018 "An Experimental Study of Seismic Structural Response With Added Viscoelastic Dampers," by R.C. Lin, Z. Liang, T.T. Soong and R.H. Zhang, 6/30/88, (PB89-122212, A05, MF-A01). This report is available only through NTIS (see address given above).

NCEER-88-0019 "Experimental Investigation of Primary - Secondary System Interaction," by G.D. Manolis, G. Juhn and A.M. Reinhorn, 5/27/88, (PB89-122204, A04, MF-A01).

NCEER-88-0020 "A Response Spectrum Approach For Analysis of Nonclassically Damped Structures," by J.N. Yang, S. Sarkani and F.X. Long, 4/22/88, (PB89-102909, A04, MF-A01).

NCEER-88-0021 "Seismic Interaction of Structures and Soils: Stochastic Approach," by A.S. Veletsos and A.M. Prasad, 7/21/88, (PB89-122196, A04, MF-A01). This report is only available through NTIS (see address given above).

NCEER-88-0022 "Identification of the Serviceability Limit State and Detection of Seismic Structural Damage," by E. DiPasquale and A.S. Cakmak, 6/15/88, (PB89-122188, A05, MF-A01). This report is available only through NTIS (see address given above).

NCEER-88-0023 "Multi-Hazard Risk Analysis: Case of a Simple Offshore Structure," by B.K. Bhartia and E.H. Vanmarcke, 7/21/88, (PB89-145213, A05, MF-A01).

NCEER-88-0024 "Automated Seismic Design of Reinforced Concrete Buildings," by Y.S. Chung, C. Meyer and M. Shinozuka, 7/5/88, (PB89-122170, A06, MF-A01). This report is available only through NTIS (see address given above).

NCEER-88-0025 "Experimental Study of Active Control of MDOF Structures Under Seismic Excitations," by L.L. Chung, R.C. Lin, T.T. Soong and A.M. Reinhorn, 7/10/88, (PB89-122600, A04, MF-A01).

NCEER-88-0026 "Earthquake Simulation Tests of a Low-Rise Metal Structure," by J.S. Hwang, K.C. Chang, G.C. Lee and R.L. Ketter, 8/1/88, (PB89-102917, A04, MF-A01).

NCEER-88-0027 "Systems Study of Urban Response and Reconstruction Due to Catastrophic Earthquakes," by F. Kozin and H.K. Zhou, 9/22/88, (PB90-162348, A04, MF-A01).

NCEER-88-0028 "Seismic Fragility Analysis of Plane Frame Structures," by H.H-M. Hwang and Y.K. Low, 7/31/88, (PB89-131445, A06, MF-A01).

NCEER-88-0029 "Response Analysis of Stochastic Structures," by A. Kardara, C. Bucher and M. Shinozuka, 9/22/88, (PB89-174429, A04, MF-A01).

NCEER-88-0030 "Nonnormal Accelerations Due to Yielding in a Primary Structure," by D.C.K. Chen and L.D. Lutes, 9/19/88, (PB89-131437, A04, MF-A01).

NCEER-88-0031 "Design Approaches for Soil-Structure Interaction," by A.S. Veletsos, A.M. Prasad and Y. Tang, 12/30/88, (PB89-174437, A03, MF-A01). This report is available only through NTIS (see address given above).

NCEER-88-0032 "A Re-evaluation of Design Spectra for Seismic Damage Control," by C.J. Turkstra and A.G. Tallin, 11/7/88, (PB89-145221, A05, MF-A01).

NCEER-88-0033 "The Behavior and Design of Noncontact Lap Splices Subjected to Repeated Inelastic Tensile Loading," by V.E. Sagan, P. Gergely and R.N. White, 12/8/88, (PB89-163737, A08, MF-A01).

NCEER-88-0034 "Seismic Response of Pile Foundations," by S.M. Mamoon, P.K. Banerjee and S. Ahmad, 11/1/88, (PB89-145239, A04, MF-A01).

NCEER-88-0035 "Modeling of R/C Building Structures With Flexible Floor Diaphragms (IDARC2)," by A.M. Reinhorn, S.K. Kunnath and N. Panahshahi, 9/7/88, (PB89-207153, A07, MF-A01).

NCEER-88-0036 "Solution of the Dam-Reservoir Interaction Problem Using a Combination of FEM, BEM with Particular Integrals, Modal Analysis, and Substructuring," by C-S. Tsai, G.C. Lee and R.L. Ketter, 12/31/88, (PB89-207146, A04, MF-A01).

NCEER-88-0037 "Optimal Placement of Actuators for Structural Control," by F.Y. Cheng and C.P. Pantelides, 8/15/88, (PB89-162846, A05, MF-A01).

NCEER-88-0038 "Teflon Bearings in Aseismic Base Isolation: Experimental Studies and Mathematical Modeling," by A. Mokha, M.C. Constantinou and A.M. Reinhorn, 12/5/88, (PB89-218457, A10, MF-A01). This report is available only through NTIS (see address given above).

NCEER-88-0039 "Seismic Behavior of Flat Slab High-Rise Buildings in the New York City Area," by P. Weidlinger and M. Ettouney, 10/15/88, (PB90-145681, A04, MF-A01).

NCEER-88-0040 "Evaluation of the Earthquake Resistance of Existing Buildings in New York City," by P. Weidlinger and M. Ettouney, 10/15/88, to be published.

NCEER-88-0041 "Small-Scale Modeling Techniques for Reinforced Concrete Structures Subjected to Seismic Loads," by W. Kim, A. El-Attar and R.N. White, 11/22/88, (PB89-189625, A05, MF-A01).

NCEER-88-0042 "Modeling Strong Ground Motion from Multiple Event Earthquakes," by G.W. Ellis and A.S. Cakmak, 10/15/88, (PB89-174445, A03, MF-A01).

NCEER-88-0043 "Nonstationary Models of Seismic Ground Acceleration," by M. Grigoriu, S.E. Ruiz and E. Rosenblueth, 7/15/88, (PB89-189617, A04, MF-A01).

NCEER-88-0044 "SARCF User's Guide: Seismic Analysis of Reinforced Concrete Frames," by Y.S. Chung, C. Meyer and M. Shinozuka, 11/9/88, (PB89-174452, A08, MF-A01).

NCEER-88-0045 "First Expert Panel Meeting on Disaster Research and Planning," edited by J. Pantelic and J. Stoyle, 9/15/88, (PB89-174460, A05, MF-A01).

NCEER-88-0046 "Preliminary Studies of the Effect of Degrading Infill Walls on the Nonlinear Seismic Response of Steel Frames," by C.Z. Chrysostomou, P. Gergely and J.F. Abel, 12/19/88, (PB89-208383, A05, MF-A01).

NCEER-88-0047 "Reinforced Concrete Frame Component Testing Facility - Design, Construction, Instrumentation and Operation," by S.P. Pessiki, C. Conley, T. Bond, P. Gergely and R.N. White, 12/16/88, (PB89-174478, A04, MF-A01).

NCEER-89-0001 "Effects of Protective Cushion and Soil Compliancy on the Response of Equipment Within a Seismically Excited Building," by J.A. HoLung, 2/16/89, (PB89-207179, A04, MF-A01).

NCEER-89-0002 "Statistical Evaluation of Response Modification Factors for Reinforced Concrete Structures," by H.H-M. Hwang and J-W. Jaw, 2/17/89, (PB89-207187, A05, MF-A01).

NCEER-89-0003 "Hysteretic Columns Under Random Excitation," by G-Q. Cai and Y.K. Lin, 1/9/89, (PB89-196513, A03, MF-A01).

NCEER-89-0004 "Experimental Study of `Elephant Foot Bulge' Instability of Thin-Walled Metal Tanks," by Z-H. Jia and R.L. Ketter, 2/22/89, (PB89-207195, A03, MF-A01).

NCEER-89-0005 "Experiment on Performance of Buried Pipelines Across San Andreas Fault," by J. Isenberg, E. Richardson and T.D. O'Rourke, 3/10/89, (PB89-218440, A04, MF-A01). This report is available only through NTIS (see address given above).

NCEER-89-0006 "A Knowledge-Based Approach to Structural Design of Earthquake-Resistant Buildings," by M. Subramani, P. Gergely, C.H. Conley, J.F. Abel and A.H. Zaghw, 1/15/89, (PB89-218465, A06, MF-A01).

NCEER-89-0007 "Liquefaction Hazards and Their Effects on Buried Pipelines," by T.D. O'Rourke and P.A. Lane, 2/1/89, (PB89-218481, A09, MF-A01).

NCEER-89-0008 "Fundamentals of System Identification in Structural Dynamics," by H. Imai, C-B. Yun, O. Maruyama and M. Shinozuka, 1/26/89, (PB89-207211, A04, MF-A01).

NCEER-89-0009 "Effects of the 1985 Michoacan Earthquake on Water Systems and Other Buried Lifelines in Mexico," by A.G. Ayala and M.J. O'Rourke, 3/8/89, (PB89-207229, A06, MF-A01).

NCEER-89-R010 "NCEER Bibliography of Earthquake Education Materials," by K.E.K. Ross, Second Revision, 9/1/89, (PB90-125352, A05, MF-A01). This report is replaced by NCEER-92-0018.

NCEER-89-0011 "Inelastic Three-Dimensional Response Analysis of Reinforced Concrete Building Structures (IDARC-3D), Part I - Modeling," by S.K. Kunnath and A.M. Reinhorn, 4/17/89, (PB90-114612, A07, MF-A01). This report is available only through NTIS (see address given above).

NCEER-89-0012 "Recommended Modifications to ATC-14," by C.D. Poland and J.O. Malley, 4/12/89, (PB90-108648, A15, MF-A01).

NCEER-89-0013 "Repair and Strengthening of Beam-to-Column Connections Subjected to Earthquake Loading," by M. Corazao and A.J. Durrani, 2/28/89, (PB90-109885, A06, MF-A01).

NCEER-89-0014 "Program EXKAL2 for Identification of Structural Dynamic Systems," by O. Maruyama, C-B. Yun, M. Hoshiya and M. Shinozuka, 5/19/89, (PB90-109877, A09, MF-A01).

NCEER-89-0015 "Response of Frames With Bolted Semi-Rigid Connections, Part I - Experimental Study and Analytical Predictions," by P.J. DiCorso, A.M. Reinhorn, J.R. Dickerson, J.B. Radziminski and W.L. Harper, 6/1/89, to be published.

NCEER-89-0016 "ARMA Monte Carlo Simulation in Probabilistic Structural Analysis," by P.D. Spanos and M.P. Mignolet, 7/10/89, (PB90-109893, A03, MF-A01).

NCEER-89-P017 "Preliminary Proceedings from the Conference on Disaster Preparedness - The Place of Earthquake Education in Our Schools," Edited by K.E.K. Ross, 6/23/89, (PB90-108606, A03, MF-A01).

NCEER-89-0017 "Proceedings from the Conference on Disaster Preparedness - The Place of Earthquake Education in Our Schools," Edited by K.E.K. Ross, 12/31/89, (PB90-207895, A012, MF-A02). This report is available only through NTIS (see address given above).

NCEER-89-0018 "Multidimensional Models of Hysteretic Material Behavior for Vibration Analysis of Shape Memory Energy Absorbing Devices, by E.J. Graesser and F.A. Cozzarelli, 6/7/89, (PB90-164146, A04, MF-A01).

NCEER-89-0019 "Nonlinear Dynamic Analysis of Three-Dimensional Base Isolated Structures (3D-BASIS)," by S. Nagarajaiah, A.M. Reinhorn and M.C. Constantinou, 8/3/89, (PB90-161936, A06, MF-A01). This report has been replaced by NCEER-93-0011.

NCEER-89-0020 "Structural Control Considering Time-Rate of Control Forces and Control Rate Constraints," by F.Y. Cheng and C.P. Pantelides, 8/3/89, (PB90-120445, A04, MF-A01).

NCEER-89-0021 "Subsurface Conditions of Memphis and Shelby County," by K.W. Ng, T-S. Chang and H-H.M. Hwang, 7/26/89, (PB90-120437, A03, MF-A01).

NCEER-89-0022 "Seismic Wave Propagation Effects on Straight Jointed Buried Pipelines," by K. Elhmadi and M.J. O'Rourke, 8/24/89, (PB90-162322, A10, MF-A02).

NCEER-89-0023 "Workshop on Serviceability Analysis of Water Delivery Systems," edited by M. Grigoriu, 3/6/89, (PB90-127424, A03, MF-A01).

NCEER-89-0024 "Shaking Table Study of a 1/5 Scale Steel Frame Composed of Tapered Members," by K.C. Chang, J.S. Hwang and G.C. Lee, 9/18/89, (PB90-160169, A04, MF-A01).

NCEER-89-0025 "DYNA1D: A Computer Program for Nonlinear Seismic Site Response Analysis - Technical Documentation," by Jean H. Prevost, 9/14/89, (PB90-161944, A07, MF-A01). This report is available only through NTIS (see address given above).

NCEER-89-0026 "1:4 Scale Model Studies of Active Tendon Systems and Active Mass Dampers for Aseismic Protection," by A.M. Reinhorn, T.T. Soong, R.C. Lin, Y.P. Yang, Y. Fukao, H. Abe and M. Nakai, 9/15/89, (PB90-173246, A10, MF-A02). This report is available only through NTIS (see address given above).

NCEER-89-0027 "Scattering of Waves by Inclusions in a Nonhomogeneous Elastic Half Space Solved by Boundary Element Methods," by P.K. Hadley, A. Askar and A.S. Cakmak, 6/15/89, (PB90-145699, A07, MF-A01).

NCEER-89-0028 "Statistical Evaluation of Deflection Amplification Factors for Reinforced Concrete Structures," by H.H.M. Hwang, J-W. Jaw and A.L. Ch'ng, 8/31/89, (PB90-164633, A05, MF-A01).

NCEER-89-0029 "Bedrock Accelerations in Memphis Area Due to Large New Madrid Earthquakes," by H.H.M. Hwang, C.H.S. Chen and G. Yu, 11/7/89, (PB90-162330, A04, MF-A01).

NCEER-89-0030 "Seismic Behavior and Response Sensitivity of Secondary Structural Systems," by Y.Q. Chen and T.T. Soong, 10/23/89, (PB90-164658, A08, MF-A01).

NCEER-89-0031 "Random Vibration and Reliability Analysis of Primary-Secondary Structural Systems," by Y. Ibrahim, M. Grigoriu and T.T. Soong, 11/10/89, (PB90-161951, A04, MF-A01).

NCEER-89-0032 "Proceedings from the Second U.S. - Japan Workshop on Liquefaction, Large Ground Deformation and Their Effects on Lifelines, September 26-29, 1989," Edited by T.D. O'Rourke and M. Hamada, 12/1/89, (PB90-209388, A22, MF-A03).

NCEER-89-0033 "Deterministic Model for Seismic Damage Evaluation of Reinforced Concrete Structures," by J.M. Bracci, A.M. Reinhorn, J.B. Mander and S.K. Kunnath, 9/27/89, (PB91-108803, A06, MF-A01).

NCEER-89-0034 "On the Relation Between Local and Global Damage Indices," by E. DiPasquale and A.S. Cakmak, 8/15/89, (PB90-173865, A05, MF-A01).

NCEER-89-0035 "Cyclic Undrained Behavior of Nonplastic and Low Plasticity Silts," by A.J. Walker and H.E. Stewart, 7/26/89, (PB90-183518, A10, MF-A01).

NCEER-89-0036 "Liquefaction Potential of Surficial Deposits in the City of Buffalo, New York," by M. Budhu, R. Giese and L. Baumgrass, 1/17/89, (PB90-208455, A04, MF-A01).

NCEER-89-0037 "A Deterministic Assessment of Effects of Ground Motion Incoherence," by A.S. Veletsos and Y. Tang, 7/15/89, (PB90-164294, A03, MF-A01).

NCEER-89-0038 "Workshop on Ground Motion Parameters for Seismic Hazard Mapping," July 17-18, 1989, edited by R.V. Whitman, 12/1/89, (PB90-173923, A04, MF-A01).

NCEER-89-0039 "Seismic Effects on Elevated Transit Lines of the New York City Transit Authority," by C.J. Costantino, C.A. Miller and E. Heymsfield, 12/26/89, (PB90-207887, A06, MF-A01).

NCEER-89-0040 "Centrifugal Modeling of Dynamic Soil-Structure Interaction," by K. Weissman, Supervised by J.H. Prevost, 5/10/89, (PB90-207879, A07, MF-A01).

NCEER-89-0041 "Linearized Identification of Buildings With Cores for Seismic Vulnerability Assessment," by I-K. Ho and A.E. Aktan, 11/1/89, (PB90-251943, A07, MF-A01).

NCEER-90-0001 "Geotechnical and Lifeline Aspects of the October 17, 1989 Loma Prieta Earthquake in San Francisco," by T.D. O'Rourke, H.E. Stewart, F.T. Blackburn and T.S. Dickerman, 1/90, (PB90-208596, A05, MF-A01).

NCEER-90-0002 "Nonnormal Secondary Response Due to Yielding in a Primary Structure," by D.C.K. Chen and L.D. Lutes, 2/28/90, (PB90-251976, A07, MF-A01).

NCEER-90-0003 "Earthquake Education Materials for Grades K-12," by K.E.K. Ross, 4/16/90, (PB91-251984, A05, MF-A05). This report has been replaced by NCEER-92-0018.

NCEER-90-0004 "Catalog of Strong Motion Stations in Eastern North America," by R.W. Busby, 4/3/90, (PB90-251984, A05, MF-A01).

NCEER-90-0005 "NCEER Strong-Motion Data Base: A User Manual for the GeoBase Release (Version 1.0 for the Sun3)," by P. Friberg and K. Jacob, 3/31/90 (PB90-258062, A04, MF-A01).

NCEER-90-0006 "Seismic Hazard Along a Crude Oil Pipeline in the Event of an 1811-1812 Type New Madrid Earthquake," by H.H.M. Hwang and C-H.S. Chen, 4/16/90, (PB90-258054, A04, MF-A01).

NCEER-90-0007 "Site-Specific Response Spectra for Memphis Sheahan Pumping Station," by H.H.M. Hwang and C.S. Lee, 5/15/90, (PB91-108811, A05, MF-A01).

NCEER-90-0008 "Pilot Study on Seismic Vulnerability of Crude Oil Transmission Systems," by T. Ariman, R. Dobry, M. Grigoriu, F. Kozin, M. O'Rourke, T. O'Rourke and M. Shinozuka, 5/25/90, (PB91-108837, A06, MF-A01).

NCEER-90-0009 "A Program to Generate Site Dependent Time Histories: EQGEN," by G.W. Ellis, M. Srinivasan and A.S. Cakmak, 1/30/90, (PB91-108829, A04, MF-A01).

NCEER-90-0010 "Active Isolation for Seismic Protection of Operating Rooms," by M.E. Talbott, Supervised by M. Shinozuka, 6/8/9, (PB91-110205, A05, MF-A01).

NCEER-90-0011 "Program LINEARID for Identification of Linear Structural Dynamic Systems," by C-B. Yun and M. Shinozuka, 6/25/90, (PB91-110312, A08, MF-A01).

NCEER-90-0012 "Two-Dimensional Two-Phase Elasto-Plastic Seismic Response of Earth Dams," by A.N. Yiagos, Supervised by J.H. Prevost, 6/20/90, (PB91-110197, A13, MF-A02).

NCEER-90-0013 "Secondary Systems in Base-Isolated Structures: Experimental Investigation, Stochastic Response and Stochastic Sensitivity," by G.D. Manolis, G. Juhn, M.C. Constantinou and A.M. Reinhorn, 7/1/90, (PB91-110320, A08, MF-A01).

NCEER-90-0014 "Seismic Behavior of Lightly-Reinforced Concrete Column and Beam-Column Joint Details," by S.P. Pessiki, C.H. Conley, P. Gergely and R.N. White, 8/22/90, (PB91-108795, A11, MF-A02).

NCEER-90-0015 "Two Hybrid Control Systems for Building Structures Under Strong Earthquakes," by J.N. Yang and A. Danielians, 6/29/90, (PB91-125393, A04, MF-A01).

NCEER-90-0016 "Instantaneous Optimal Control with Acceleration and Velocity Feedback," by J.N. Yang and Z. Li, 6/29/90, (PB91-125401, A03, MF-A01).

NCEER-90-0017 "Reconnaissance Report on the Northern Iran Earthquake of June 21, 1990," by M. Mehrain, 10/4/90, (PB91-125377, A03, MF-A01).

NCEER-90-0018 "Evaluation of Liquefaction Potential in Memphis and Shelby County," by T.S. Chang, P.S. Tang, C.S. Lee and H. Hwang, 8/10/90, (PB91-125427, A09, MF-A01).

NCEER-90-0019 "Experimental and Analytical Study of a Combined Sliding Disc Bearing and Helical Steel Spring Isolation System," by M.C. Constantinou, A.S. Mokha and A.M. Reinhorn, 10/4/90, (PB91-125385, A06, MF-A01). This report is available only through NTIS (see address given above).

NCEER-90-0020 "Experimental Study and Analytical Prediction of Earthquake Response of a Sliding Isolation System with a Spherical Surface," by A.S. Mokha, M.C. Constantinou and A.M. Reinhorn, 10/11/90, (PB91-125419, A05, MF-A01).

NCEER-90-0021 "Dynamic Interaction Factors for Floating Pile Groups," by G. Gazetas, K. Fan, A. Kaynia and E. Kausel, 9/10/90, (PB91-170381, A05, MF-A01).

NCEER-90-0022 "Evaluation of Seismic Damage Indices for Reinforced Concrete Structures," by S. Rodriguez-Gomez and A.S. Cakmak, 9/30/90, PB91-171322, A06, MF-A01).

NCEER-90-0023 "Study of Site Response at a Selected Memphis Site," by H. Desai, S. Ahmad, E.S. Gazetas and M.R. Oh, 10/11/90, (PB91-196857, A03, MF-A01).

NCEER-90-0024 "A User's Guide to Strongmo: Version 1.0 of NCEER's Strong-Motion Data Access Tool for PCs and Terminals," by P.A. Friberg and C.A.T. Susch, 11/15/90, (PB91-171272, A03, MF-A01).

NCEER-90-0025 "A Three-Dimensional Analytical Study of Spatial Variability of Seismic Ground Motions," by L-L. Hong and A.H.-S. Ang, 10/30/90, (PB91-170399, A09, MF-A01).

NCEER-90-0026 "MUMOID User's Guide - A Program for the Identification of Modal Parameters," by S. Rodriguez-Gomez and E. DiPasquale, 9/30/90, (PB91-171298, A04, MF-A01).

NCEER-90-0027 "SARCF-II User's Guide - Seismic Analysis of Reinforced Concrete Frames," by S. Rodriguez-Gomez, Y.S. Chung and C. Meyer, 9/30/90, (PB91-171280, A05, MF-A01).

NCEER-90-0028 "Viscous Dampers: Testing, Modeling and Application in Vibration and Seismic Isolation," by N. Makris and M.C. Constantinou, 12/20/90 (PB91-190561, A06, MF-A01).

NCEER-90-0029 "Soil Effects on Earthquake Ground Motions in the Memphis Area," by H. Hwang, C.S. Lee, K.W. Ng and T.S. Chang, 8/2/90, (PB91-190751, A05, MF-A01).

NCEER-91-0001 "Proceedings from the Third Japan-U.S. Workshop on Earthquake Resistant Design of Lifeline Facilities and Countermeasures for Soil Liquefaction, December 17-19, 1990," edited by T.D. O'Rourke and M. Hamada, 2/1/91, (PB91-179259, A99, MF-A04).

NCEER-91-0002 "Physical Space Solutions of Non-Proportionally Damped Systems," by M. Tong, Z. Liang and G.C. Lee, 1/15/91, (PB91-179242, A04, MF-A01).

NCEER-91-0003 "Seismic Response of Single Piles and Pile Groups," by K. Fan and G. Gazetas, 1/10/91, (PB92-174994, A04, MF-A01).

NCEER-91-0004 "Damping of Structures: Part 1 - Theory of Complex Damping," by Z. Liang and G. Lee, 10/10/91, (PB92-197235, A12, MF-A03).

NCEER-91-0005 "3D-BASIS - Nonlinear Dynamic Analysis of Three Dimensional Base Isolated Structures: Part II," by S. Nagarajaiah, A.M. Reinhorn and M.C. Constantinou, 2/28/91, (PB91-190553, A07, MF-A01). This report has been replaced by NCEER-93-0011.

NCEER-91-0006 "A Multidimensional Hysteretic Model for Plasticity Deforming Metals in Energy Absorbing Devices," by E.J. Graesser and F.A. Cozzarelli, 4/9/91, (PB92-108364, A04, MF-A01).

NCEER-91-0007 "A Framework for Customizable Knowledge-Based Expert Systems with an Application to a KBES for Evaluating the Seismic Resistance of Existing Buildings," by E.G. Ibarra-Anaya and S.J. Fenves, 4/9/91, (PB91-210930, A08, MF-A01).

NCEER-91-0008 "Nonlinear Analysis of Steel Frames with Semi-Rigid Connections Using the Capacity Spectrum Method," by G.G. Deierlein, S-H. Hsieh, Y-J. Shen and J.F. Abel, 7/2/91, (PB92-113828, A05, MF-A01).

NCEER-91-0009 "Earthquake Education Materials for Grades K-12," by K.E.K. Ross, 4/30/91, (PB91-212142, A06, MF-A01). This report has been replaced by NCEER-92-0018.

NCEER-91-0010 "Phase Wave Velocities and Displacement Phase Differences in a Harmonically Oscillating Pile," by N. Makris and G. Gazetas, 7/8/91, (PB92-108356, A04, MF-A01).

NCEER-91-0011 "Dynamic Characteristics of a Full-Size Five-Story Steel Structure and a 2/5 Scale Model," by K.C. Chang, G.C. Yao, G.C. Lee, D.S. Hao and Y.C. Yeh," 7/2/91, (PB93-116648, A06, MF-A02).

NCEER-91-0012 "Seismic Response of a 2/5 Scale Steel Structure with Added Viscoelastic Dampers," by K.C. Chang, T.T. Soong, S-T. Oh and M.L. Lai, 5/17/91, (PB92-110816, A05, MF-A01).

NCEER-91-0013 "Earthquake Response of Retaining Walls; Full-Scale Testing and Computational Modeling," by S. Alampalli and A-W.M. Elgamal, 6/20/91, to be published.

NCEER-91-0014 "3D-BASIS-M: Nonlinear Dynamic Analysis of Multiple Building Base Isolated Structures," by P.C. Tsopelas, S. Nagarajaiah, M.C. Constantinou and A.M. Reinhorn, 5/28/91, (PB92-113885, A09, MF-A02).

NCEER-91-0015 "Evaluation of SEAOC Design Requirements for Sliding Isolated Structures," by D. Theodossiou and M.C. Constantinou, 6/10/91, (PB92-114602, A11, MF-A03).

NCEER-91-0016 "Closed-Loop Modal Testing of a 27-Story Reinforced Concrete Flat Plate-Core Building," by H.R. Somaprasad, T. Toksoy, H. Yoshiyuki and A.E. Aktan, 7/15/91, (PB92-129980, A07, MF-A02).

NCEER-91-0017 "Shake Table Test of a 1/6 Scale Two-Story Lightly Reinforced Concrete Building," by A.G. El-Attar, R.N. White and P. Gergely, 2/28/91, (PB92-222447, A06, MF-A02).

NCEER-91-0018 "Shake Table Test of a 1/8 Scale Three-Story Lightly Reinforced Concrete Building," by A.G. El-Attar, R.N. White and P. Gergely, 2/28/91, (PB93-116630, A08, MF-A02).

NCEER-91-0019 "Transfer Functions for Rigid Rectangular Foundations," by A.S. Veletsos, A.M. Prasad and W.H. Wu, 7/31/91, to be published.

NCEER-91-0020 "Hybrid Control of Seismic-Excited Nonlinear and Inelastic Structural Systems," by J.N. Yang, Z. Li and A. Danielians, 8/1/91, (PB92-143171, A06, MF-A02).

NCEER-91-0021 "The NCEER-91 Earthquake Catalog: Improved Intensity-Based Magnitudes and Recurrence Relations for U.S. Earthquakes East of New Madrid," by L. Seeber and J.G. Armbruster, 8/28/91, (PB92-176742, A06, MF-A02).

NCEER-91-0022 "Proceedings from the Implementation of Earthquake Planning and Education in Schools: The Need for Change - The Roles of the Changemakers," by K.E.K. Ross and F. Winslow, 7/23/91, (PB92-129998, A12, MF-A03).

NCEER-91-0023 "A Study of Reliability-Based Criteria for Seismic Design of Reinforced Concrete Frame Buildings," by H.H.M. Hwang and H-M. Hsu, 8/10/91, (PB92-140235, A09, MF-A02).

NCEER-91-0024 "Experimental Verification of a Number of Structural System Identification Algorithms," by R.G. Ghanem, H. Gavin and M. Shinozuka, 9/18/91, (PB92-176577, A18, MF-A04).

NCEER-91-0025 "Probabilistic Evaluation of Liquefaction Potential," by H.H.M. Hwang and C.S. Lee," 11/25/91, (PB92-143429, A05, MF-A01).

NCEER-91-0026 "Instantaneous Optimal Control for Linear, Nonlinear and Hysteretic Structures - Stable Controllers," by J.N. Yang and Z. Li, 11/15/91, (PB92-163807, A04, MF-A01).

NCEER-91-0027 "Experimental and Theoretical Study of a Sliding Isolation System for Bridges," by M.C. Constantinou, A. Kartoum, A.M. Reinhorn and P. Bradford, 11/15/91, (PB92-176973, A10, MF-A03).

NCEER-92-0001 "Case Studies of Liquefaction and Lifeline Performance During Past Earthquakes, Volume 1: Japanese Case Studies," Edited by M. Hamada and T. O'Rourke, 2/17/92, (PB92-197243, A18, MF-A04).

NCEER-92-0002 "Case Studies of Liquefaction and Lifeline Performance During Past Earthquakes, Volume 2: United States Case Studies," Edited by T. O'Rourke and M. Hamada, 2/17/92, (PB92-197250, A20, MF-A04).

NCEER-92-0003 "Issues in Earthquake Education," Edited by K. Ross, 2/3/92, (PB92-222389, A07, MF-A02).

NCEER-92-0004 "Proceedings from the First U.S. - Japan Workshop on Earthquake Protective Systems for Bridges," Edited by I.G. Buckle, 2/4/92, (PB94-142239, A99, MF-A06).

NCEER-92-0005 "Seismic Ground Motion from a Haskell-Type Source in a Multiple-Layered Half-Space," A.P. Theoharis, G. Deodatis and M. Shinozuka, 1/2/92, to be published.

NCEER-92-0006 "Proceedings from the Site Effects Workshop," Edited by R. Whitman, 2/29/92, (PB92-197201, A04, MF-A01).

NCEER-92-0007 "Engineering Evaluation of Permanent Ground Deformations Due to Seismically-Induced Liquefaction," by M.H. Baziar, R. Dobry and A-W.M. Elgamal, 3/24/92, (PB92-222421, A13, MF-A03).

NCEER-92-0008 "A Procedure for the Seismic Evaluation of Buildings in the Central and Eastern United States," by C.D. Poland and J.O. Malley, 4/2/92, (PB92-222439, A20, MF-A04).

NCEER-92-0009 "Experimental and Analytical Study of a Hybrid Isolation System Using Friction Controllable Sliding Bearings," by M.Q. Feng, S. Fujii and M. Shinozuka, 5/15/92, (PB93-150282, A06, MF-A02).

NCEER-92-0010 "Seismic Resistance of Slab-Column Connections in Existing Non-Ductile Flat-Plate Buildings," by A.J. Durrani and Y. Du, 5/18/92, (PB93-116812, A06, MF-A02).

NCEER-92-0011 "The Hysteretic and Dynamic Behavior of Brick Masonry Walls Upgraded by Ferrocement Coatings Under Cyclic Loading and Strong Simulated Ground Motion," by H. Lee and S.P. Prawel, 5/11/92, to be published.

NCEER-92-0012 "Study of Wire Rope Systems for Seismic Protection of Equipment in Buildings," by G.F. Demetriades, M.C. Constantinou and A.M. Reinhorn, 5/20/92, (PB93-116655, A08, MF-A02).

NCEER-92-0013 "Shape Memory Structural Dampers: Material Properties, Design and Seismic Testing," by P.R. Witting and F.A. Cozzarelli, 5/26/92, (PB93-116663, A05, MF-A01).

NCEER-92-0014 "Longitudinal Permanent Ground Deformation Effects on Buried Continuous Pipelines," by M.J. O'Rourke, and C. Nordberg, 6/15/92, (PB93-116671, A08, MF-A02).

NCEER-92-0015 "A Simulation Method for Stationary Gaussian Random Functions Based on the Sampling Theorem," by M. Grigoriu and S. Balopoulou, 6/11/92, (PB93-127496, A05, MF-A01).

NCEER-92-0016 "Gravity-Load-Designed Reinforced Concrete Buildings: Seismic Evaluation of Existing Construction and Detailing Strategies for Improved Seismic Resistance," by G.W. Hoffmann, S.K. Kunnath, A.M. Reinhorn and J.B. Mander, 7/15/92, (PB94-142007, A08, MF-A02).

NCEER-92-0017 "Observations on Water System and Pipeline Performance in the Limón Area of Costa Rica Due to the April 22, 1991 Earthquake," by M. O'Rourke and D. Ballantyne, 6/30/92, (PB93-126811, A06, MF-A02).

NCEER-92-0018 "Fourth Edition of Earthquake Education Materials for Grades K-12," Edited by K.E.K. Ross, 8/10/92, (PB93-114023, A07, MF-A02).

NCEER-92-0019 "Proceedings from the Fourth Japan-U.S. Workshop on Earthquake Resistant Design of Lifeline Facilities and Countermeasures for Soil Liquefaction," Edited by M. Hamada and T.D. O'Rourke, 8/12/92, (PB93-163939, A99, MF-E11).

NCEER-92-0020 "Active Bracing System: A Full Scale Implementation of Active Control," by A.M. Reinhorn, T.T. Soong, R.C. Lin, M.A. Riley, Y.P. Wang, S. Aizawa and M. Higashino, 8/14/92, (PB93-127512, A06, MF-A02).

NCEER-92-0021 "Empirical Analysis of Horizontal Ground Displacement Generated by Liquefaction-Induced Lateral Spreads," by S.F. Bartlett and T.L. Youd, 8/17/92, (PB93-188241, A06, MF-A02).

NCEER-92-0022 "IDARC Version 3.0: Inelastic Damage Analysis of Reinforced Concrete Structures," by S.K. Kunnath, A.M. Reinhorn and R.F. Lobo, 8/31/92, (PB93-227502, A07, MF-A02).

NCEER-92-0023 "A Semi-Empirical Analysis of Strong-Motion Peaks in Terms of Seismic Source, Propagation Path and Local Site Conditions, by M. Kamiyama, M.J. O'Rourke and R. Flores-Berrones, 9/9/92, (PB93-150266, A08, MF-A02).

NCEER-92-0024 "Seismic Behavior of Reinforced Concrete Frame Structures with Nonductile Details, Part I: Summary of Experimental Findings of Full Scale Beam-Column Joint Tests," by A. Beres, R.N. White and P. Gergely, 9/30/92, (PB93-227783, A05, MF-A01).

NCEER-92-0025 "Experimental Results of Repaired and Retrofitted Beam-Column Joint Tests in Lightly Reinforced Concrete Frame Buildings," by A. Beres, S. El-Borgi, R.N. White and P. Gergely, 10/29/92, (PB93-227791, A05, MF-A01).

NCEER-92-0026 "A Generalization of Optimal Control Theory: Linear and Nonlinear Structures," by J.N. Yang, Z. Li and S. Vongchavalitkul, 11/2/92, (PB93-188621, A05, MF-A01).

NCEER-92-0027 "Seismic Resistance of Reinforced Concrete Frame Structures Designed Only for Gravity Loads: Part I - Design and Properties of a One-Third Scale Model Structure," by J.M. Bracci, A.M. Reinhorn and J.B. Mander, 12/1/92, (PB94-104502, A08, MF-A02).

NCEER-92-0028 "Seismic Resistance of Reinforced Concrete Frame Structures Designed Only for Gravity Loads: Part II - Experimental Performance of Subassemblages," by L.E. Aycardi, J.B. Mander and A.M. Reinhorn, 12/1/92, (PB94-104510, A08, MF-A02).

NCEER-92-0029 "Seismic Resistance of Reinforced Concrete Frame Structures Designed Only for Gravity Loads: Part III - Experimental Performance and Analytical Study of a Structural Model," by J.M. Bracci, A.M. Reinhorn and J.B. Mander, 12/1/92, (PB93-227528, A09, MF-A01).

NCEER-92-0030 "Evaluation of Seismic Retrofit of Reinforced Concrete Frame Structures: Part I - Experimental Performance of Retrofitted Subassemblages," by D. Choudhuri, J.B. Mander and A.M. Reinhorn, 12/8/92, (PB93-198307, A07, MF-A02).

NCEER-92-0031 "Evaluation of Seismic Retrofit of Reinforced Concrete Frame Structures: Part II - Experimental Performance and Analytical Study of a Retrofitted Structural Model," by J.M. Bracci, A.M. Reinhorn and J.B. Mander, 12/8/92, (PB93-198315, A09, MF-A03).

NCEER-92-0032 "Experimental and Analytical Investigation of Seismic Response of Structures with Supplemental Fluid Viscous Dampers," by M.C. Constantinou and M.D. Symans, 12/21/92, (PB93-191435, A10, MF-A03). This report is available only through NTIS (see address given above).

NCEER-92-0033 "Reconnaissance Report on the Cairo, Egypt Earthquake of October 12, 1992," by M. Khater, 12/23/92, (PB93-188621, A03, MF-A01).

NCEER-92-0034 "Low-Level Dynamic Characteristics of Four Tall Flat-Plate Buildings in New York City," by H. Gavin, S. Yuan, J. Grossman, E. Pekelis and K. Jacob, 12/28/92, (PB93-188217, A07, MF-A02).

NCEER-93-0001 "An Experimental Study on the Seismic Performance of Brick-Infilled Steel Frames With and Without Retrofit," by J.B. Mander, B. Nair, K. Wojtkowski and J. Ma, 1/29/93, (PB93-227510, A07, MF-A02).

NCEER-93-0002 "Social Accounting for Disaster Preparedness and Recovery Planning," by S. Cole, E. Pantoja and V. Razak, 2/22/93, (PB94-142114, A12, MF-A03).

NCEER-93-0003 "Assessment of 1991 NEHRP Provisions for Nonstructural Components and Recommended Revisions," by T.T. Soong, G. Chen, Z. Wu, R-H. Zhang and M. Grigoriu, 3/1/93, (PB93-188639, A06, MF-A02).

NCEER-93-0004 "Evaluation of Static and Response Spectrum Analysis Procedures of SEAOC/UBC for Seismic Isolated Structures," by C.W. Winters and M.C. Constantinou, 3/23/93, (PB93-198299, A10, MF-A03).

NCEER-93-0005 "Earthquakes in the Northeast - Are We Ignoring the Hazard? A Workshop on Earthquake Science and Safety for Educators," edited by K.E.K. Ross, 4/2/93, (PB94-103066, A09, MF-A02).

NCEER-93-0006 "Inelastic Response of Reinforced Concrete Structures with Viscoelastic Braces," by R.F. Lobo, J.M. Bracci, K.L. Shen, A.M. Reinhorn and T.T. Soong, 4/5/93, (PB93-227486, A05, MF-A02).

NCEER-93-0007 "Seismic Testing of Installation Methods for Computers and Data Processing Equipment," by K. Kosar, T.T. Soong, K.L. Shen, J.A. HoLung and Y.K. Lin, 4/12/93, (PB93-198299, A07, MF-A02).

NCEER-93-0008 "Retrofit of Reinforced Concrete Frames Using Added Dampers," by A. Reinhorn, M. Constantinou and C. Li, to be published.

NCEER-93-0009 "Seismic Behavior and Design Guidelines for Steel Frame Structures with Added Viscoelastic Dampers," by K.C. Chang, M.L. Lai, T.T. Soong, D.S. Hao and Y.C. Yeh, 5/1/93, (PB94-141959, A07, MF-A02).

NCEER-93-0010 "Seismic Performance of Shear-Critical Reinforced Concrete Bridge Piers," by J.B. Mander, S.M. Waheed, M.T.A. Chaudhary and S.S. Chen, 5/12/93, (PB93-227494, A08, MF-A02).

NCEER-93-0011 "3D-BASIS-TABS: Computer Program for Nonlinear Dynamic Analysis of Three Dimensional Base Isolated Structures," by S. Nagarajaiah, C. Li, A.M. Reinhorn and M.C. Constantinou, 8/2/93, (PB94-141819, A09, MF-A02).

NCEER-93-0012 "Effects of Hydrocarbon Spills from an Oil Pipeline Break on Ground Water," by O.J. Helweg and H.H.M. Hwang, 8/3/93, (PB94-141942, A06, MF-A02).

NCEER-93-0013 "Simplified Procedures for Seismic Design of Nonstructural Components and Assessment of Current Code Provisions," by M.P. Singh, L.E. Suarez, E.E. Matheu and G.O. Maldonado, 8/4/93, (PB94-141827, A09, MF-A02).

NCEER-93-0014 "An Energy Approach to Seismic Analysis and Design of Secondary Systems," by G. Chen and T.T. Soong, 8/6/93, (PB94-142767, A11, MF-A03).

NCEER-93-0015 "Proceedings from School Sites: Becoming Prepared for Earthquakes - Commemorating the Third Anniversary of the Loma Prieta Earthquake," Edited by F.E. Winslow and K.E.K. Ross, 8/16/93, (PB94-154275, A16, MF-A02).

NCEER-93-0016 "Reconnaissance Report of Damage to Historic Monuments in Cairo, Egypt Following the October 12, 1992 Dahshur Earthquake," by D. Sykora, D. Look, G. Croci, E. Karaesmen and E. Karaesmen, 8/19/93, (PB94-142221, A08, MF-A02).

NCEER-93-0017 "The Island of Guam Earthquake of August 8, 1993," by S.W. Swan and S.K. Harris, 9/30/93, (PB94-141843, A04, MF-A01).

NCEER-93-0018 "Engineering Aspects of the October 12, 1992 Egyptian Earthquake," by A.W. Elgamal, M. Amer, K. Adalier and A. Abul-Fadl, 10/7/93, (PB94-141983, A05, MF-A01).

NCEER-93-0019 "Development of an Earthquake Motion Simulator and its Application in Dynamic Centrifuge Testing," by I. Krstelj, Supervised by J.H. Prevost, 10/23/93, (PB94-181773, A-10, MF-A03).

NCEER-93-0020 "NCEER-Taisei Corporation Research Program on Sliding Seismic Isolation Systems for Bridges: Experimental and Analytical Study of a Friction Pendulum System (FPS)," by M.C. Constantinou, P. Tsopelas, Y-S. Kim and S. Okamoto, 11/1/93, (PB94-142775, A08, MF-A02).

NCEER-93-0021 "Finite Element Modeling of Elastomeric Seismic Isolation Bearings," by L.J. Billings, Supervised by R. Shepherd, 11/8/93, to be published.

NCEER-93-0022 "Seismic Vulnerability of Equipment in Critical Facilities: Life-Safety and Operational Consequences," by K. Porter, G.S. Johnson, M.M. Zadeh, C. Scawthorn and S. Eder, 11/24/93, (PB94-181765, A16, MF-A03).

NCEER-93-0023 "Hokkaido Nansei-oki, Japan Earthquake of July 12, 1993, by P.I. Yanev and C.R. Scawthorn, 12/23/93, (PB94-181500, A07, MF-A01).

NCEER-94-0001 "An Evaluation of Seismic Serviceability of Water Supply Networks with Application to the San Francisco Auxiliary Water Supply System," by I. Markov, Supervised by M. Grigoriu and T. O'Rourke, 1/21/94, (PB94-204013, A07, MF-A02).

NCEER-94-0002 "NCEER-Taisei Corporation Research Program on Sliding Seismic Isolation Systems for Bridges: Experimental and Analytical Study of Systems Consisting of Sliding Bearings, Rubber Restoring Force Devices and Fluid Dampers," Volumes I and II, by P. Tsopelas, S. Okamoto, M.C. Constantinou, D. Ozaki and S. Fujii, 2/4/94, (PB94-181740, A09, MF-A02 and PB94-181757, A12, MF-A03).

NCEER-94-0003 "A Markov Model for Local and Global Damage Indices in Seismic Analysis," by S. Rahman and M. Grigoriu, 2/18/94, (PB94-206000, A12, MF-A03).

NCEER-94-0004 "Proceedings from the NCEER Workshop on Seismic Response of Masonry Infills," edited by D.P. Abrams, 3/1/94, (PB94-180783, A07, MF-A02).

NCEER-94-0005 "The Northridge, California Earthquake of January 17, 1994: General Reconnaissance Report," edited by J.D. Goltz, 3/11/94, (PB94-193943, A10, MF-A03).

NCEER-94-0006 "Seismic Energy Based Fatigue Damage Analysis of Bridge Columns: Part I - Evaluation of Seismic Capacity," by G.A. Chang and J.B. Mander, 3/14/94, (PB94-219185, A11, MF-A03).

NCEER-94-0007 "Seismic Isolation of Multi-Story Frame Structures Using Spherical Sliding Isolation Systems," by T.M. Al-Hussaini, V.A. Zayas and M.C. Constantinou, 3/17/94, (PB94-193745, A09, MF-A02).

NCEER-94-0008 "The Northridge, California Earthquake of January 17, 1994: Performance of Highway Bridges," edited by I.G. Buckle, 3/24/94, (PB94-193851, A06, MF-A02).

NCEER-94-0009 "Proceedings of the Third U.S.-Japan Workshop on Earthquake Protective Systems for Bridges," edited by I.G. Buckle and I. Friedland, 3/31/94, (PB94-195815, A99, MF-A06).

NCEER-94-0010 "3D-BASIS-ME: Computer Program for Nonlinear Dynamic Analysis of Seismically Isolated Single and Multiple Structures and Liquid Storage Tanks," by P.C. Tsopelas, M.C. Constantinou and A.M. Reinhorn, 4/12/94, (PB94-204922, A09, MF-A02).

NCEER-94-0011 "The Northridge, California Earthquake of January 17, 1994: Performance of Gas Transmission Pipelines," by T.D. O'Rourke and M.C. Palmer, 5/16/94, (PB94-204989, A05, MF-A01).

NCEER-94-0012 "Feasibility Study of Replacement Procedures and Earthquake Performance Related to Gas Transmission Pipelines," by T.D. O'Rourke and M.C. Palmer, 5/25/94, (PB94-206638, A09, MF-A02).

NCEER-94-0013 "Seismic Energy Based Fatigue Damage Analysis of Bridge Columns: Part II - Evaluation of Seismic Demand," by G.A. Chang and J.B. Mander, 6/1/94, (PB95-18106, A08, MF-A02).

NCEER-94-0014 "NCEER-Taisei Corporation Research Program on Sliding Seismic Isolation Systems for Bridges: Experimental and Analytical Study of a System Consisting of Sliding Bearings and Fluid Restoring Force/Damping Devices," by P. Tsopelas and M.C. Constantinou, 6/13/94, (PB94-219144, A10, MF-A03).

NCEER-94-0015 "Generation of Hazard-Consistent Fragility Curves for Seismic Loss Estimation Studies," by H. Hwang and J-R. Huo, 6/14/94, (PB95-181996, A09, MF-A02).

NCEER-94-0016 "Seismic Study of Building Frames with Added Energy-Absorbing Devices," by W.S. Pong, C.S. Tsai and G.C. Lee, 6/20/94, (PB94-219136, A10, A03).

NCEER-94-0017 "Sliding Mode Control for Seismic-Excited Linear and Nonlinear Civil Engineering Structures," by J. Yang, J. Wu, A. Agrawal and Z. Li, 6/21/94, (PB95-138483, A06, MF-A02).

NCEER-94-0018 "3D-BASIS-TABS Version 2.0: Computer Program for Nonlinear Dynamic Analysis of Three Dimensional Base Isolated Structures," by A.M. Reinhorn, S. Nagarajaiah, M.C. Constantinou, P. Tsopelas and R. Li, 6/22/94, (PB95-182176, A08, MF-A02).

NCEER-94-0019 "Proceedings of the International Workshop on Civil Infrastructure Systems: Application of Intelligent Systems and Advanced Materials on Bridge Systems," Edited by G.C. Lee and K.C. Chang, 7/18/94, (PB95-252474, A20, MF-A04).

NCEER-94-0020 "Study of Seismic Isolation Systems for Computer Floors," by V. Lambrou and M.C. Constantinou, 7/19/94, (PB95-138533, A10, MF-A03).

NCEER-94-0021 "Proceedings of the U.S.-Italian Workshop on Guidelines for Seismic Evaluation and Rehabilitation of Unreinforced Masonry Buildings," Edited by D.P. Abrams and G.M. Calvi, 7/20/94, (PB95-138749, A13, MF-A03).

NCEER-94-0022 "NCEER-Taisei Corporation Research Program on Sliding Seismic Isolation Systems for Bridges: Experimental and Analytical Study of a System Consisting of Lubricated PTFE Sliding Bearings and Mild Steel Dampers," by P. Tsopelas and M.C. Constantinou, 7/22/94, (PB95-182184, A08, MF-A02).

NCEER-94-0023 “Development of Reliability-Based Design Criteria for Buildings Under Seismic Load,” by Y.K. Wen, H. Hwang and M. Shinozuka, 8/1/94, (PB95-211934, A08, MF-A02).

NCEER-94-0024 “Experimental Verification of Acceleration Feedback Control Strategies for an Active Tendon System,” by S.J. Dyke, B.F. Spencer, Jr., P. Quast, M.K. Sain, D.C. Kaspari, Jr. and T.T. Soong, 8/29/94, (PB95-212320, A05, MF-A01).

NCEER-94-0025 “Seismic Retrofitting Manual for Highway Bridges,” Edited by I.G. Buckle and I.F. Friedland, published by the Federal Highway Administration (PB95-212676, A15, MF-A03).

NCEER-94-0026 “Proceedings from the Fifth U.S.-Japan Workshop on Earthquake Resistant Design of Lifeline Facilities and Countermeasures Against Soil Liquefaction,” Edited by T.D. O’Rourke and M. Hamada, 11/7/94, (PB95-220802, A99, MF-E08).

NCEER-95-0001 "Experimental and Analytical Investigation of Seismic Retrofit of Structures with Supplemental Damping: Part 1 - Fluid Viscous Damping Devices," by A.M. Reinhorn, C. Li and M.C. Constantinou, 1/3/95, (PB95-266599, A09, MF-A02).

NCEER-95-0002 "Experimental and Analytical Study of Low-Cycle Fatigue Behavior of Semi-Rigid Top-And-Seat Angle Connections," by G. Pekcan, J.B. Mander and S.S. Chen, 1/5/95, (PB95-220042, A07, MF-A02).

NCEER-95-0003 "NCEER-ATC Joint Study on Fragility of Buildings," by T. Anagnos, C. Rojahn and A.S. Kiremidjian, 1/20/95, (PB95-220026, A06, MF-A02).

NCEER-95-0004 "Nonlinear Control Algorithms for Peak Response Reduction," by Z. Wu, T.T. Soong, V. Gattulli and R.C. Lin, 2/16/95, (PB95-220349, A05, MF-A01).

NCEER-95-0005 "Pipeline Replacement Feasibility Study: A Methodology for Minimizing Seismic and Corrosion Risks to Underground Natural Gas Pipelines," by R.T. Eguchi, H.A. Seligson and D.G. Honegger, 3/2/95, (PB95-252326, A06, MF-A02).

NCEER-95-0006 "Evaluation of Seismic Performance of an 11-Story Frame Building During the 1994 Northridge Earthquake," by F. Naeim, R. DiSulio, K. Benuska, A. Reinhorn and C. Li, to be published.

NCEER-95-0007 "Prioritization of Bridges for Seismic Retrofitting," by N. Basöz and A.S. Kiremidjian, 4/24/95, (PB95-252300, A08, MF-A02).

NCEER-95-0008 "Method for Developing Motion Damage Relationships for Reinforced Concrete Frames," by A. Singhal and A.S. Kiremidjian, 5/11/95, (PB95-266607, A06, MF-A02).

NCEER-95-0009 "Experimental and Analytical Investigation of Seismic Retrofit of Structures with Supplemental Damping: Part II - Friction Devices," by C. Li and A.M. Reinhorn, 7/6/95, (PB96-128087, A11, MF-A03).

NCEER-95-0010 "Experimental Performance and Analytical Study of a Non-Ductile Reinforced Concrete Frame Structure Retrofitted with Elastomeric Spring Dampers," by G. Pekcan, J.B. Mander and S.S. Chen, 7/14/95, (PB96-137161, A08, MF-A02).

NCEER-95-0011 "Development and Experimental Study of Semi-Active Fluid Damping Devices for Seismic Protection of Structures," by M.D. Symans and M.C. Constantinou, 8/3/95, (PB96-136940, A23, MF-A04).

NCEER-95-0012 "Real-Time Structural Parameter Modification (RSPM): Development of Innervated Structures," by Z. Liang, M. Tong and G.C. Lee, 4/11/95, (PB96-137153, A06, MF-A01).

NCEER-95-0013 "Experimental and Analytical Investigation of Seismic Retrofit of Structures with Supplemental Damping: Part III - Viscous Damping Walls," by A.M. Reinhorn and C. Li, 10/1/95, (PB96-176409, A11, MF-A03).

NCEER-95-0014 "Seismic Fragility Analysis of Equipment and Structures in a Memphis Electric Substation," by J-R. Huo and H.H.M. Hwang, 8/10/95, (PB96-128087, A09, MF-A02).

NCEER-95-0015 "The Hanshin-Awaji Earthquake of January 17, 1995: Performance of Lifelines," Edited by M. Shinozuka, 11/3/95, (PB96-176383, A15, MF-A03).

NCEER-95-0016 "Highway Culvert Performance During Earthquakes," by T.L. Youd and C.J. Beckman, available as NCEER-96-0015.

NCEER-95-0017 "The Hanshin-Awaji Earthquake of January 17, 1995: Performance of Highway Bridges," Edited by I.G. Buckle, 12/1/95, to be published.

NCEER-95-0018 "Modeling of Masonry Infill Panels for Structural Analysis," by A.M. Reinhorn, A. Madan, R.E. Valles, Y. Reichmann and J.B. Mander, 12/8/95, (PB97-110886, MF-A01, A06).

NCEER-95-0019 "Optimal Polynomial Control for Linear and Nonlinear Structures," by A.K. Agrawal and J.N. Yang, 12/11/95, (PB96-168737, A07, MF-A02).

NCEER-95-0020 "Retrofit of Non-Ductile Reinforced Concrete Frames Using Friction Dampers," by R.S. Rao, P. Gergely and R.N. White, 12/22/95, (PB97-133508, A10, MF-A02).

NCEER-95-0021 "Parametric Results for Seismic Response of Pile-Supported Bridge Bents," by G. Mylonakis, A. Nikolaou and G. Gazetas, 12/22/95, (PB97-100242, A12, MF-A03).

NCEER-95-0022 "Kinematic Bending Moments in Seismically Stressed Piles," by A. Nikolaou, G. Mylonakis and G. Gazetas, 12/23/95, (PB97-113914, MF-A03, A13).

NCEER-96-0001 "Dynamic Response of Unreinforced Masonry Buildings with Flexible Diaphragms," by A.C. Costley and D.P. Abrams," 10/10/96, (PB97-133573, MF-A03, A15).

NCEER-96-0002 "State of the Art Review: Foundations and Retaining Structures," by I. Po Lam, to be published.

NCEER-96-0003 "Ductility of Rectangular Reinforced Concrete Bridge Columns with Moderate Confinement," by N. Wehbe, M. Saiidi, D. Sanders and B. Douglas, 11/7/96, (PB97-133557, A06, MF-A02).

NCEER-96-0004 "Proceedings of the Long-Span Bridge Seismic Research Workshop," edited by I.G. Buckle and I.M. Friedland, to be published.

NCEER-96-0005 "Establish Representative Pier Types for Comprehensive Study: Eastern United States," by J. Kulicki and Z. Prucz, 5/28/96, (PB98-119217, A07, MF-A02).

NCEER-96-0006 "Establish Representative Pier Types for Comprehensive Study: Western United States," by R. Imbsen, R.A. Schamber and T.A. Osterkamp, 5/28/96, (PB98-118607, A07, MF-A02).

NCEER-96-0007 "Nonlinear Control Techniques for Dynamical Systems with Uncertain Parameters," by R.G. Ghanem and M.I. Bujakov, 5/27/96, (PB97-100259, A17, MF-A03).

NCEER-96-0008 "Seismic Evaluation of a 30-Year Old Non-Ductile Highway Bridge Pier and Its Retrofit," by J.B. Mander, B. Mahmoodzadegan, S. Bhadra and S.S. Chen, 5/31/96, (PB97-110902, MF-A03, A10).

NCEER-96-0009 "Seismic Performance of a Model Reinforced Concrete Bridge Pier Before and After Retrofit," by J.B. Mander, J.H. Kim and C.A. Ligozio, 5/31/96, (PB97-110910, MF-A02, A10).

NCEER-96-0010 "IDARC2D Version 4.0: A Computer Program for the Inelastic Damage Analysis of Buildings," by R.E. Valles, A.M. Reinhorn, S.K. Kunnath, C. Li and A. Madan, 6/3/96, (PB97-100234, A17, MF-A03).

NCEER-96-0011 "Estimation of the Economic Impact of Multiple Lifeline Disruption: Memphis Light, Gas and Water Division Case Study," by S.E. Chang, H.A. Seligson and R.T. Eguchi, 8/16/96, (PB97-133490, A11, MF-A03).

NCEER-96-0012 "Proceedings from the Sixth Japan-U.S. Workshop on Earthquake Resistant Design of Lifeline Facilities and Countermeasures Against Soil Liquefaction, Edited by M. Hamada and T. O'Rourke, 9/11/96, (PB97-133581, A99, MF-A06).

NCEER-96-0013 "Chemical Hazards, Mitigation and Preparedness in Areas of High Seismic Risk: A Methodology for Estimating the Risk of Post-Earthquake Hazardous Materials Release," by H.A. Seligson, R.T. Eguchi, K.J. Tierney and K. Richmond, 11/7/96, (PB97-133565, MF-A02, A08).

NCEER-96-0014 "Response of Steel Bridge Bearings to Reversed Cyclic Loading," by J.B. Mander, D-K. Kim, S.S. Chen and G.J. Premus, 11/13/96, (PB97-140735, A12, MF-A03).

NCEER-96-0015 "Highway Culvert Performance During Past Earthquakes," by T.L. Youd and C.J. Beckman, 11/25/96, (PB97-133532, A06, MF-A01).

NCEER-97-0001 "Evaluation, Prevention and Mitigation of Pounding Effects in Building Structures," by R.E. Valles and A.M. Reinhorn, 2/20/97, (PB97-159552, A14, MF-A03).

NCEER-97-0002 "Seismic Design Criteria for Bridges and Other Highway Structures," by C. Rojahn, R. Mayes, D.G. Anderson, J. Clark, J.H. Hom, R.V. Nutt and M.J. O'Rourke, 4/30/97, (PB97-194658, A06, MF-A03).

NCEER-97-0003 “Proceedings of the U.S.-Italian Workshop on Seismic Evaluation and Retrofit,” Edited by D.P. Abrams and G.M. Calvi, 3/19/97, (PB97-194666, A13, MF-A03).

NCEER-97-0004 "Investigation of Seismic Response of Buildings with Linear and Nonlinear Fluid Viscous Dampers," by A.A. Seleemah and M.C. Constantinou, 5/21/97, (PB98-109002, A15, MF-A03).

NCEER-97-0005 "Proceedings of the Workshop on Earthquake Engineering Frontiers in Transportation Facilities," edited by G.C. Lee and I.M. Friedland, 8/29/97, (PB98-128911, A25, MR-A04).

NCEER-97-0006 "Cumulative Seismic Damage of Reinforced Concrete Bridge Piers," by S.K. Kunnath, A. El-Bahy, A. Taylor and W. Stone, 9/2/97, (PB98-108814, A11, MF-A03).

NCEER-97-0007 "Structural Details to Accommodate Seismic Movements of Highway Bridges and Retaining Walls," by R.A. Imbsen, R.A. Schamber, E. Thorkildsen, A. Kartoum, B.T. Martin, T.N. Rosser and J.M. Kulicki, 9/3/97, (PB98-108996, A09, MF-A02).

NCEER-97-0008 "A Method for Earthquake Motion-Damage Relationships with Application to Reinforced Concrete Frames," by A. Singhal and A.S. Kiremidjian, 9/10/97, (PB98-108988, A13, MF-A03).

NCEER-97-0009 "Seismic Analysis and Design of Bridge Abutments Considering Sliding and Rotation," by K. Fishman and R. Richards, Jr., 9/15/97, (PB98-108897, A06, MF-A02).

NCEER-97-0010 "Proceedings of the FHWA/NCEER Workshop on the National Representation of Seismic Ground Motion for New and Existing Highway Facilities," edited by I.M. Friedland, M.S. Power and R.L. Mayes, 9/22/97, (PB98-128903, A21, MF-A04).

NCEER-97-0011 "Seismic Analysis for Design or Retrofit of Gravity Bridge Abutments," by K.L. Fishman, R. Richards, Jr. and R.C. Divito, 10/2/97, (PB98-128937, A08, MF-A02).

NCEER-97-0012 "Evaluation of Simplified Methods of Analysis for Yielding Structures," by P. Tsopelas, M.C. Constantinou, C.A. Kircher and A.S. Whittaker, 10/31/97, (PB98-128929, A10, MF-A03).

NCEER-97-0013 "Seismic Design of Bridge Columns Based on Control and Repairability of Damage," by C-T. Cheng and J.B. Mander, 12/8/97, (PB98-144249, A11, MF-A03).

NCEER-97-0014 "Seismic Resistance of Bridge Piers Based on Damage Avoidance Design," by J.B. Mander and C-T. Cheng, 12/10/97, (PB98-144223, A09, MF-A02).

NCEER-97-0015 “Seismic Response of Nominally Symmetric Systems with Strength Uncertainty,” by S. Balopoulou and M. Grigoriu, 12/23/97, (PB98-153422, A11, MF-A03).

NCEER-97-0016 “Evaluation of Seismic Retrofit Methods for Reinforced Concrete Bridge Columns,” by T.J. Wipf, F.W. Klaiber and F.M. Russo, 12/28/97, (PB98-144215, A12, MF-A03).

NCEER-97-0017 “Seismic Fragility of Existing Conventional Reinforced Concrete Highway Bridges,” by C.L. Mullen and A.S. Cakmak, 12/30/97, (PB98-153406, A08, MF-A02).

NCEER-97-0018 “Loss Asssessment of Memphis Buildings,” edited by D.P. Abrams and M. Shinozuka, 12/31/97, (PB98-144231, A13, MF-A03).

NCEER-97-0019 “Seismic Evaluation of Frames with Infill Walls Using Quasi-static Experiments,” by K.M. Mosalam, R.N. White and P. Gergely, 12/31/97, (PB98-153455, A07, MF-A02).

NCEER-97-0020 “Seismic Evaluation of Frames with Infill Walls Using Pseudo-dynamic Experiments,” by K.M. Mosalam, R.N. White and P. Gergely, 12/31/97, (PB98-153430, A07, MF-A02).

NCEER-97-0021 “Computational Strategies for Frames with Infill Walls: Discrete and Smeared Crack Analyses and Seismic Fragility,” by K.M. Mosalam, R.N. White and P. Gergely, 12/31/97, (PB98-153414, A10, MF-A02).

NCEER-97-0022 "Proceedings of the NCEER Workshop on Evaluation of Liquefaction Resistance of Soils," edited by T.L. Youd and I.M. Idriss, 12/31/97, (PB98-155617, A15, MF-A03).

MCEER-98-0001 "Extraction of Nonlinear Hysteretic Properties of Seismically Isolated Bridges from Quick-Release Field Tests," by Q. Chen, B.M. Douglas, E.M. Maragakis and I.G. Buckle, 5/26/98, (PB99-118838, A06, MF-A01).

MCEER-98-0002 "Methodologies for Evaluating the Importance of Highway Bridges," by A. Thomas, S. Eshenaur and J. Kulicki, 5/29/98, (PB99-118846, A10, MF-A02).

MCEER-98-0003 "Capacity Design of Bridge Piers and the Analysis of Overstrength," by J.B. Mander, A. Dutta and P. Goel, 6/1/98, (PB99-118853, A09, MF-A02).

MCEER-98-0004 "Evaluation of Bridge Damage Data from the Loma Prieta and Northridge, California Earthquakes," by N. Basoz and A. Kiremidjian, 6/2/98, (PB99-118861, A15, MF-A03).

MCEER-98-0005 "Screening Guide for Rapid Assessment of Liquefaction Hazard at Highway Bridge Sites," by T. L. Youd, 6/16/98, (PB99-118879, A06, not available on microfiche).

MCEER-98-0006 "Structural Steel and Steel/Concrete Interface Details for Bridges," by P. Ritchie, N. Kauhl and J. Kulicki, 7/13/98, (PB99-118945, A06, MF-A01).

MCEER-98-0007 "Capacity Design and Fatigue Analysis of Confined Concrete Columns," by A. Dutta and J.B. Mander, 7/14/98, (PB99-118960, A14, MF-A03).

MCEER-98-0008 "Proceedings of the Workshop on Performance Criteria for Telecommunication Services Under Earthquake Conditions," edited by A.J. Schiff, 7/15/98, (PB99-118952, A08, MF-A02).

MCEER-98-0009 "Fatigue Analysis of Unconfined Concrete Columns," by J.B. Mander, A. Dutta and J.H. Kim, 9/12/98, (PB99-123655, A10, MF-A02).

MCEER-98-0010 "Centrifuge Modeling of Cyclic Lateral Response of Pile-Cap Systems and Seat-Type Abutments in Dry Sands," by A.D. Gadre and R. Dobry, 10/2/98, (PB99-123606, A13, MF-A03).

MCEER-98-0011 "IDARC-BRIDGE: A Computational Platform for Seismic Damage Assessment of Bridge Structures," by A.M. Reinhorn, V. Simeonov, G. Mylonakis and Y. Reichman, 10/2/98, (PB99-162919, A15, MF-A03).

MCEER-98-0012 "Experimental Investigation of the Dynamic Response of Two Bridges Before and After Retrofitting with Elastomeric Bearings," by D.A. Wendichansky, S.S. Chen and J.B. Mander, 10/2/98, (PB99-162927, A15, MF-A03).

MCEER-98-0013 "Design Procedures for Hinge Restrainers and Hinge Sear Width for Multiple-Frame Bridges," by R. Des Roches and G.L. Fenves, 11/3/98, (PB99-140477, A13, MF-A03).

MCEER-98-0014 "Response Modification Factors for Seismically Isolated Bridges," by M.C. Constantinou and J.K. Quarshie, 11/3/98, (PB99-140485, A14, MF-A03).

MCEER-98-0015 "Proceedings of the U.S.-Italy Workshop on Seismic Protective Systems for Bridges," edited by I.M. Friedland and M.C. Constantinou, 11/3/98, (PB2000-101711, A22, MF-A04).

MCEER-98-0016 "Appropriate Seismic Reliability for Critical Equipment Systems: Recommendations Based on Regional Analysis of Financial and Life Loss," by K. Porter, C. Scawthorn, C. Taylor and N. Blais, 11/10/98, (PB99-157265, A08, MF-A02).

MCEER-98-0017 "Proceedings of the U.S. Japan Joint Seminar on Civil Infrastructure Systems Research," edited by M. Shinozuka and A. Rose, 11/12/98, (PB99-156713, A16, MF-A03).

MCEER-98-0018 "Modeling of Pile Footings and Drilled Shafts for Seismic Design," by I. PoLam, M. Kapuskar and D. Chaudhuri, 12/21/98, (PB99-157257, A09, MF-A02).

MCEER-99-0001 "Seismic Evaluation of a Masonry Infilled Reinforced Concrete Frame by Pseudodynamic Testing," by S.G. Buonopane and R.N. White, 2/16/99, (PB99-162851, A09, MF-A02).

MCEER-99-0002 "Response History Analysis of Structures with Seismic Isolation and Energy Dissipation Systems: Verification Examples for Program SAP2000," by J. Scheller and M.C. Constantinou, 2/22/99, (PB99-162869, A08, MF-A02).

MCEER-99-0003 "Experimental Study on the Seismic Design and Retrofit of Bridge Columns Including Axial Load Effects," by A. Dutta, T. Kokorina and J.B. Mander, 2/22/99, (PB99-162877, A09, MF-A02).

MCEER-99-0004 "Experimental Study of Bridge Elastomeric and Other Isolation and Energy Dissipation Systems with Emphasis on Uplift Prevention and High Velocity Near-source Seismic Excitation," by A. Kasalanati and M. C. Constantinou, 2/26/99, (PB99-162885, A12, MF-A03).

MCEER-99-0005 "Truss Modeling of Reinforced Concrete Shear-flexure Behavior," by J.H. Kim and J.B. Mander, 3/8/99, (PB99-163693, A12, MF-A03).

MCEER-99-0006 "Experimental Investigation and Computational Modeling of Seismic Response of a 1:4 Scale Model Steel Structure with a Load Balancing Supplemental Damping System," by G. Pekcan, J.B. Mander and S.S. Chen, 4/2/99, (PB99-162893, A11, MF-A03).

MCEER-99-0007 "Effect of Vertical Ground Motions on the Structural Response of Highway Bridges," by M.R. Button, C.J. Cronin and R.L. Mayes, 4/10/99, (PB2000-101411, A10, MF-A03).

MCEER-99-0008 "Seismic Reliability Assessment of Critical Facilities: A Handbook, Supporting Documentation, and Model Code Provisions," by G.S. Johnson, R.E. Sheppard, M.D. Quilici, S.J. Eder and C.R. Scawthorn, 4/12/99, (PB2000-101701, A18, MF-A04).

MCEER-99-0009 "Impact Assessment of Selected MCEER Highway Project Research on the Seismic Design of Highway Structures," by C. Rojahn, R. Mayes, D.G. Anderson, J.H. Clark, D'Appolonia Engineering, S. Gloyd and R.V. Nutt, 4/14/99, (PB99-162901, A10, MF-A02).

MCEER-99-0010 "Site Factors and Site Categories in Seismic Codes," by R. Dobry, R. Ramos and M.S. Power, 7/19/99, (PB2000-101705, A08, MF-A02).

MCEER-99-0011 "Restrainer Design Procedures for Multi-Span Simply-Supported Bridges," by M.J. Randall, M. Saiidi, E. Maragakis and T. Isakovic, 7/20/99, (PB2000-101702, A10, MF-A02).

MCEER-99-0012 "Property Modification Factors for Seismic Isolation Bearings," by M.C. Constantinou, P. Tsopelas, A. Kasalanati and E. Wolff, 7/20/99, (PB2000-103387, A11, MF-A03).

MCEER-99-0013 "Critical Seismic Issues for Existing Steel Bridges," by P. Ritchie, N. Kauhl and J. Kulicki, 7/20/99, (PB2000-101697, A09, MF-A02).

MCEER-99-0014 "Nonstructural Damage Database," by A. Kao, T.T. Soong and A. Vender, 7/24/99, (PB2000-101407, A06, MF-A01).

MCEER-99-0015 "Guide to Remedial Measures for Liquefaction Mitigation at Existing Highway Bridge Sites," by H.G. Cooke and J. K. Mitchell, 7/26/99, (PB2000-101703, A11, MF-A03).

MCEER-99-0016 "Proceedings of the MCEER Workshop on Ground Motion Methodologies for the Eastern United States," edited by N. Abrahamson and A. Becker, 8/11/99, (PB2000-103385, A07, MF-A02).

MCEER-99-0017 "Quindío, Colombia Earthquake of January 25, 1999: Reconnaissance Report," by A.P. Asfura and P.J. Flores, 10/4/99, (PB2000-106893, A06, MF-A01).

MCEER-99-0018 "Hysteretic Models for Cyclic Behavior of Deteriorating Inelastic Structures," by M.V. Sivaselvan and A.M. Reinhorn, 11/5/99, (PB2000-103386, A08, MF-A02).

MCEER-99-0019 "Proceedings of the 7th U.S.- Japan Workshop on Earthquake Resistant Design of Lifeline Facilities and Countermeasures Against Soil Liquefaction," edited by T.D. O'Rourke, J.P. Bardet and M. Hamada, 11/19/99, (PB2000-103354, A99, MF-A06).

MCEER-99-0020 "Development of Measurement Capability for Micro-Vibration Evaluations with Application to Chip Fabrication Facilities," by G.C. Lee, Z. Liang, J.W. Song, J.D. Shen and W.C. Liu, 12/1/99, (PB2000-105993, A08, MF-A02).

MCEER-99-0021 "Design and Retrofit Methodology for Building Structures with Supplemental Energy Dissipating Systems," by G. Pekcan, J.B. Mander and S.S. Chen, 12/31/99, (PB2000-105994, A11, MF-A03).

MCEER-00-0001 "The Marmara, Turkey Earthquake of August 17, 1999: Reconnaissance Report," edited by C. Scawthorn; with major contributions by M. Bruneau, R. Eguchi, T. Holzer, G. Johnson, J. Mander, J. Mitchell, W. Mitchell, A. Papageorgiou, C. Scaethorn, and G. Webb, 3/23/00, (PB2000-106200, A11, MF-A03).

MCEER-00-0002 "Proceedings of the MCEER Workshop for Seismic Hazard Mitigation of Health Care Facilities," edited by G.C. Lee, M. Ettouney, M. Grigoriu, J. Hauer and J. Nigg, 3/29/00, (PB2000-106892, A08, MF-A02).

MCEER-00-0003 "The Chi-Chi, Taiwan Earthquake of September 21, 1999: Reconnaissance Report," edited by G.C. Lee and C.H. Loh, with major contributions by G.C. Lee, M. Bruneau, I.G. Buckle, S.E. Chang, P.J. Flores, T.D. O'Rourke, M. Shinozuka, T.T. Soong, C-H. Loh, K-C. Chang, Z-J. Chen, J-S. Hwang, M-L. Lin, G-Y. Liu, K-C. Tsai, G.C. Yao and C-L. Yen, 4/30/00, (PB2001-100980, A10, MF-A02).

MCEER-00-0004 "Seismic Retrofit of End-Sway Frames of Steel Deck-Truss Bridges with a Supplemental Tendon System: Experimental and Analytical Investigation," by G. Pekcan, J.B. Mander and S.S. Chen, 7/1/00, (PB2001-100982, A10, MF-A02).

MCEER-00-0005 "Sliding Fragility of Unrestrained Equipment in Critical Facilities," by W.H. Chong and T.T. Soong, 7/5/00, (PB2001-100983, A08, MF-A02).

MCEER-00-0006 "Seismic Response of Reinforced Concrete Bridge Pier Walls in the Weak Direction," by N. Abo-Shadi, M. Saiidi and D. Sanders, 7/17/00, (PB2001-100981, A17, MF-A03).

MCEER-00-0007 "Low-Cycle Fatigue Behavior of Longitudinal Reinforcement in Reinforced Concrete Bridge Columns," by J. Brown and S.K. Kunnath, 7/23/00, (PB2001-104392, A08, MF-A02).

MCEER-00-0008 "Soil Structure Interaction of Bridges for Seismic Analysis," I. PoLam and H. Law, 9/25/00, (PB2001-105397, A08, MF-A02).

MCEER-00-0009 "Proceedings of the First MCEER Workshop on Mitigation of Earthquake Disaster by Advanced Technologies (MEDAT-1), edited by M. Shinozuka, D.J. Inman and T.D. O'Rourke, 11/10/00, (PB2001-105399, A14, MF-A03).

MCEER-00-0010 "Development and Evaluation of Simplified Procedures for Analysis and Design of Buildings with Passive Energy Dissipation Systems," by O.M. Ramirez, M.C. Constantinou, C.A. Kircher, A.S. Whittaker, M.W. Johnson, J.D. Gomez and C. Chrysostomou, 11/16/01, (PB2001-105523, A23, MF-A04).

MCEER-00-0011 "Dynamic Soil-Foundation-Structure Interaction Analyses of Large Caissons," by C-Y. Chang, C-M. Mok, Z-L. Wang, R. Settgast, F. Waggoner, M.A. Ketchum, H.M. Gonnermann and C-C. Chin, 12/30/00, (PB2001-104373, A07, MF-A02).

MCEER-00-0012 "Experimental Evaluation of Seismic Performance of Bridge Restrainers," by A.G. Vlassis, E.M. Maragakis and M. Saiid Saiidi, 12/30/00, (PB2001-104354, A09, MF-A02).

MCEER-00-0013 "Effect of Spatial Variation of Ground Motion on Highway Structures," by M. Shinozuka, V. Saxena and G. Deodatis, 12/31/00, (PB2001-108755, A13, MF-A03).

MCEER-00-0014 "A Risk-Based Methodology for Assessing the Seismic Performance of Highway Systems," by S.D. Werner, C.E. Taylor, J.E. Moore, II, J.S. Walton and S. Cho, 12/31/00, (PB2001-108756, A14, MF-A03).

MCEER-01-0001 "Experimental Investigation of P-Delta Effects to Collapse During Earthquakes," by D. Vian and M. Bruneau, 6/25/01, (PB2002-100534, A17, MF-A03).

MCEER-01-0002 "Proceedings of the Second MCEER Workshop on Mitigation of Earthquake Disaster by Advanced Technologies (MEDAT-2)," edited by M. Bruneau and D.J. Inman, 7/23/01, (PB2002-100434, A16, MF-A03).

MCEER-01-0003 "Sensitivity Analysis of Dynamic Systems Subjected to Seismic Loads," by C. Roth and M. Grigoriu, 9/18/01, (PB2003-100884, A12, MF-A03).

MCEER-01-0004 "Overcoming Obstacles to Implementing Earthquake Hazard Mitigation Policies: Stage 1 Report," by D.J. Alesch and W.J. Petak, 12/17/01, (PB2002-107949, A07, MF-A02).

MCEER-01-0005 "Updating Real-Time Earthquake Loss Estimates: Methods, Problems and Insights," by C.E. Taylor, S.E. Chang and R.T. Eguchi, 12/17/01, (PB2002-107948, A05, MF-A01).

MCEER-01-0006 "Experimental Investigation and Retrofit of Steel Pile Foundations and Pile Bents Under Cyclic Lateral Loadings," by A. Shama, J. Mander, B. Blabac and S. Chen, 12/31/01, (PB2002-107950, A13, MF-A03).

MCEER-02-0001 "Assessment of Performance of Bolu Viaduct in the 1999 Duzce Earthquake in Turkey" by P.C. Roussis, M.C. Constantinou, M. Erdik, E. Durukal and M. Dicleli, 5/8/02, (PB2003-100883, A08, MF-A02).

MCEER-02-0002 "Seismic Behavior of Rail Counterweight Systems of Elevators in Buildings," by M.P. Singh, Rildova and L.E. Suarez, 5/27/02. (PB2003-100882, A11, MF-A03).

MCEER-02-0003 "Development of Analysis and Design Procedures for Spread Footings," by G. Mylonakis, G. Gazetas, S. Nikolaou and A. Chauncey, 10/02/02, (PB2004-101636, A13, MF-A03, CD-A13).

MCEER-02-0004 "Bare-Earth Algorithms for Use with SAR and LIDAR Digital Elevation Models," by C.K. Huyck, R.T. Eguchi and B. Houshmand, 10/16/02, (PB2004-101637, A07, CD-A07).

MCEER-02-0005 "Review of Energy Dissipation of Compression Members in Concentrically Braced Frames," by K.Lee and M. Bruneau, 10/18/02, (PB2004-101638, A10, CD-A10).

MCEER-03-0001 "Experimental Investigation of Light-Gauge Steel Plate Shear Walls for the Seismic Retrofit of Buildings" by J. Berman and M. Bruneau, 5/2/03, (PB2004-101622, A10, MF-A03, CD-A10).

MCEER-03-0002 "Statistical Analysis of Fragility Curves," by M. Shinozuka, M.Q. Feng, H. Kim, T. Uzawa and T. Ueda, 6/16/03, (PB2004-101849, A09, CD-A09).

MCEER-03-0003 "Proceedings of the Eighth U.S.-Japan Workshop on Earthquake Resistant Design f Lifeline Facilities and Countermeasures Against Liquefaction," edited by M. Hamada, J.P. Bardet and T.D. O'Rourke, 6/30/03, (PB2004-104386, A99, CD-A99).

MCEER-03-0004 "Proceedings of the PRC-US Workshop on Seismic Analysis and Design of Special Bridges," edited by L.C. Fan and G.C. Lee, 7/15/03, (PB2004-104387, A14, CD-A14).

MCEER-03-0005 "Urban Disaster Recovery: A Framework and Simulation Model," by S.B. Miles and S.E. Chang, 7/25/03, (PB2004-104388, A07, CD-A07).

MCEER-03-0006 "Behavior of Underground Piping Joints Due to Static and Dynamic Loading," by R.D. Meis, M. Maragakis and R. Siddharthan, 11/17/03, (PB2005-102194, A13, MF-A03, CD-A00).

MCEER-03-0007 "Seismic Vulnerability of Timber Bridges and Timber Substructures," by A.A. Shama, J.B. Mander, I.M. Friedland and D.R. Allicock, 12/15/03.

MCEER-04-0001 "Experimental Study of Seismic Isolation Systems with Emphasis on Secondary System Response and Verification of Accuracy of Dynamic Response History Analysis Methods," by E. Wolff and M. Constantinou, 1/16/04 (PB2005-102195, A99, MF-E08, CD-A00).

MCEER-04-0002 "Tension, Compression and Cyclic Testing of Engineered Cementitious Composite Materials," by K. Kesner and S.L. Billington, 3/1/04, (PB2005-102196, A08, CD-A08).

MCEER-04-0003 "Cyclic Testing of Braces Laterally Restrained by Steel Studs to Enhance Performance During Earthquakes," by O.C. Celik, J.W. Berman and M. Bruneau, 3/16/04, (PB2005-102197, A13, MF-A03, CD-A00).

MCEER-04-0004 "Methodologies for Post Earthquake Building Damage Detection Using SAR and Optical Remote Sensing: Application to the August 17, 1999 Marmara, Turkey Earthquake," by C.K. Huyck, B.J. Adams, S. Cho, R.T. Eguchi, B. Mansouri and B. Houshmand, 6/15/04, (PB2005-104888, A10, CD-A00).

MCEER-04-0005 "Nonlinear Structural Analysis Towards Collapse Simulation: A Dynamical Systems Approach," by M.V. Sivaselvan and A.M. Reinhorn, 6/16/04, (PB2005-104889, A11, MF-A03, CD-A00).

MCEER-04-0006 "Proceedings of the Second PRC-US Workshop on Seismic Analysis and Design of Special Bridges," edited by G.C. Lee and L.C. Fan, 6/25/04, (PB2005-104890, A16, CD-A00).

MCEER-04-0007 "Seismic Vulnerability Evaluation of Axially Loaded Steel Built-up Laced Members," by K. Lee and M. Bruneau, 6/30/04, (PB2005-104891, A16, CD-A00).

MCEER-04-0008 "Evaluation of Accuracy of Simplified Methods of Analysis and Design of Buildings with Damping Systems for Near-Fault and for Soft-Soil Seismic Motions," by E.A. Pavlou and M.C. Constantinou, 8/16/04, (PB2005-104892, A08, MF-A02, CD-A00).

MCEER-04-0009 "Assessment of Geotechnical Issues in Acute Care Facilities in California," by M. Lew, T.D. O'Rourke, R. Dobry and M. Koch, 9/15/04, (PB2005-104893, A08, CD-A00).

MCEER-04-0010 "Scissor-Jack-Damper Energy Dissipation System," by A.N. Sigaher-Boyle and M.C. Constantinou, 12/1/04.

MCEER-04-0011 "Seismic Retrofit of Bridge Steel Truss Piers Using a Controlled Rocking Approach," by M. Pollino and M. Bruneau, 12/20/04.

MCEER-05-0001 "Experimental and Analytical Studies of Structures Seismically Isolated with an Uplift-Restraint Isolation System," by P.C. Roussis and M.C. Constantinou, 1/10/05.

MCEER-05-0002 "A Versatile Experimentation Model for Study of Structures Near Collapse Applied to Seismic Evaluation of Irregular Structures," by D. Kusumastuti, A.M. Reinhorn and A. Rutenberg, 3/31/05.

MCEER-05-0003 "Proceedings of the Third PRC-US Workshop on Seismic Analysis and Design of Special Bridges," edited by L.C. Fan and G.C. Lee, 4/20/05.

MCEER-05-0004 "Approaches for the Seismic Retrofit of Braced Steel Bridge Piers and Proof-of-Concept Testing of an Eccentrically Braced Frame with Tubular Link," by J.W. Berman and M. Bruneau, 4/21/05.

MCEER-05-0005 "Simulation of Strong Ground Motions for Seismic Fragility Evaluation of Nonstructural Components in Hospitals," by A. Wanitkorkul and A. Filiatrault, 5/26/05.

MCEER-05-0006 "Seismic Safety in California Hospitals: Assessing an Attempt to Accelerate the Replacement or Seismic Retrofit of Older Hospital Facilities," by D.J. Alesch, L.A. Arendt and W.J. Petak, 6/6/05.

MCEER-05-0007 "Development of Seismic Strengthening and Retrofit Strategies for Critical Facilities Using Engineered Cementitious Composite Materials," by K. Kesner and S.L. Billington, 8/29/05.

MCEER-05-0008 "Experimental and Analytical Studies of Base Isolation Systems for Seismic Protection of Power Transformers," by N. Murota, M.Q. Feng and G-Y. Liu, 9/30/05.

MCEER-05-0009 "3D-BASIS-ME-MB: Computer Program for Nonlinear Dynamic Analysis of Seismically Isolated Structures," by P.C. Tsopelas, P.C. Roussis, M.C. Constantinou, R. Buchanan and A.M. Reinhorn, 10/3/05.

MCEER-05-0010 "Steel Plate Shear Walls for Seismic Design and Retrofit of Building Structures," by D. Vian and M. Bruneau, 12/15/05.

MCEER-05-0011 "The Performance-Based Design Paradigm," by M.J. Astrella and A. Whittaker, 12/15/05.

MULTIDISCIPLINARY CENTER FOR EARTHQUAKE ENGINEERING RESEARCH

A National Center of Excellence in Advanced Technology Applications

University at Buffalo, State University of New York
Red Jacket Quadrangle ▪ Buffalo, New York 14261
Phone: (716) 645-3391 ▪ Fax: (716) 645-3399
E-mail: *mceer@mceermail.buffalo.edu* ▪ WWW Site *http://mceer.buffalo.edu*

University at Buffalo *The State University of New York*

ISSN 1520-295X